Technical University of Crete
School of Electrical and Computer Engineering

Diploma Thesis

Movement Strategies for Emergency Vehicles in Lane-Free Environment

Ismini Pavlaki

Thesis Committee
Prof. Michail G. Lagoudakis
Prof. Georgios Chalkiadakis
Prof. Ioannis Papamichail (School of PEM)

Chania, July 2023

Πολυτεχνείο Κρήτης
Σχολή Ηλεκτρολόγων Μηχανικών και Μηχανικών Υπολογιστών

Διπλωματική Εργασία

Στρατηγικές Κίνησης για Οχήματα Έκτακτης Ανάγκης σε Δρόμους Χωρίς Λωρίδες

Ισμήνη Παυλάκη

Εξεταστική Επιτροπή

Καθ. Μιχαήλ Γ. Λαγουδάκης
Καθ. Γεώργιος Χαλκιαδάκης
Καθ. Ιωάννης Παπαμιχαήλ (Σχολή ΜΠΔ)

Χανιά, Ιούλιος 2023

Acknowledgements

I would firstly like to thank Prof. Papageorgiou and Prof. Papamichail for the opportunity they gave me to join their team and have a closer look on their work and research. I would also like to thank Prof. Michail Lagoudakis, and Prof. Georgios Chalkiadakis for their willingness to collaborate with the aforementioned professors in order for my thesis project to be successfully completed. Moreover, I give special thanks to Dr. Panagiotis Typaldos and Dr. Venkata Karteek Yanumula for their thoughtful comments and recommendations on this dissertation. They were both happy to assist me in any way throughout the whole project. Finally, I cannot forget to thank my family and friends for their continuous support throughout my college years.

Abstract

Road congestion and road accidents persist as major problems, even after decades of research and developments in road safety and traffic management and call for comprehensive solutions. Automated vehicles receive high-quality information in a fraction of a second through an array of sensors that scan the surroundings frequently. With high-quality information and split-second decisions, automated vehicles have the potential to deliver safe and efficient traffic flow. Road traffic lanes were introduced to help human drivers for safe navigation at the cost of reduced utilization of the road space. Moreover, lane changing is a high-risk task, which has the potential to trigger congestion and possibly lead to road capacity drop. Full automation of traffic makes the lanes unnecessary and calls for the novel idea of lane-free traffic. In a futuristic scenario of 100% automated vehicles, there is no need for the vehicles to follow the rules designed for human drivers. A lane-free environment is considered for the current work with fully automated vehicles for safe and efficient movement.

Emergency situations may arise due to various reasons, for example an ambulance or a fire truck navigating through traffic needs a "green corridor", especially when human lives are at stake. With cooperation among the automated vehicles, emergency situations can be handled in an efficient manner. To this end, this diploma thesis investigates the case of an automated Emergency Vehicle (EmV), which aims at driving through traffic, while maintaining its desired speed. Regarding the connectivity capabilities of the EmV, we consider different approaches, where the EmV has no direct interaction with the rest of the traffic in terms of changing their behavior (passive approach); or cases where the EmV is capable of exchanging enhanced information with the surrounding vehicles in order to facilitate its movement, e.g. by creating "green corridors" (active approach).

The aforementioned problem is formulated as an Optimal Control Problem (OCP) and is solved numerically with use of a Feasible Direction Algorithm (FDA). The objective function of the OCP aims at minimizing several terms, regarding the safety and comfort of the passengers, fuel efficiency, and advancement goals of EmV by penalizing deviations from longitudinal and lateral desired speeds. State-dependent bounds on control inputs are used to ensure that the vehicles stay within the road boundaries and prevent crashes in emergency situations. The OCP is solved repeatedly for short-time horizons within a model predictive control (MPC) framework, while the vehicle advances.

The performance of the EmV is evaluated for both passive and active approaches and for different scenarios and traffic densities. The simulations were conducted in a lane-free environment, using a custom-made extension, named TrafficFluid-Sim, which is built for the SUMO (Simulation of Urban MObility) simulator. The results indicate that, at low-traffic densities, connectivity/cooperation between the EmV and the surrounding traffic has minor effect on the EmV's performance, as there is sufficient space for manoeuvring. On the other hand, as the traffic density rises, the cooperation seems to be crucial and measures, like the formation of "green corridors", are demonstrated to be extremely efficient, allowing the EmV to maintain high speeds, despite the limited space.

Περίληψη

Η οδική συμφόρηση και τα τροχαία ατυχήματα εξακολουθούν να αποτελούν μείζονα προβλήματα, ακόμη και μετά από δεκαετίες έρευνας και εξελίξεων στην οδική ασφάλεια και τη διαχείριση της κυκλοφορίας και απαιτούν ουσιαστικές λύσεις. Τα αυτοματοποιημένα οχήματα λαμβάνουν πληροφορίες υψηλής ποιότητας σε ένα κλάσμα του δευτερολέπτου μέσω μιας σειράς αισθητήρων που σαρώνουν συχνά το περιβάλλον. Με υψηλής ποιότητας πληροφορίες και αποφάσεις σε κλάσματα δευτερολέπτου, τα αυτοματοποιημένα οχήματα έχουν τη δυνατότητα να παρέχουν ασφαλή και αποτελεσματική κυκλοφοριακή ροή. Οι οδικές λωρίδες κυκλοφορίας εισήχθησαν για να παρέχουν στους οδηγούς ασφαλή πλοήγηση, όμως με κόστος τη μειωμένη χρήση του οδικού χώρου. Επιπλέον, η αλλαγή λωρίδας είναι μια διαδικασία υψηλού κινδύνου, η οποία έχει τη δυνατότητα να προκαλέσει συμφόρηση και πιθανώς να οδηγήσει σε μείωση της οδικής χωρητικότητας. Η πλήρης αυτοματοποίηση της κυκλοφορίας καθιστά τις λωρίδες περιττές και εισάγει τη καινοφανή ιδέα της κυκλοφορίας χωρίς λωρίδες. Σε ένα φουτουριστικό σενάριο, με χρήση 100% αυτοματοποιημένων οχημάτων, δεν υπάρχει ανάγκη τα οχήματα να ακολουθούν τους κανόνες που έχουν σχεδιαστεί για τους ανθρώπους-οδηγούς. Στη παρούσα εργασία, θεωρούμε ένα περιβάλλον χωρίς λωρίδες, με πλήρη χρήση αυτοματοποιημένων οχημάτων για ασφαλή και αποτελεσματική μετακίνηση.

Καταστάσεις έκτακτης ανάγκης ενδέχεται να προκύψουν για διάφορους λόγους, για παράδειγμα ένα ασθενοφόρο ή ένα πυροσβεστικό όχημα που πλοηγείται στην κυκλοφορία χρειάζεται έναν «πράσινο διάδρομο», ειδικά όταν διακυβεύονται ανθρώπινες ζωές. Με τη συνεργασία μεταξύ των αυτοματοποιημένων οχημάτων, οι καταστάσεις έκτακτης ανάγκης μπορούν να αντιμετωπιστούν με αποτελεσματικό τρόπο. Για το σκοπό αυτό, η παρούσα διπλωματική εργασία διερευνά την περίπτωση ενός αυτοματοποιημένου οχήματος έκτακτης ανάγκης (Emergency Vehicle - EmV), το οποίο στοχεύει στη διέλευση του οχήματος μέσα από την κυκλοφορία, διατηρώντας την επιθυμητή του ταχύτητα. Όσον αφορά τις δυνατότητες συνδεσιμότητας του EmV, εξετάζουμε διαφορετικές προσεγγίσεις, όπου το EmV δεν έχει άμεση αλληλεπίδραση με την υπόλοιπη κίνηση όσον αφορά την αλλαγή της συμπεριφοράς τους (παθητική προσέγγιση), καθώς και περιπτώσεις όπου το EmV είναι ικανό να ανταλλάσσει βελτιωμένες πληροφορίες με τα γύρω οχήματα για να διευκολύνει την κίνησή του, π.χ. με τη δημιουργία «πράσινων διαδρόμων» (ενεργητική προσέγγιση).

Το προαναφερθέν πρόβλημα διατυπώνεται ως Πρόβλημα Βέλτιστου Ελέγχου (Optimal Control Problem - OCP) και επιλύεται αριθμητικά με τη χρήση ενός αλγόριθμου εφικτής κατεύθυνσης (Feasible Direction Algorithm - FDA). Η αντικειμενική συνάρτηση του OCP στοχεύει στην ελαχιστοποίηση πολλών όρων σχετικά με την ασφάλεια και την άνεση των επιβατών, την κατανάλωση καυσίμου και άλλους στόχους βελτίωσης της ποιότητας κίνησης του EmV με αριθμητικές ποινές αποκλίσεων από τις διαμήκεις και πλευρικές επιθυμητές ταχύτητες. Τα όρια που εξαρτώνται από τις εξισώσεις κατάστασης στις εισόδους ελέγχου χρησιμοποιούνται για να διασφαλιστεί ότι τα οχήματα παραμένουν εντός των ορίων του δρόμου και αποτρέπουν ατυχήματα σε καταστάσεις έκτακτης ανάγκης. Το OCP επιλύεται επαναληπτικά για σύντομους χρονικούς ορίζοντες μέσα σε ένα πλαίσιο προβλεπτικού ελέγχου βάσει μοντέλου (Model Predictive Control - MPC), ενώ το όχημα προχωρά.

Η απόδοση του EmV αξιολογείται, τόσο στις παθητικές, όσο και στις ενεργητικές, προσεγγίσεις, για διαφορετικά σενάρια και πυκνότητες κυκλοφορίας. Οι προσομοιώσεις έλαβαν χώρα σε ένα περιβάλλον χωρίς λωρίδες, χρησιμοποιώντας την προσαρμοσμένη επέκταση με την ονομασία TrafficFluid-Sim, η οποία έχει κατασκευαστεί για τον προσομοιωτή SUMO (Simulation of Urban MObility). Τα αποτελέσματα υποδεικνύουν ότι, σε χαμηλές πυκνότητες κυκλοφορίας, η συνδεσιμότητα/συνεργασία μεταξύ του EmV και της γύρω κυκλοφορίας έχει μικρή επίδραση στην απόδοση του EmV, καθώς υπάρχει επαρκής χώρος για ελιγμούς. Από την άλλη, καθώς αυξάνεται η πυκνότητα κυκλοφορίας, η συνεργασία φαίνεται να είναι κρίσιμη και μέτρα, όπως ο σχηματισμός «πράσινων διαδρόμων», αποδεικνύονται εξαιρετικά αποτελεσματικά, επιτρέποντας στο EmV να διατηρεί υψηλές ταχύτητες, παρά τον περιορισμένο χώρο.

Contents

List of Figures

List of Tables

1

Introduction

1.1 Introduction

Connected and Automated Vehicles (CAVs) will soon be the main form of transportation in urban highways. The driving task may be implemented by Artificially Intelligent (AI) Vehicles that not only find an optimal route, but also choose their driving behavior and their location on the road. By continuously staying connected with each other, in fully automated roads, or by being trained to adapt and coexist with human driven vehicles through Reinforcement Learning (RL), CAVs will soon be able to complete the driving task without the need of human intervention. Regarding another approach, in which the Traffic Fluid research group is highly interested in, instead of AI, vehicles with high sensory levels will use a path-planning algorithm for automated road vehicles on lane-free motorways, which are derived from the opportune formulation of an optimal control problem, as proposed in [52]. Unlike similar research conducted in the field, Traffic Fluid is based into two innovative principles: *Lane-free traffic* and *Nudging*, making research more complex and interesting.

When roads were firstly invented there was no need for lanes, since the road utilization was very low. As automobiles became more affordable and popular, the need of lane markings gradually emerged for segmentation of opposite directions to avoid collisions and later on, in the 1950s, dashed lines, separating parallel lanes on the same traffic direction, were introduced with rules for lane-changing tasks. Parallel lanes help maintain traffic safety by making it easier for human drivers to keep on track and avoid collisions with neighboring vehicles. Within a lane, a driver only has focus on the speed of its downstream vehicle, ensuring that he keeps a safe distance from it. Unfortunately, switching lanes makes things more difficult since the driver has to search for a free spot on the target lane, predict its potential trajectory based on the speeds of many vehicles (including his own), and keep an eye on the distance to the vehicle in front. When frequent lane changes take place, caused by lane drops or roadways or merging on-ramps, the task of changing lanes becomes more dangerous. Lane changes do, in fact, cause 10% of

collisions. By automating the task, these numbers would immediately drop. Additional capacity losses result from dynamic events linked to lane-changing maneuvers, in addition to the static capacity loss brought on by the requirement for broad lanes on high-speed motorways and arterials when driving manually. As for space utilization, human lanes are designed wide enough to fit the wider type of vehicle. So, with lane-free traffic, the carriageway capacity could be significantly increased by utilizing every free space on the road. Vehicle sensors within connected and automated vehicles (CAVs) allow them to quickly, concurrently, continuously, and reliably monitor their surrounding vehicles on a 360-degree basis and make quick (computer-based) driving decisions.

Based on proper movement techniques, a CAV can "float" securely and effectively in a stream of collaborating CAVs, thanks its enhanced capabilities compared to human driving. As a result, lane-free highways, motorways and even urban roads may improve traffic safety while regaining capacity.

Regarding the second TrafficFluid principle, nudging: Vehicles communicate their presence to other vehicles in front of them (or are sensed by them), and this may exert a "nudging" effect on the downstream vehicles [1]. The phenomenon of anisotropy in macroscopic traffic flow models is a significant and even "sacred" principle in traffic flow theory [2]. The groundwork for macroscopic traffic flow theory was laid by the seminal paper [2], which compared the movement of traffic in open channels to that of water. Traffic states behave similarly to gas in a pipe or water flow in an open channel, moving as waves with a speed higher than the speed of the fluid particles. Shock waves also arise as fast cars catch up to slower ones in front. There is a significant difference, however, between the flow of water or gas and the flow of vehicular traffic. The movement of a vehicle, as contributed by a human driver, is typically unaffected by what is happening behind it (basically, it depends only on the distance and speed of the vehicle in front), while it is typically affected by what is happening upstream. For example, fast particles may be "pushing" slower particles ahead, causing them to accelerate. On the other hand, water or gas flow particles may have an impact on the condition of other particles downstream [3]. Without the anisotropic limitation given by human driving, the suggested nudge effect allows for the purposeful conception of vehicle traffic flow in a number of conceivable ways, to achieve the necessary design goals, such as increasing the flow and the road capacity [56].

Finally, in automated vehicle models, we have higher levels of intervention, so in case of an emergency it is much easier to communicate and prioritize mobility of certain vehicles, open the way, or slow down other vehicles.

1.2 Thesis Objectives

Emergency vehicles (EmV's), such as ambulances, fire trucks, police cars, and engineering rescue vehicles, are essential for providing efficient emergency services. More than 5 million people die each year due to delayed trauma care, according to the World Health Organization. If emergency resuscitation is administered on time, the mortality rate can be decreased by roughly 10%. The distance between a starting place and the scene of an emergency is represented by an EmV's reaction time [5].

The present thesis aims to investigate the behavior of an EmV driving in a lane-free environment, following the principles of the Traffic-Fluid concept [4]. It is based on the path-planning problem, as proposed in [52], where a nonlinear Optimal Control Problem (OCP) with state-dependent constraints in a lane-free environment is established. To the aforementioned work, several extensions and modifications are made in order to test the case of an EmV entering the existing model. The tool used to simulate and investigate the reaction of the CAVs' population to this addition was TrafficFluid Sim, as proposed in [40].

In this diploma thesis, changes are gradually made in every scenario taking place, regarding the behavior of an individual vehicle, which is marked as an EmV. At first, in the Passive (or Non-Cooperative) Approach, the EmV's presence does not affect other vehicles' driving behavior within traffic. Instead, alterations on the EmV's goals and characteristics take place individually, such as an increment in target speed or use of a smaller time-gap to become more flexible on the road. Neighboring CAVs are called to adapt to the change without any further intervention.

Similarly, in the Active (or Cooperative) Approach, cooperation takes place with small changes of parameters in the present algorithm in order to help the EmV reach higher speeds and travel independently of other traffic conditions. At this point, the lateral positioning strategy proposed in [57] is used to direct the EmV towards a prespecified lateral position, as it has to be directed toward a green corridor created to reach its goals. Moreover, other vehicles' behavior is also altered by adding the case where a vehicle within the CAV population, is downstream to the EmV. Different methodologies are implemented in order to open the way for the EmV to pass through traffic. As different scenarios are tested many questions arise regarding the model's ability to adapt to the changes and maintain safety. Is the present model ready to complete our mission? Do our alterations affect the overall performance of our model negatively? Through experiments and testing, the reaction of the system is observed, and decisions regarding the creation of a green corridor for the EmV to pass through, as a realistic and implantable solution were made.

1.3 Thesis Structure

This thesis begins with Chapter 1, which is an introduction to the current research related to the path planning for CAVs in a lane-free environment. Chapter 2, gives a brief description of the background required to understand this diploma thesis by reviewing the fundamental principles and concepts of current traffic systems. Chapter 3 accurately defines the problem with all its constraints, as considered in [52] such as the objective function, and the OCP solution. Moreover, Chapter 4 firstly gives a brief description of the extension TrafficFluid-Sim in SUMO, as been proposed in [40], in which the simulations take place. And additionally, presents the emergency vehicle entrance to the given model. Chapter 5 sets up experiment configurations and benchmarks of our approach with multiple difficulty levels to evaluate its performance. Finally, Chapter 6 summarizes our strategy and the improvement of the EmV's performance.

2

Background

The fundamental principles and concepts of current traffic systems are presented in Chapter 2. The principle of Vehicle Automation and Communication Systems is mentioned in Section 2.1. A brief overview of connected and automated vehicles (CAVs) and their effects are provided in Section 2.2. Moreover, the Traffic Fluid paradigm which was developed in [4] is presented in Section 2.3. Finally, in Section 2.4, the concept of discrete-time optimal control is briefly described as established in [52].

2.1 Vehicular Traffic

Vehicle traffic is crucial for the transportation of people and products and improves the social and economic health of a modern life. Urbanization causes many problems to human mobility, since people living in the cities tend to increase the vehicular traffic flow. In densely populated urban centers, traffic congestion results from city road infrastructure not evolving at a rate that keeps up with the number of vehicles. As a result, human mobility suffers greatly due to urbanization. Beyond causing travel delays, vehicle traffic congestion has major negative effects on people's health (e.g., stress-related health issues, in emergency cases with delayed arrival of the vehicle), the environment (e.g., a rise in pollution), and the economy (e.g., money being spent due to time spent in traffic jams). However, despite decades of research, problems like traffic congestion and accidents still occur often, particularly in urban locations around the world. Creative solutions are required.

The development of various Vehicle Automation and Communication Systems (VACS) and control strategies has been a significant endeavor in the last few years to address the aforementioned problems, where developments projected aim to enhance the capabilities of the various vehicles.

2.1.1 Vehicle automation and communication systems - VACS

VACS are systems that automate some vehicle tasks to varying degrees, from simple driver assistance to complete automation. Only a portion of the multiple VACS described in current literature actually correspond to various systems. The goal of marketing or differentiation is to get manufacturers and researchers refer to systems that are essentially the same under different labels. Numerous classifications have been offered, each with a particular function and reflecting various VACS facets.

For instance, Bishop divides VACS applications into the four groups listed below based on their intended functionality, [7]:

- ***Safety systems:*** The systems that ensure safety for crash avoidance.
- ***Convenience systems:*** Products in this category help drivers manage their vehicles and reduce the stress associated with driving.
- ***Productivity systems:*** This category includes systems that are suitable for buses and commercial vehicles and are designed to enhance productivity in terms of operating expenses (such as fuel consumption) or time (such as more effective maneuvering).
- ***Traffic assist systems:*** These are systems that combine advanced vehicle control methods with vehicle communications to potentially improve traffic flow over time.

The aforesaid classification is flexible in that it allows the inclusion of a certain system in more than one category.

To the contrary side, Popescu-Zeletin et al. [8] offer a classification that is better suited for the analysis of the VACS communication requirements. They start off by defining VACS application domains for this purpose in a different way than Bishop [7], and afterwards establish communication systems that are not related to the application domains. This helps VACS to be categorized based on both the application domains in which they are employed such as the communication policies that are necessary to perform their functions.

Three application domains for VACS are identified under the scheme put forth by Popescu-Zeletin et al. [8]:

- ***Safety*:** Applications for VACS are included in this domain with the aim of improving vehicle and passenger safety.
- ***Resource efficiency:*** Applications for VACS in this domain work to increase both traffic and environmental efficiency.
- ***Infotainment and advanced driver assistance systems (ADAS):*** This category consists of VACS programs that offer passengers and drivers entertainment or information.

Additionally, the utilization (transmission type) and necessary technology (transmission method) are taken into account while establishing the VACS communication rules. According to the required technology, two communication domains are specified.:

- *The bidirectional regime* that enables connection between two vehicles or vehicle and roadside for bidirectional exchange of information; and
- *The position-based regime* by means of which data is shared instantly to a certain vehicle population within a certain range. Roadside units, which are viewed as fixed-position vehicles, are the only method of spreading information in a single direction.

Finally, three communication protocols are developed based on their application. [13]:

- *In-vehicle regime* refers to communication types that are based on electronic units inside the vehicle;
- *Vehicle-to-vehicle (V2V)*: refers to communication methods that allow the transmission of data between vehicles; and
- *Vehicle-to-infrastructure (V2I)* corresponds to the multiple forms of communication that include transmission of data between infrastructure and vehicles.

2.1.2 Freeway Traffic Management and Control

Due to the continuous increase in traffic congestion, it becomes crucial to create systems of surveillance and control for highway traffic networks. Despite being built to accommodate the mobility demands of heavy traffic, freeway networks have recently been challenged by increased traffic densities, which is hardly handled through adequate infrastructure improvements [8]. As a result, implementing control techniques may serve as the only method to enhance the efficiency of motorway traffic systems. In a lane environment, control solutions have been created to address issues like congestion and as a result offer safer, more effective, and less polluting transportation. The quality of the control techniques determines how effective traffic control is.

Traffic signals play a central role in traffic management in many major cities. Although it has been studied for many years, it is widely accepted that its benefits are not fully realized. Even in cities with advanced traffic management centers (TMCs), it is not uncommon to intervene manually in the timing plans, especially during peak hours [9]. Those attests that indeed there is plenty of room for improvement.

In addition, thanks to advancements in detection, transmission, and data processing technologies, the development of information systems assisting drivers, while they are traveling on freeways, has significantly expanded in recent years. In fact, the implementation of a trusted traffic monitoring system, or, analogously, a traffic surveillance system, is essential for the efficient management of a freeway network. These systems can elaborate the relevant information coming from sensors placed throughout the network, to detect potential critical situations, and to give controllers and road users

useful information about the system's current state and, in some cases, a prediction of its evolution [9].

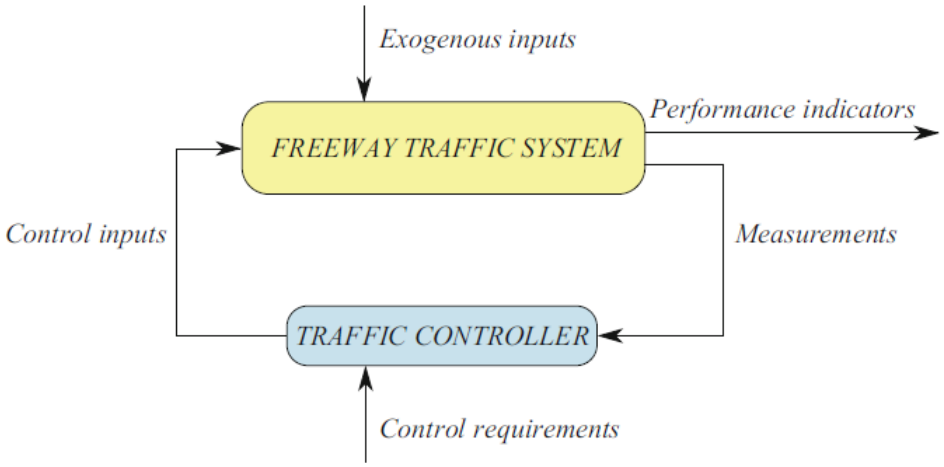

Figure 2. 1: A controlled freeway traffic system
(Source [11])

Besides monitoring the traffic state, improving the efficiency of the freeway system, overall, requires controlling and regulating traffic flows. The scientific community has developed and is now looking into highway traffic control systems that may react to the system in real time based on the existing system status and, in certain cases, also on its predicted evolution. Reduced congestion, or shorter travel times for cars, is one of the key goals of a highway traffic control instrument.

There is little doubt that reducing traffic congestion and delays for travelers frequently implies reducing other negative impacts of traffic, which are more connected to sustainability and the quality of life for inhabitants. However, some newer freeway traffic control systems expressly consider these linked aims, i.e., certain traffic controllers are designed specifically to decrease traffic emissions, noise, accidents, and so on [11].

The huge variety of existing methods that have already been proposed and documented in the literature [11], [12] serve as an illustration of how the computational architectures of automated vehicle controls are quite different. However, several of the methods describe architectural designs that are now well-known and respected for their qualities and possibilities [12], as shown in the following examples:

- ***Reactive Control:*** A sensorimotor response system makes up reactive control. This type of control is typically the simplest to create, because it uses the fewest computational resources. Reactive control employs a loop that scans the sensors, immediately processes the data, and then sends an actuator order in response. A reactive control strategy typically only takes into account the sensory readings made in the present for the purpose of formulating decisions and generating action orders [13]. A reactive system is very useful to implement actions, such as preventing collisions.

- ***Cognitive Control***: The use of an action planning mechanism falls under the category of cognitive control. So, based on the information the system possesses regarding an issue that needs to be solved, a previous plan of execution of a series of activities can be developed. The deliberative control assumes the existence of a high-level decision-making and reasoning process, which is usually more difficult to implement than reactive control. Actions can be planned, using this procedure in order to manage and complete tasks that call for a more complex level of control. These tasks could be the definition and execution of tasks for navigating one's environment by using a map to get from one point to another. Pure deliberative control, however, has limitations in the context of unexpected situations, such as a block obstructing a specific route [14]. Pure deliberative control struggles to respond in this situation to a new environmental configuration that was not predicted during initial planning. A control system should ideally combine reactive and deliberative elements in a hierarchical/hybrid system, demonstrating the reactive capabilities of a reactive system as well as the ability to manage and complete the challenging tasks involved in a deliberative system.
- ***Hierarchical/hybrid control:*** Multiple reactive and deliberative control modules are combined to provide hierarchical or hybrid control, which is composed of layers with the arrangement allowing for either parallel or hierarchical operation. These control systems are frequently encountered in hierarchical systems with vertical and horizontal decompositions, and the pairing of multiple control modules results in the implementation of a priority scheme, addressing the various layers of the system [15]. The advantage of hierarchical/hybrid systems is that they can combine the behaviors learned from each of their individual parts to produce a more reliable behavior and more complex task execution. A collection of parallel-operating, communicative modules is used to provide hybrid control.

2.1.3 Combining Automation with Human Driving

Due to their advanced capabilities, connected and automated vehicles (CAVs) have taken on a strategic lead in the global automotive industry [16], such as automated navigation and vehicle-to-everything connectivity [17]. CAVs can gather more precise traffic data than human-driven vehicles (HVs) and conduct synchronized control [18]. They can significantly increase the efficiency and safety of traffic flows [19]. However, upgrading from an exclusively Human Driven (HV) traffic system to a genuine CAV traffic system may require a few years. Hence, the use of the same road by HVs and CAVs during this transitional phase is possible [20]. When the two types of vehicles interact, the corresponding mixed traffic flows, may exhibit characteristics not seen in pure HV traffic flows because the two types of vehicles have different behaviors [21].

Related research has used computer simulation, which receives traffic models and traffic situations as input, to examine the dynamics and capabilities of diverse traffic flows [22]. The modeling of HV and CAV mixed traffic flows is a topic that has extensively

been studied in the literature. Machine learning and physics-based models are two types within which the modeling techniques can be separated. Contemporary algorithms that employ deep neural networks, reinforcement learning, imitation learning, etc. to imitate human intelligence are also referred by the term machine learning. In recent years, it extensively used for autonomous vehicle decision-making [23]. Guo et al. developed a cooperative lane-changing strategy to enable farsighted lane-changing behavior by CAVs in favor of traffic efficiency based on improving learning skills [24]. To enhance the simulation system's ability to accurately imitate the car-following and lane-changing behavior of CAVs in mixed traffic, Guo et al. applied the deep reinforcement learning approach [25]. On [16] the dynamics of CAVs and HVs, Manhbub et al. [26] established a strict framework for controlling CAVs in mixed traffic. This framework was based on a machine learning algorithm.

2.2 Connected Automated Vehicles (CAVs)

2.2.1 Connectivity

Connected and Automated Vehicles (CAVs) are cars that can operate independently and are equipped with a variety of sensors to collect data from their environment [27]. One of the most important inventions from the first two decades of the twenty-first century is automated driving, which has the potential to revolutionize both the urban and rural transportation infrastructure as well as the way of life of those who travel frequently. Thanks to Artificial Intelligence (AI) onboard cars, automated driving technology has advanced over the past ten years.

In a world where CAVs are widely used, there will always be a coexistence of private and shared use, when it comes to human transportation. The former will be identical to a private car, with the automation's technological equipment being the only significant difference from contemporary vehicles.

Modern cutting-edge technologies are incorporated into automated vehicles to enable self-driving functionality and improve the experience of drivers and passengers. Systems built on these technologies typically rely on ever-more-advanced controllers and sensors, which enable vehicles to detect environmental events, provide their embedded systems the ability to infer and decide on routes and navigation, and assist vehicles with more driving autonomy. The full adoption of self-driving cars still raises a number of issues regarding the potential effects and dangers that minor errors in the system may bring to public safety; these flaws could result in accidents and consequently, to loss of people's lives. As a result, it is necessary to evaluate the driving system's reliability and safety, as an independent vehicle is being developed [12].

Several names for a class of transport vehicle for people or goods using a digital control system include automobiles without drivers, independent vehicles, and robotic cars. This control system incorporates several sensors and actuators that, beginning with a user-established initial mission, serve the purpose of travelling safely and automatedly through

streets, roads, and other terrestrial surfaces [28], [29]. The navigation procedure comprises a few automated phases to collect data from the environment, locate the vehicle, avoid accidents with other environmental features, and take the best possible actions for the specified mission [30].

The design and implementation of the lowest levels of the control pyramid are the first steps in creating a control system for an automated vehicle. The implementation of a computer system that controls the various components and modules of this system follows the creation of lower layers. Simpler duties that can be handled by programmable logic controllers (PLCs) can be easily included in a computerized control system. However, more advanced computational control architectures are needed for systems that are designed to manage the performance of more complex tasks [31]. Several skills may be required to complete the objectives of this control architecture:

- Reading and analyzing inputs from the vehicle's sensors.
- Avoiding obstacles.
- Reacting to events, even unexpected ones, like the sudden appearance of moving obstacles.
- Managing the various system components to generate commands in the right order and with the appropriate parameters, so that the planned task may be performed.
- Developing routes from point A to point B without using a map of the area for planning trajectories. Ensuring that a vehicle is positioned appropriately.
- Mapping its surroundings by drawing a diagram that symbolizes your "memories" of the paths it has taken.
- Acquiring information of the environment and how to interact with it, adapting essentially.
- Interacting, collaborating, and even exchanging information with other computing devices.
- Outlining methods for putting fault-sensing and fault-tolerance into practice when locating and correcting for localized flaws in a vehicle's components.

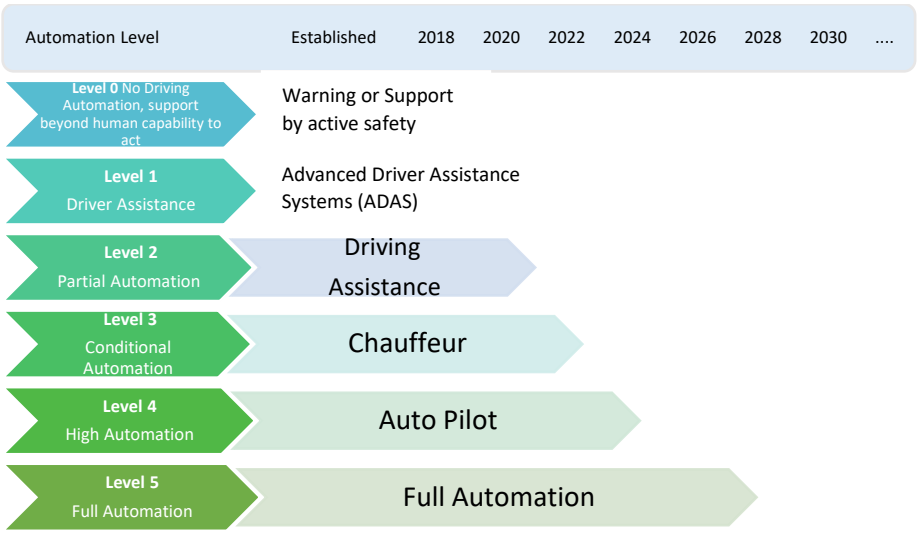

Figure 2.2: Levels of Automation
(Source: [55])

2.2.2 Types of linked car communication systems

Networking tools, such as communication devices with cutting-edge wireless connections, like 5G, enable communication and information transmission between vehicles and other road elements, like cars, traffic lights, etc. The ability to process information in a network manner, sense the environment, and communicate with other devices, all enable intelligent vehicles to be directed. The three following categories [1] are used to group the linked car communication systems:

Vehicle-to-vehicle (V2V)

A design that enables immediate interaction between cars without the use of a permanent infrastructure. Road safety, which is one of the most important applications of telematics in the vehicle field, several works for collision avoidance support, and warning mechanisms in general, have been widely studied by researchers. Using an appropriate V2V paradigm, vehicles could communicate with each other and propagate security issues.

Vehicle to Infrastructure (V2I)

Communication with the road infrastructure, such as traffic lights, signs, and other roadside objects. In this case, on-board services require a connection with the infrastructure located at the roadside. This kind of connectivity is known as Vehicle to Infrastructure (V2I) communication. An example of such technology can be found in electronic fee collection systems, where drivers are charged automatically, according to some road and vehicle parameters [32].

Hybrid architecture

A combination of both V2V and V2I: Connected and Automated vehicles (CAVs) will be a reality in the near future and have the potential to reduce traffic congestion, road crashes and vehicle emissions [33],[34].

Safety

Given that human error contributes to 94% of crashes, the idea of CAVs has raised expectations for the safety performance of future road transportation systems. Based on this statistic, recent studies have assessed the possible safety impact of CAVs, indicating a safety benefit of about 90% during the fully automated era [35].

During the last years, many researchers have focused on the simulation-based studies in order to evaluate the benefits of CAVs, due to the lack of real-world data. Although there are many vehicle-centric applications available on the market, such as lane departure warning systems and speed updates, these technologies only somewhat assist human drivers, and accidents still happen due to human error. The focus of current research is the deployment of CAVs on public roads and the operation of lane-free environments in traffic without human drivers.

Mobility

CAVs have the potential to evolve the way people travel in the near future. Road congestion will be noticeably improved, since the use of CAVs allows the detection of events like a sudden increase in traffic volume or speed, and the lane-free model will utilize a bigger part of the road, allowing a denser traffic flow and as a result, a better one. So, vehicles may be directed to different possible routes to avoid traffic. The most crucial aspect, however, is that incident responders can reach the scene more swiftly and safely, due to the communication between CAVs and emergency technologies [36].

Environment

The need to transition to a more sustainable transportation system is driven by the problems posed by climate change and urban population development. More than 70% of all carbon dioxide (CO_2) emissions in Europe are linked to road transportation, with passenger vehicles playing a major role [39]. The expansion in transportation demand has contributed to the fact that, despite recent technology advancements and emission standard laws, road transport emission reductions have been less significant than initially projected [39]. Diesel car use has been linked to an increase in some pollutants, including nitrogen oxides (NOx) [41]. Additionally, many individuals choose sport utility vehicles, or SUVs, which are bigger and less fuel-efficient, according to the International Energy Agency [42]. According to the European Environment Agency (EEA), average CO_2 emissions from recently registered passenger automobiles in the European Union (EU) climbed yet again in 2019 [42].

Moreover, it has been noted that plug-in hybrid vehicles are becoming more and more popular in demand for electric vehicles, while 100% electric vehicles are losing ground.

Plug-in hybrid electric vehicles' (PHEV) emissions are 28 to 89% higher than claimed, even under ideal test settings [42]. Hybrid electric vehicles (HEV) made up 6% of newly registered cars and more than 55% of alternatively powered vehicles marketed in the EU in 2019 [43].

In total, excessive vehicle tailpipe emissions were linked to about 40,000 deaths worldwide in 2015, including 10% of all ozone-related premature deaths in the EU [44]. As a result, the impact of road transportation on the environment and human health is still significant.

The development of cooperative intelligent transport systems (C-ITS) and the gradual entrance of vehicles with increasing autonomy levels will result in significant change for the transportation industry. These technologies are expected to improve the efficiency of the transportation system and decrease human error [45], [46]. At some point, automated operational and strategic mechanisms can be put into place to minimize harmful environmental effects by controlling the nearby conventional cars (CVs). Since connected and automated vehicles (CAVs) will definitely coexist on the road with conventional cars (CVs) for a significant period of time, it is appropriate to investigate the potential network-wide effects of various market penetration rates (MPRs) of CAVs [47].

Connected and automated vehicles (CAVs') potential effects on the environment are presently unclear. Little is known about how CAV operation behavior affects network traffic, including conventional vehicles, in terms of environmental performance (CVs). On [48], the operation of CAVs in Motorway, Rural, and Urban Road segments of a medium-sized European city was modelled using a microscopic traffic and emission modeling platform, assuming various configurations of the car-following model parameters associated with a pre-determined or cooperative adaptative behavior of the CAVs. The main focus was the examination of the effects of CAV operation on the distribution of accelerations, Vehicle Specific Power (VSP) modal distribution, carbon dioxide (CO_2) and nitrogen oxides (NOx) emissions for various road types, and Market Penetration Rates (MPR). According to the results, depending on the driving conditions and type of road, CAV operational behavior may have a positive or negative impact on CV environmental performance. According to the type of route and Market Penetration Rates (MPR), it was estimated that network-wide CO_2 savings can range from 18% to 4% improvements. System NOx could be reduced up to 13%-23% with CAVs' modified driving parameters for MPRs between 10% and 90%.

Economic Development

Vehicles that are fully automated and connected, also known as CAVs, may soon govern the automobile industry. When CAVs are sufficiently reliable and reasonably priced, they will enter markets and cause economic ripples throughout various industries. With software accounting for a larger portion of vehicle value than before, CAVs will eventually play a crucial role in the automotive sector. Vehicle sharing may result in fewer vehicles being purchased each year, but longer travels could result in more vehicle sales. The ability of heavy-truck drivers to complete other tasks or take a break during lengthy trips may reduce freight costs and boost capacity. The use of shared automated vehicle operations

for private transport could replace those of taxis, buses, and other types of public transportation. There will be less need for auto maintenance, traffic police, medical, insurance, and legal services, since there will be fewer collisions and more law-abiding vehicles on the road. CAVs will also result in novel strategies of regulating travel demand, the repositioning of curbside and off-street parking, and significant cost savings from increased productivity brought on by hands-free travel and lower crash-related expenditures for injuries. The predicted economic impact of CAVs, if they eventually take a sizable portion of the automobile sector, is $1.2 trillion, or $3,800 per American citizen annually [49].

2.3 Traffic Fluid

A novel paradigm, called TrafficFluid, has been proposed in [4] in order to study movement control strategies for various type of vehicles and sizes, e.g. cars, vans, trucks etc., in a new road environment. The paradigm proposes the following three principles:

- Lane-free Traffic
- Nudging
- Traffic as an Artificial Fluid

At first, the TrafficFluid concept, as proposed in [4], had two main inventive principles: Lane-free traffic and Nudging. In a lane-free environment, smooth vehicle movement makes vehicle movement strategies for CAVs simpler to develop, safer, and more effective, making it unnecessary to use accident-prone, thus cautious, laterally "discontinuous" displacements to other lanes. Vehicles can be in any lateral position within the road boundaries, thus lifting the lane changing task. Moreover, road space is being fully utilized, unlike lane-based traffic. With the suggested nudge effect, vehicles can push forward vehicles in the form of a "nudging" effect. This idea suggests that slower downstream vehicles may be nudged to make space for faster upstream vehicles to pass. More significantly, nudging has a capacity-increasing and stabilizing influence on traffic flow at a macro level [4], [61].

Moreover, a simulator named TrafficFluid Sim was built as an extension of the Simulation of Urban Mobility (SUMO) simulator, proposed in [40], in order to possess the aforementioned desired characteristics of the TrafficFluid concept. Control inputs and other data are communicated with SUMO via the extension of the open-source codebase of SUMO. Additionally, in [52] a nonlinear Optimal Control Problem (OCP) with state-dependent constraints in a lane-free environment is established and provides the basis for the model in which CAVs will move.

In [60], Lane-free traffic suggests that incremental road widening or narrowing results in a corresponding incremental increase or decrease in capacity. This opens the door to the consideration of real-time internal boundary control on highways and arterials in order to flexibly share the total (both directions) road width and capacity along the two traffic

directions in dependence to the bi-directional demand and traffic conditions, in order to maximize the total (two directions) flow efficiency.

Related work also involves a Deep Reinforcement Learning (DRL) formulation [40], which focuses on the reward function of a lane-free autonomous driving agent. An effective reward function was designed, as the reward model is crucial in determining the overall efficiency of the resulting policy. Different components of reward functions connected to the environment at various information levels were constructed and then they were combined and collated to the existing components with main concern to reduce the collisions among vehicles and address their requirement of maintaining a desired speed. Additionally, two well-known DRL algorithms: deep Q-networks (improved with several commonly used extensions) and deep deterministic policy gradient (DDPG), are applied, leading to better policies. As a conclusion made in this study [40], it is confirmed that the DRL-employing autonomous vehicle is capable of gradually learning effective policies in environments with a range of levels of difficulty, especially when all of the proposed rewards components are properly combined. A thorough investigation into the effectiveness of various combinations among the various reward components proposed, is also proposed.

2.3.1 Lane-Free Traffic

Till a few decades ago, there was no need for road lanes, since transportation activity and road utilization were low. To reduce the risk of case of accidents and crashes, roads and highways had to be marked with lane markings to separate opposite traffic directions, when cars started to get widely used in the early 20th century. However, dashed lines, which separate parallel lanes on the same traffic direction, weren't adopted until the 1950s along with the regulations governing lane changing. Parallel lanes improve traffic safety since they make manual driving simpler for human drivers. When driving in a lane, a driver basically only needs to keep an eye on the front vehicle's distance from him and speed, and not to the left, right, or back sides. However, when a driver wants to switch lanes, things become more challenging, since it must be done while paying attention to the distance towards the vehicle in front and searching for an open space on the target lane and predicting its expansion based on observed speeds of multiple vehicles (including his own). The task of changing lanes becomes considerably harder, when there are frequent lane changes brought on by lane dips or merging on-ramps or roads. In fact, 10% of accidents are caused by lane changes [11]. In conclusion, unidirectional lanes are essential in manual driving situations, because they promote safety; yet, the requirement for lanes requires lane-changing, which is known to be an accident-prone maneuver.

American interstate highways have lanes that are 3.7 meters wide, while German automobiles have lanes that are 3.5 to 3.75 meters wide. Given that a truck is roughly 2.5 m wide, and a medium-sized automobile is roughly 1.8 m, we come to the conclusion that the lateral utilization on motorways may only be somewhat more than 50%. Consequently,

even if only a portion of the available lateral space is occupied, as with lane-free traffic, the roadway capacity could be significantly enhanced. Extra capacity losses result from dynamic phenomena linked to lane-changing maneuvers, in addition to the static capacity loss brought on by the need for broad lanes on high-speed roads and arterials with manual driving.

In summary, unidirectional traffic lanes appeared in the middle of the twentieth century as a crucial measure for ensuring traffic safety, when driving manually, even at the expense of lowering the highway's capacity. According to the TrafficFluid concept, there is no need to mimic the human lane-based driving task in the era of high-level vehicle automation and connectivity (in fact, there are solid reasons to avoid imitation, as well). Vehicle sensors and communications allow connected and automated vehicles (CAVs) to monitor their immediate (and even further away) surroundings quickly, simultaneously, continuously, and reliably, and to make quick (computer-based) driving decisions. Based on proper movement strategies, a CAV can "float" securely and effectively in a stream of other, potentially collaborating, CAVs thanks to these phenomenally expanded capabilities compared to human driving. As a result, lane-free highways, motorways, arterials, and even urban roads may return, regaining lost capacity and improving traffic safety. Smooth 2-D vehicle movement makes it easier, safer, and more efficient to develop vehicle movement strategies for CAVs in a lane-free environment. And as a result, makes it unnecessary to use accident-prone, hence conservative, laterally "discontinuous" displacements to other lanes. Furthermore, front-back vehicle crashes, which may involve dozens of vehicles in a traffic accident and occur in manual lane-based driving, may result in more severe damage than their counterpart side-side incidents, which are more likely to happen in lane-free traffic.

In a lane-free environment, vehicle movement patterns that are met may differ depending on the infrastructure or other vehicles (such as EmV's). The notion of allowing a small number of manually controlled vehicles raises an interesting challenge, one that would necessitate the CAV moving around them activating a unique movement plan [3].

2.3.2 Nudging

The property of anisotropy in macroscopic traffic flow models is a significant and perhaps "sacred" principle in traffic flow theory [50], [1], [2]. The groundwork for macroscopic traffic flow theory was established by the seminal paper [2], which compared the movement of traffic in open channels to that of water.

In fact, the qualitative characteristics of vehicular traffic are very similar to those of gas in a pipe or water flow in an open channel. Like water flow, traffic states propagate as waves with a speed different from the speed of the fluid particles, and shock waves form when fast vehicles overtake slower vehicles in front [3].

Adversely, there is a significant difference between the flow of water or gas and the flow of vehicular traffic. The movement of a vehicle, as prompted by a human driver, is typically

unlikely to be affected by what happens behind it. For example, fast particles may be "pushing" slower particles ahead, causing them to accelerate. In contrast, water or gas flow particles may influence the movement of other downstream particles. The anisotropic aspect of traffic flow, which refers to the notion that drivers only respond to forehead inputs, has some mathematical implications, such as the fact that traffic waves cannot move more quickly than moving vehicles [50].

Without the anisotropic restriction given by human driving, the proposed nudge effect allows for the deliberate conception of vehicular traffic flow in a variety of possible ways to achieve the necessary design goals, such as increasing the flow and the road capacity.

In Figure 2.3, the results of four series of simulations were run, with each series being condensed into a fundamental diagram (FD) that shows stationary flow (veh/h) vs. density (veh/km) for that series. As the goal is to maintain high flow at high density, having points near the upper-right part of a Fundamental Diagram indicates better performance compared to points in the other parts. The first simulation has no nudging forces applied, the second and third have weaker and stronger nudging applied, and the fourth has the same conditions as the third, but with a wider road, that is additionally 1.7 m wide, or additionally half the width of a typical motorway lane.

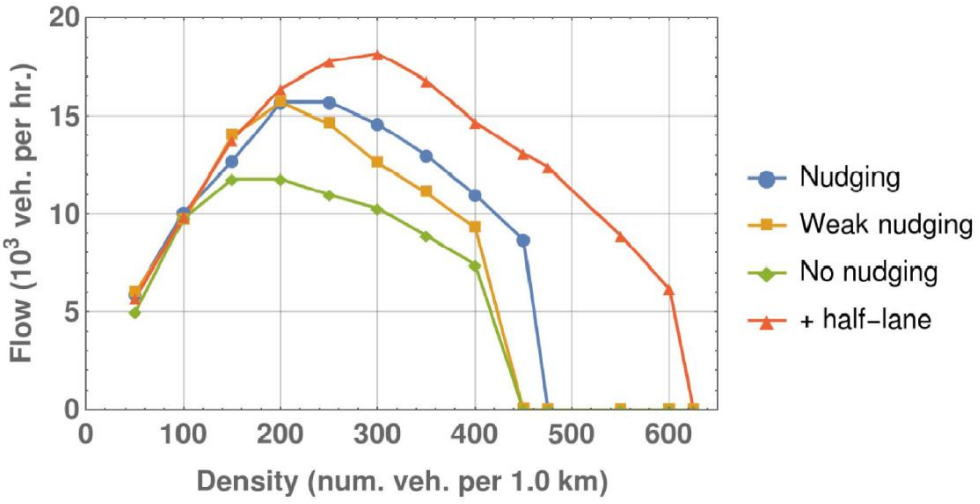

Figure 2. 3: Emerging flow-density curves (fundamental diagrams) for various simulated scenarios (Source: [3])

The summarized simulation results prove that:

1. Nudging increases the flows and the capacity.
2. The lane-free traffic feature is mainly responsible for the achieved flows and capacity, which are significantly higher than those typically recorded on a standard three-lane highway.
3. Enlarging the road (by half “lane”) brings an additional increase in flow and capacity. Surprisingly, the observed capacity increase is roughly proportional to the widening of the road.

The details of the movement control strategy and simulation are provided in [4].

2.3.3 Traffic as an Artificial Fluid

According to TrafficFluid, the development of automated vehicle movement strategies ought not be based on the history of human driving, but rather should be detached from pointless constraints like lane discipline and consideration of downstream conditions that have an impact on traffic flow effectiveness and safety. Vehicle nudging and lane-free flow provide the opportunity to design (rather than describe or model) the traffic flow characteristics in an ideal manner, under constraints, but without the need to satisfy anisotropy or other conditions originating from the era of human driving. In essence, we face the challenge of defining the characteristics of the traffic flow as an artificial fluid for the first time, since the advent of the automobile, and this is in fact the main idea behind the TrafficFluid concept [4].

The basic requirements for a practical implementation of the suggested concept are low. Given that vehicle motions, including the lateral component, may be smooth, the necessary movement strategy at the vehicle level should be simpler to develop than current automated vehicle lane-based driving (including lane change) techniques (no abrupt lane-changing is required).

There are no necessary requirements that go beyond the CAVs' current equipment or plans in terms of onboard sensors and connection (V2V and V2I). Finally, TrafficFluid does not require the addition of novel or expensive new features to the road system.

Instead of needing to extend traditional highways by lane "quanta" in order to enhance their capacity, the TrafficFluid concept leads to gradual capacity increases, because of the road's lane-free character.

Therefore, a minimal percentage of road widening around problematic bottleneck regions (such as on-ramps, strong upgrades, or curves) might be enough to solve the local capacity issues which cause congestion in regular traffic [4].

2.4 The Theory of Discrete -Time Optimal Control

The optimal control theory was developed in the 1960s for both continuous and discrete time systems. Different applications of optimal control in various technical fields have been documented, particularly in the fields of robotics, transportation, and space technology.

2.4.1 Problem Formulation

A discrete-time dynamic process described by the following set of difference equations organized in vector form is considered in vector form:

$$\boldsymbol{x}(k+1) = \boldsymbol{f}[\boldsymbol{x}(k), \boldsymbol{u}(k), k], k = 0, \dots K-1 \qquad (2.1)$$

where $\boldsymbol{x} \in R^n$ is the system state variable vector and $\boldsymbol{u} \in R^m$ is the control variable vector. And $\boldsymbol{f} \in R^n$ is a twice continuous differentiable vector function. Additionally, $\cdot(k)$ denotes the value of the corresponding variable at time $t = kT$, where T is the sample time interval, and k is the discrete time index, and K (or $K \cdot T$) is the fixed time horizon. The system has a known initial state

$$\boldsymbol{x}(0) = \boldsymbol{x}_0 \tag{2.2}$$

The problem is formulated as a constrained optimization problem in [52] with the following objective function to be minimized

$$J = \theta[\mathbf{x}(K)] + \sum_{\mathrm{k=o}}^{K-1} \{\phi[\boldsymbol{x}(k), \boldsymbol{u}(k), k]\} \tag{2.3}$$

subject to (2.1), (2.2) the constraints:

$$\boldsymbol{h}[\boldsymbol{x}(k), \boldsymbol{u}(k), k] \leq 0, \ k = 0, \dots, K-1 \tag{2.4}$$

where $\theta, \phi, \mathbf{h}, \in R^q$ are twice continuous differentiable functions. The final state may be free or may be required to satisfy a final condition and the final condition:

$$\boldsymbol{g}[\boldsymbol{x}(K)] = \mathbf{0} \tag{2.5}$$

$\boldsymbol{g} \in \mathbb{R}^l, l \leq n$, is a twice continuous differentiable vector function.

Although expressing a dynamic physical procedure, the above formulated problem is, from a mathematical point of view, a static optimization problem due to the discrete time nature of the involved process model.

It is necessary to define the vectors:

$$\boldsymbol{X} = [\boldsymbol{x}(1)^T \dots \boldsymbol{x}(K)^T]^T$$

$$\boldsymbol{U} = [\boldsymbol{u}(1)^T \dots \boldsymbol{u}(K)^T]^T$$

The discrete-time optimal control problem may be expressed in terms of optimization as:

$Minimize\ \Phi(\boldsymbol{X}, \boldsymbol{U})$

subject to

$\boldsymbol{F}(\boldsymbol{X}, \boldsymbol{U} = \mathbf{0}), \boldsymbol{H}(\boldsymbol{x}, \boldsymbol{U}) \leq \mathbf{0}$

where Φ expresses the discrete time cost function (2.3) , $\boldsymbol{H}$ the inequality constraints and $\boldsymbol{F}$ the state equation (2.1) for all $k \in [0, K-1]$ and the terminal condition (2.5).

2.4.2 Optimality Conditions

To derive the optimality conditions, the Lagrangian Function for this problem is constructed:

$$L[\boldsymbol{x}(k), \boldsymbol{u}(k), \boldsymbol{\lambda}(k), \boldsymbol{\mu}(k), v, k] = \theta[\boldsymbol{x}(K)] + \sum_{k=0}^{K-1} \phi[\boldsymbol{x}(k), \boldsymbol{u}(k), k] + \sum_{k=0}^{K-1} \{\boldsymbol{\lambda}(k+1)^T [f[\boldsymbol{x}(k), \boldsymbol{u}(k), k]] + \boldsymbol{\mu}(k)^T \boldsymbol{h}[\boldsymbol{x}(k), \boldsymbol{u}, k]\} + \boldsymbol{v}^T \boldsymbol{g}[x(K)] \quad (2.6)$$

The following components comprise the Lagrangian Function: Where $\boldsymbol{\lambda}(k+1) \in R^n$ and $\boldsymbol{\mu}(k) \in R^q, k = 0, \dots, K-1$ are **Lagrange** and **Kuhn-Tucker** multipliers, respectively, for the corresponding equality and inequality conditions.

$$\boldsymbol{\Lambda} = [\boldsymbol{\lambda}(\mathbf{1})^T \dots \boldsymbol{\lambda}(\boldsymbol{K})^T \boldsymbol{v}^T], \quad \boldsymbol{M} = [\boldsymbol{\mu}(\mathbf{0})^T \dots \boldsymbol{\mu}(K-1)^T]^T$$

In more comprehensive from, equation (2.6) can be written:

$$L[\boldsymbol{x}(k), \boldsymbol{u}(k), \boldsymbol{\lambda}(k), \boldsymbol{\mu}(k), v, k] = \Phi(\boldsymbol{X}, \boldsymbol{U}) + \boldsymbol{\Lambda}^T \boldsymbol{F}(\boldsymbol{X}, \boldsymbol{U}) + \boldsymbol{M}^T \boldsymbol{H}(\boldsymbol{X}, \boldsymbol{U})$$

The multipliers $\mathbf{v} \in \mathbb{R}^l$ are assigned to the final condition (2.5). Applying the necessary conditions of optimality, i.e.

$$\frac{dL}{d\boldsymbol{X}} = 0, \qquad \frac{dL}{d\boldsymbol{U}} = 0, \qquad \frac{dL}{d\boldsymbol{\Lambda}} = 0, \quad \boldsymbol{H}(\boldsymbol{X}, \boldsymbol{U}) \leq \mathbf{0}, \qquad \boldsymbol{H}^T M = 0, \quad M \geq 0 \qquad (2.7)$$

We derive the necessary conditions of optimality for the discrete-time optimal control problem. These conditions are usually expressed in terms of the -extended- **Hamiltonian Function** as described below.

$$H[\boldsymbol{x}(k), \boldsymbol{u}, \boldsymbol{\lambda}(k), k] = \phi[\boldsymbol{x}(k), \boldsymbol{u}(k)] + \boldsymbol{\lambda}(k+1)^T \boldsymbol{f}[\boldsymbol{x}(k), \boldsymbol{u}(k), k] \qquad (2.8)$$

The **extended** discrete-time Hamiltonian is also defined

$$\widetilde{H}[\boldsymbol{x}(k),\boldsymbol{u}(k),\boldsymbol{\lambda}(k),\boldsymbol{\mu}(k),k] = \phi[\boldsymbol{x}(k),\boldsymbol{u}(k),k] + \boldsymbol{\lambda}(k+1)^T\boldsymbol{f}[\boldsymbol{x}(k),\boldsymbol{u}(k),k] + \boldsymbol{\mu}(k)^T\boldsymbol{h}[\boldsymbol{x}(k),\boldsymbol{u}(k),k] \tag{2.9}$$

In which exist multipliers $\boldsymbol{v}$ and $\boldsymbol{\lambda}(k+1)$, $\boldsymbol{\mu}(k)$, $k = 0,\dots,K-1$, such that the following equations are satisfied for $k = 0,\dots,K-1$ (notation: $x_y = dx/dy$):

$$\boldsymbol{x}(k+1) = \widetilde{H}_{\lambda(k+1)} = \boldsymbol{f}[\boldsymbol{x}(k),\boldsymbol{u}(k),k] \tag{2.10}$$

$$\boldsymbol{\lambda}(k) = \widetilde{H}_{x(k)} = \phi_{\boldsymbol{x}(k)} + \boldsymbol{f}_{\boldsymbol{x}(k)}^T\,\boldsymbol{\lambda}(k+1) + \boldsymbol{h}_{x(k)}^T\boldsymbol{\mu}(k) \tag{2.11}$$

$$\widetilde{H}_{\boldsymbol{u}(k)} = \phi_{\boldsymbol{u}(k)} + \boldsymbol{f}_{\boldsymbol{u}(k)}^{\boldsymbol{T}}\,\boldsymbol{\lambda}(k+1) + \boldsymbol{h}_{\boldsymbol{u}(k)}^T\boldsymbol{\mu}(k) = 0 \tag{2.12}$$

$$\boldsymbol{\mu}(k)^T\boldsymbol{h}[\boldsymbol{x}(k),\boldsymbol{u}(k),k] = 0 \tag{2.13}$$

$$\boldsymbol{\mu} \geq 0 \tag{2.14}$$

$$\boldsymbol{h}[\boldsymbol{x}(k),\boldsymbol{u}(k),k] \leq 0 \tag{2.15}$$

In addition, the boundary and transversality conditions must be satisfied:

$$\boldsymbol{x}(0) = \boldsymbol{x}_0 \tag{2.16}$$

$$\boldsymbol{g}[\boldsymbol{x}(K)] = 0 \tag{2.17}$$

$$\boldsymbol{\lambda}(K) = \theta_{x(K)} + \boldsymbol{g}_{x(K)}^T\boldsymbol{v} \tag{2.18}$$

Equations are called the state and costate difference equations respectively, and together consist of the system of canonical difference equations of the problem.

2.4.3 State-Dependent Control Bounds

The state-dependent control bounds are of the form:

$$\boldsymbol{u}_{min}(\boldsymbol{x}(k),k) \leq \boldsymbol{u}(k) \leq \boldsymbol{u}_{max}(\boldsymbol{x}(k),k) \tag{2.19}$$

where $\boldsymbol{u}_{min}(\boldsymbol{x}(k),k)$ and $\boldsymbol{u}_{max}(\boldsymbol{x}(k),k)$ are twice continuously differentiable functions. The equations in the form of (2.4) may be reduced to (2.19) if the state equation is of the form of (2.2). By replacing x from the state equation in the inequality constraint and by resolving for $u(k)$, if possible, the state-dependent control bound is obtained. However, the state dependence of the bounds, needs some further measures to guarantee fulfillment of the necessary optimality conditions. By writing the equation (2.19) as:

$$h[\boldsymbol{x}(k), u(k), k] = [\boldsymbol{u}(k) - \boldsymbol{u}_{max}(\boldsymbol{x}(k), k)\,][\boldsymbol{u}(k) - \boldsymbol{u}_{min}(\boldsymbol{x}(k), k)\,] \leq 0 \tag{2.20}$$

following two equations are derived:

$$\frac{\partial \boldsymbol{h}}{\partial \boldsymbol{x}} \neq 0 \tag{2.21}$$

$$\frac{\partial h}{\partial u(k)} = 2u(k) - u_{max}(x(k), k) - \; u_{min}(\boldsymbol{x}(k), k) \tag{2.22}$$

3

Path Planning for CAVs

In the present chapter the formulation of the problem is presented with all its constraints, such as the objective function, and the OCP solution as proposed in [52]. The problem's kinematics and constraints will be described in Section 3.1 while the Optimal Control Problem and its solution as formed in [52] are described in Section 3.2. This chapter will first review existing work that will subsequently be used for the current thesis. Firstly, the paper referred in [55] establishes a nonlinear Optimal Control Problem (OCP) with state-dependent constraints in a lane-free environment and provides the basis for the model in which CAVs move. On the existing model, special cases or vehicles with different characteristics were added in order to create different scenarios and test the adjustment of the environment to the entering of an EmV. Moreover, a lateral positioning strategy as proposed in [56], is utilized in order to give the EmV the tendency to reach a prespecified lateral position.

3.1 Problem formulation

3.1.1 Kinematics and Constraints

The problem consists of a dynamic model with an objective function that must be minimized under certain constraints to achieve certain qualities, such as moving smoothly in a lane-free environment without colliding with neighbor vehicles. Four equations, two in the longitudinal direction and two in the lateral direction, are used to describe each vehicle. The so-called *state equations* are derived from the kinematics rules.

The following equations are obtained by taking into account a 2-D plane and discrete time:

For the q^{th} vehicle, the state equations are the following in optimization form:

$$x_1^q(k\ +\ 1) =\ x_1^q(k) +\ Tx_3^q(k) + \frac{1}{2}T^2u_1^q(k) \quad (3.1(a))$$

$$x_3^q(k\ +\ 1) =\ x_3^q(k) +\ Tu_1^q(k) \quad (3.1(b))$$

$$x_2^q(k+1) =\ x_2^q(k) +\ Tx_4^q(k) + \frac{1}{2}T^2\ u_2^q(k) \quad (3.1(c))$$

$$x_4^q(k\ +\ 1) =\ x_4^q(k) +\ Tu_2^q(k) \quad (3.1(d))$$

According to state equation (3.1), the state variables $x_1^q, x_2^q, x_3^q, x_4^q$ stand for longitudinal position, lateral position, longitudinal speed, and lateral speed, respectively, while the control inputs u_1^q, u_2^q represent the longitudinal and lateral accelerations, respectively.

The time step, or interval duration variable T, is related to discrete time through the formula $t\ =\ kT$, where k is the discrete time index. The parameters of an automobile are shown in a 2-D plane in Figure 3.1 while, path generation is provided for every vehicle, for every time horizon. The route is determined by the upcoming routes of nearby cars, which is feasible under the condition that vehicles communicate with each other via V2V communications.

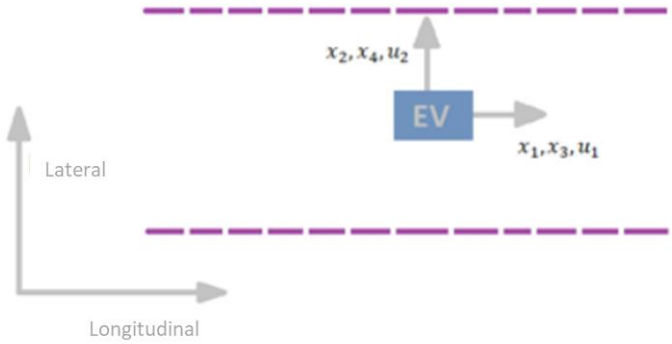

Figure 3. 1: Ego Vehicle (EV) Kinematics

The limitations of this issue revolve around avoiding negative longitudinal speeds, cross-directional collisions, and route deviations. These constraints are provided as state-dependent equations in an inequality form on accelerations.

The following equation provides the general form for the q^{th} vehicle in the longitudinal direction:

$$u_{min1}^q(k) \leq\ u_1^q(k) \leq\ u_{max1}^q(k) \quad (3.2)$$

For the lower limit, it is assumed that the longitudinal speed is non-negative in the time $k+1$, i.e. $x_4^q(k+1) \geq 0$. By replacing the equation (3.1(d)) in (3.2) , the following equation is derived:

$$u_1^q(k) \geq -\frac{1}{T} x_3^{q(k)} \tag{3.3}$$

and hence the state-dependent lower limit is: $U_{min1}^q(k) = \frac{1}{T} x_3^q(k)$. However, due to constrained deceleration capabilities of the vehicle, a constant lower limit is also assumed: U_{min1}^q. Consequently, the lower limit might take values in:

$$u_{min1}^q(k) = max\,[U_{min1}^q(k), U_{min1}^q] \tag{3.4}$$

due to the vehicle's constrained acceleration capabilities, a constant upper limitation U_{max1}^q is determined with respect to the upper limit for the longitudinal control bound. The state-dependent constraint for the upper limit, on the other hand, is only applied in exceptional conditions, which are typically when the OCP returns a collision. If a collision is found, the state-dependent bound becomes active. To prevent a collision with the vehicle in front, a longitudinal position restriction is set; the ego vehicle must not cross such limit at the $k+2$ time-step. The position limit $\hat{x}_1^q$ can be expressed as follows and has the same meaning as in equation (3.1):

$$\hat{x}_1^q(k+1) = \hat{x}_1^q(k) + T\,\hat{x}_3^q + \frac{1}{2}T^2\hat{u}_1^q \tag{3.5}$$

$$\hat{x}_3^q(k+1) = \hat{x}_3^q + T^2\hat{u}_1^q(k) \tag{3.6}$$

Consider the following dynamics for the moving boundary in the form of state equations, where all $\hat{}$ variables have similar meanings as in equation (3.1).

Hence, the condition of non-collision is given by the following equation:

$$x_1^q(k+2) \leq \hat{x}_1^q(k+2) \tag{3.7}$$

If the EV reaches the moving boundary and constraint (3.7) is activated, then ego vehicle should have its longitudinal speed equal the speed of the moving boundary [52]:

$$x_3^q(k+2) = \hat{x}_3^q(k+2) \tag{3.8}$$

By replacing in the (3.1(a)), (3.1(b)), (3.6), where $k = k+2$, we obtain:

$$x_1^q(k+2) = x_1^q(k+1) + Tx_3^q(k+1) + \frac{1}{2}T^2u_1^q(k+1) \tag{3.9}$$

$$\hat{x}_1^q(k+2) = \hat{x}_1^q(k+1) + T\hat{x}_3^q(k+1) + \frac{1}{2}T^2\hat{u}_1^q(k+1) \tag{3.10}$$

Subtracting equations (3.9) and (3.10) (3.10)
we have the following rearrangements:

$$0 = x_1^q(k+1) + Tx_3^q(k+1) + \frac{1}{2}T^2u_1^q(k+1) - \hat{x}_1^q(k+1) - T\hat{x}_3^q(k+1) - \frac{1}{2}T^2\hat{u}_1^q(k+1) \quad (3.11)$$

By replacing, where $x_1^q(k+1)$ and $\hat{x}_1^q(k+1)$ their formula from the state equation respectively, equation (3.11) can be reduced to:

$$0 = x_1^q(k) - \hat{x}_1^q(k) + 2T\left[x_3^q(k) - \hat{x}_3^q(k)\right] + \frac{3}{2}T^2\left[u_1^q(k) - \hat{u}_1^q(k)\right] + \frac{1}{2}T^2[u_1^q(k+1) - \hat{u}_1^q(k+1)] \quad (3.12)$$

Finally, by using equation (3.8) and solving for $u_1^q(k)$ occurs:

$$u_1^q(\mathrm{k}) \leq -\frac{1}{T^2}\left[x_1^q(k) - \widehat{x_1^q}(k)\right] - \frac{3}{2\mathrm{T}}\left[x_3^q(k) - \widehat{x_3^q}(k)\right] + \widehat{u_1^q}(k) \quad (3.13)$$

To lead the vehicle in exactly two timesteps to the moving boundaries, the right-hand side of equation (3.13) can be viewed as a dead-beat controller. The amplitude of the longitudinal acceleration can be correctly selected by some feedback gain, and (3.13) can then be replaced by the maximum control input in the longitudinal direction to prevent this situation:

$$u_{max1}^q(k) = -K_{long1}e_1^{q(k)} - K_{long2}\,e_2^q(k) + \widehat{u_1^q}(k) \quad (3.14)$$

where, $K_{long1} \in (0, \frac{T^2}{2}]$, $K_{long2} \in (0, \frac{3}{2T}]$ and e_1^q, e_2^q are the tracking errors.

When the limit is activated, the gain values of K_{long1} and K_{long2} must be chosen to achieve aperiodic tracking. After various arrangements and using the equations (3.1 (a)), (3.1(c)) and (3.14) the following occurs in matrix form:

$$\begin{bmatrix} e_1^q(k+1) \\ e_2^q(k+1) \end{bmatrix} = \begin{bmatrix} 1 - \frac{1}{2}T^2\,K_{long1} & T - \frac{1}{2}T^2K_{long2} \\ TK_{long1} & 1 - T^2K_{long2} \end{bmatrix} \begin{bmatrix} e_1^q(k) \\ e_2^q(k) \end{bmatrix} \quad (3.15)$$

To ensure stability and aperiodic behavior, the characteristic equation's roots must be in a unit circle, and be non-negative real. To keep the design process simple and to allow the roots to be non-negative and similar, we choose

$$K_{long2} = 2\sqrt{K_{long1}} - K_{long1}\frac{T}{2}$$

Summing up, the upper limit can take two values:

$u^q_{max1}(k) = U_{max1}$ or $u^q_{max1}(k) = U_{max1}(k)$ for normal or collision situations, respectively.

The vehicle must follow the lateral road boundaries or travel on a road boundary in accordance with the lateral limits.

To prevent collision in the lateral direction, a hypothetical barrier is also constructed, similar to that for the longitudinal direction. First, in the $k + 2$ time step, the ego car must keep within the limits of the road. The acceleration gets smoother when we look at its behavior two time- steps in advance, hence the $k + 2$ time step is utilized. The lateral position is therefore bounded by equation (3.16), where $\tilde{x}^q_2$ refers to the half of the vehicle's width ($W_v/2$) and the $\hat{x}^q_2$ refers to the road width minus half of the ego vehicle's width ($W_r - W_v/2$).

$$\tilde{x}^q_2(k + 2) \leq x^q_2(k + 2) \leq \hat{x}^q_2(k + 2) \qquad (3.16)$$

The lateral speed of the ego vehicle must be zero if it stays on the left or right side of the road boundary, i.e. $x^q_4(k + 2) = 0$. From the state equation derives that :

$$x^q_4(k + 1) + Tu^q_2(k + 1) = 0.$$

After rearrangements and replacements in (3.1(c)) and (3.1(d)), where k = k + 1, we conclude that:

$$\begin{aligned} x^q_2(k + 1) &= x^q_2(k) + Tx^q_4(k) + \frac{1}{2}T^2 u^q_2(k) \rightarrow x^q_2(k + 2) \\ &= x^q_2(k + 1) + Tx^q_4(k + 1) + \frac{1}{2}T^2 u^q_2(k + 1) \end{aligned} \qquad (3.17)$$

$$x^q_4(k + 1) = x^q_4(k) + \frac{1}{2}Tu^q_2 \rightarrow x^q_4(k + 2) = x^q_4(k + 1) + Tu^q_2(k + 1) = 0 \qquad (3.18)$$

By replacing $x^q_2(k + 1)$ with the state equation in (3.17)
we obtain:

$$x^q_2(k + 2) = x^q_2(k) + 2Tx^q_4(k) + \frac{3}{2}T^2 u^q_2(k) + \frac{1}{2}T^2 u^q_2(k + 1) \qquad (3.19)$$

By replacing $u_2^q\ (k+1)$ in (3.19) with the equation (3.18) we obtain:

$$x_2^q(k\ +\ 2) =\ x_2^q(k) + \frac{3}{2} T x_4^q(k) T^2 u_2^q(k) \qquad (3.20)$$

Finally, by replacing the above equation in inequality (3.16), we obtain the state-dependent constraint:

$$-\frac{1}{T^2}\left[x_2^q(k) - \tilde{x}_2^q(k\ +\ 2)\right] - \frac{3}{2T}\ x_4^q(k) \leq\ u_2^{q(k)} \leq -\frac{1}{T^2}\left[x_2^q\ (k) - \hat{x}_2^q(k\ +\ 2)\right] - \frac{3}{2T}\ x_4^q(k) \qquad (3.21)$$

If (3.22)is considered an equality, then it acts similarly on the longitudinal direction with the lateral direction and can guide the ego vehicle to the road boundary in exactly two timesteps. Additionally, the magnitudes brought on by lateral accelerations may lead to passenger discomfort due to high values. This causes the lateral "controller" to remain smoother, get the vehicle asymptotically within the road boundaries and is given by the equation: $K_{lat2}\ =\ 2\sqrt{K_{lat1}} - K_{lat1}\frac{T}{2}$.

$$U_{min2}^q(x_2(k), x_4^q(k))\ =\ -K_{lat1}[x_2^q(k) -\ \tilde{x}_2^q(k)] -\ K_{lat2} x_4^q(k) \qquad (3.22)$$

$$U_{max2}^q(x_2^q(k), x_4^q(k))\ =\ -K_{lat1}[x_2^q(k) -\ \hat{x}_2^q(k)] -\ K_{lat2} x_4^q(k) \qquad (3.23)$$

where $K_{lat1} \in$ (o, $\frac{1}{T^2}$] and $K_{lat2} \in$ (o, $\frac{3}{2T}$].

Inferentially, equations (3.22),(3.22)can be used either for keeping the Ego Vehicle within the road boundaries or in emergency situations, for preventing the ego vehicle to have a lateral crash with an obstacle.

Since the ego car and an obstruction are preventing a lateral crash, equation (3.22) can be applied both to remaining within the bounds of the road and to emergency situations.

So, lower and higher limits are determined as:

$u_{min2}^q(k)\ =\ U_{min2}^q(k)$ and $u_{max2}^q(k)\ =\ U_{max2}^q(k)$, accordingly.

Concluding, the following state-dependent constraints can be used to represent the longitudinal and lateral control bounds as shown in (3.4),(3.14)

(3.14), (3.22), and (3.23):

$$h_1^q =\ \left[u_1^q(k) -\ u_{max1}^q(k)\right]\left[u_1^q(k) -\ u_{min1}^q(k)\right] \leq\ 0 \qquad (3.23\ (a))$$

$$h_2^q =\ \left[u_2^q(k) -\ u_{max2}^q(k)\right]\left[u_2^q(k) -\ u_{min2}^q(k)\right] \leq\ 0 \qquad (3.24\ (b))$$

3.1.2 Objective Function

The objective function [2.3] to be minimized consists of five sub-objectives that engage: fuel economy, passenger comfort, achieving target speeds, avoiding obstacles, and coupling longitudinal and lateral speeds. Those are illustrated in Figure 3. 2.

Fuel Consumption and Passenger Comfort

Fuel consumption improvement contributes to environmentally friendly CAV traffic and hence reduced emissions. As shown in [22], this is accomplished using a longitudinal acceleration cost term $\left(u_1(k)\right)^2$. Additionally, the moderate and smooth accelerations given by the quadratic cost terms of longitudinal and lateral accelerations $u_1(k)^2$ and $u_2(k)^2$, respectively, improve passenger comfort.

$$u_1^q(k)^2 + u_2^q(k)^2 \tag{3.24}$$

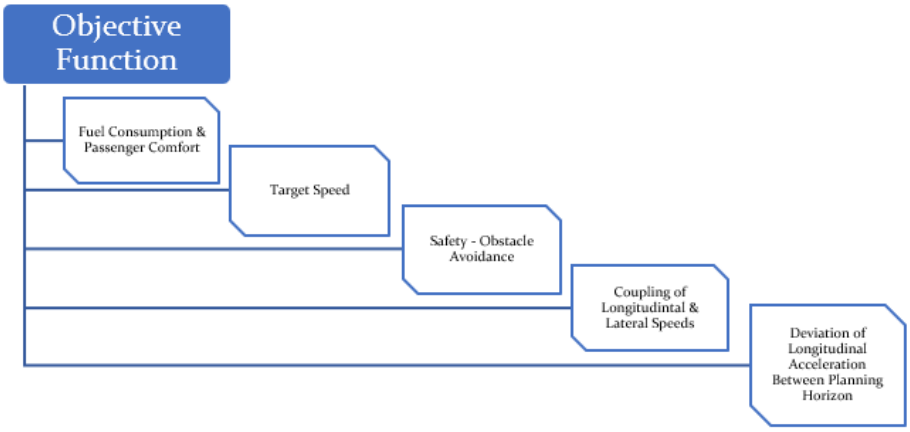

Figure 3. 2: Objective Function Components

Desired Speed

For a vehicle to travel and reach an exit, it must reach the appropriate speeds in both the longitudinal and lateral directions. This study takes an unfolded ring road into consideration, which necessitates a positive longitudinal desired speed and a zero lateral desired speed. The Ego Vehicle (EV) attempts to reach its intended speed because of the quadratic cost term $(x_3^q(k) - v_{d1}^q(k))^2$ with longitudinal goal speed v_{d1}. Passengers travel faster when cars are moving close to their desired speeds. To mitigate lateral movement, the quadratic cost term $(x_4^q(k) - v_{d2}^q(k))^2$ is used, where $v_{d2} = 0$ is the lateral ideal speed. Unnecessary lateral movements might affect traffic efficiency.

$$\left(x_3^q(k) - v_{d1}^q(k)\right)^2 + \left(x_4^q(k) - v_{d2}^q(k)\right)^2 \tag{3.25}$$

Obstacle Avoidance

One of the most important requirements that must be reflected in a designed sub-objective is collision avoidance with other vehicles. Appropriate consideration of the novel aspects stemming from the lane-free vehicle movement, as well as from the possibility of vehicle nudging is taken into consideration.

It is essential that the EV sensors and V2V communication have access to the current states (position and speed) of vehicles within their Interaction Zone (IZ) in order to avoid collisions, while generating the trajectory of the EV. Each vehicle shares its created path plan to surrounding vehicles. Naturally, the accuracy of short-term predictions of the motion of nearby vehicles may be limited, and this may result in the generation of a different path.

The product of the longitudinal intended speed and the length of the planning horizon determines the length of the interaction zone (IZ) in both the upstream and downstream directions. The constant time-gap (CTG), which uses a linear function of the follower's speed multiplied by a coefficient known as time gap, is employed in the lane-based approach to maintain safe distances between the cars. As proposed in [52], an imaginary positive-valued, smooth, longitudinally and laterally symmetric ellipsoid hemisphere around each obstacle is designed, which determines the cost incurred if the EV is positioned within the ellipsoid range. This cost aims to discourage the EV from intruding the ellipsoid range, i.e., from approaching too closely (or colliding with) with the obstacle. While designing the ellipsoid hemisphere, time-gap like safety parameters ω_1, ω_2 are considered in longitudinal and lateral directions, respectively, along with the obstacle's corresponding physical dimensions.

The position and speed of the i^{th} obstacle among the n obstacles in both directions, as well as the time gap parameters $(\omega_{x1}, \omega_{x2})$, are each being considered.

Assuming there are n obstacles inside the Interaction Zone (IZ), we determine the longitudinal and lateral coordinates (o_{i1}, o_{i2}) and speeds for the i^{th}obstacle (o_{i3}, o_{i4}).

The ellipsoid's length and position (center) in the longitudinal direction must meet the following criteria:

- The ellipsoid should surround completely the physical dimensions of both ego and obstacle vehicles, even at zero speed, when the vehicle is not moving. l_e and l_{oi} are the lengths of the ego and obstacle vehicles, respectively, and μ_x is a coefficient where, L_i is defined as: $L_i = x\ (l_e + l_{oi})$. The length of the longitudinal axis of the ellipsoid is L_i when both ego and obstacle cars are moving at zero speed, hence x makes sure that vehicles are not bumper to bumper at stillstand. The constant time-gap policy dictates that if the EV is positioned behind the obstacle, a safety gap proportional to its current speed should be considered (in addition to L_i).

$$Safety\ Gap = \begin{cases} \omega_{x1} x_3^q, & if\ the\ obstacle\ is\ in\ front\ of\ the\ ego\ vehicle \\ \omega_{x1} o_{i3}, & if\ the\ obstacle\ is\ behind\ the\ ego\ vehicle \end{cases} \quad (3.26)$$

The center of the ellipsoid is set in the longitudinal direction and is affected by the speed difference between the ego vehicle and the obstacle. If the two vehicles are

traveling at the same speed, the ellipse's center will be at the obstacle's center; however, if the two vehicles are traveling at different speeds, the ellipsoid will be moved laterally to satisfy the previous safety gap requirements. So, for the ellipsoid, the longitudinal axis and longitudinal centers are set and positioned, respectively, as follows:

$$s_{d1} = L_i + \omega_{x1} x_3^q + \omega_{x1} o_{i3} \tag{3.27}$$

All mentioned requirements are fulfilled, if the length of the longitudinal ellipsoid axis is equal to $d_1 = Li + \omega_1 x_3 + \omega_1 o_{i3}$, while the ellipsoid's longitudinal center is positioned at

$$\delta_{o1} = o_{i1} - \frac{\left(\omega_{x1}\left(x_3^q - o_{i3}\right)\right)}{2} \tag{3.28}$$

In the lateral direction :

- Laterally, the only case that is taken into consideration is the one where the vehicles are approaching one another. The following equation demonstrates how the safety gap is set in this direction to prevent collision:

$$Safety\ Gap = \begin{cases} \omega_{x2} |x_4^q - o_{i4}|, & if\ vehicles\ approach\ each\ other \\ 0, & otherwise \end{cases} \tag{3.29}$$

The center of the obstacle and the midpoint of the ellipsis coincide in the lateral direction; however, the center's positioning in the lateral direction should be defined in terms of the following features:

$$d_2 = W_1 + \omega_2 \left[tanh(o_{i2} - x_2)\,(x_4 - o_{i4}) + \sqrt{[tanh(o_{i2} = x_2)(x_4 - o_{i4})]^2} + \varepsilon_\omega\right] \tag{3.30}$$

where $W_i = \mu_y(w_e + w_{oi})$ with the w_e and w_{oi} being the widths of ego vehicles and obstacles, ϵ_ω being a small number for safety distance, and μ_y being a coefficient, slightly greater than 1, which ensures that the corners of the (rectangular) obstacle are sufficiently covered.

The ellipsoid's function penalizes vehicle approach and acts as a collision avoidance term in the objective function. The ellipsoid function should also meet two other

crucial criteria. To allow the rapid ego vehicles to slide around the slower obstacles in front of them, the form of the ellipsoid should first cover the corners of the obstacle and be sufficiently curved. In order for the ellipsoid's gradient to extend sufficiently far from zero, it must be sufficiently steep in the three-dimensional plane. Considering these extra constraints, the ellipsoid has the following form:

$$c_i\,(\boldsymbol{x}, \boldsymbol{o_i}) = \left\{1 - tanh\left[\left(\frac{x_1 - \delta_{o1}}{0.5d_1}\right)^{p_1} + \left(\frac{x_2 - o_{i2}}{0.5d_2}\right)^{p_2}\right]\right\} + \left\{\left[\left(\frac{x_1 - \delta_{o1}}{0.25d_1}\right)^{p_3} + \left(\frac{x_2 - o_{i2}}{0.25d_2}\right)^{p_4}\right]^{p_5} + 1\right\}^{-1} \tag{3.31}$$

Therefore, the first component of equation (3.31) satisfies the first additional requirement, while the second term satisfies the second additional factor. Additionally, the ellipsis accepts values in the range [0, 1], and its universal form for all barriers is:

$$\sum_{i=1}^{n}[c_i(\boldsymbol{x}, \mathbf{o}_i)] \tag{3.32}$$

where $\boldsymbol{x}$ and $\boldsymbol{o}_i$ are state vectors comprising the four state variables of the ego and obstacle$-i$ vehicles, respectively. n is the number of timesteps for which the cost c_i is calculated.

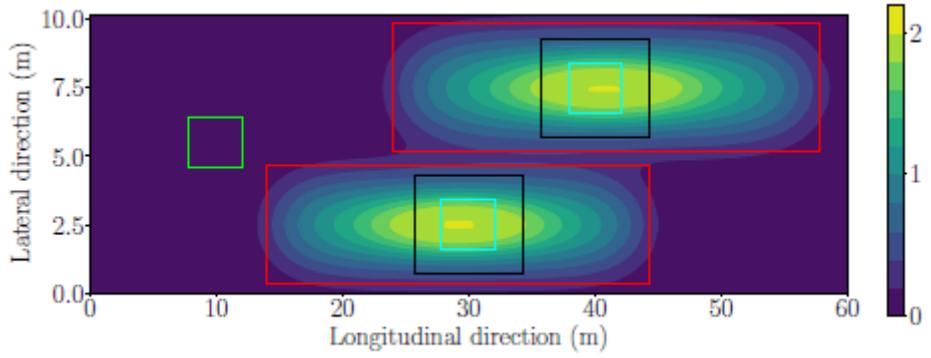

Figure 3.3 : Obstacle Avoidance Function
(Source: [52])

Coupling of Longitudinal and Lateral Speeds

The connection of longitudinal and lateral speeds is the subject of the fourth sub-objective function, which is described in equation (3.33). It is employed when the longitudinal speed is low and the equations of motion model could result in unrealistic and impractical

moves, such as just traveling with a higher lateral than longitudinal speed, which is not possible for cars as designed till this point. Due to their design, cars and possibly CAVs must have a longitudinal speed in order to make turns.

$$f_c = \begin{cases} \left(\beta x_3(k)^q - x_4^q(k)\right)^2, & x_4^q > \beta x_3^q(k) \\ \left(\beta x_3^q(k)^q - x_4^q(k)\right)^2, & x_4^q < -\beta x_3^q(k) \\ 0, & otherwise \end{cases} \tag{3.33}$$

Deviation of Longitudinal Acceleration Between Planning Horizons

Equation (3.34) defines the fifth sub-objective function, which corresponds to the deviation of longitudinal acceleration between planning horizons. Each finite time planning horizon can start with any acceleration. Due to the difference between the last applied and the first applied acceleration in the longitudinal direction, this may result in discontinuities in the acceleration between the planning horizons. These discontinuities can be reduced by penalizing the difference between a planning horizon's initial acceleration ($u_1^q(0)$) and the final acceleration ($u_{1prev}^q(K-1)$) of the preceding planning horizon.

$$f_d^q = \left[u_1^q(0) - u_{1prev}^q(K-1)\right]^2 \tag{3.34}$$

3.2 Optimal Control Problem (OCP) Formulation

According to Section 2.4 the optimal path planning problem could be formulated as an optimal control problem [56], in which the objective function to be minimized has the following OCP form:

$$J = \sum_{k=0}^{K-1} \Big\{ w_1\left(u_1(k)\right)^2 + w_2\left(u_2^q(k)\right)^2 + w_3\left(x_3^q(k) - v_{d1}\right)^2 + w_4\left(x_4^q(k) - v_{d2}\right)^2 + w_5 \sum_{i=1}^{n} \{c_i(x, o_i)\} + w_6 f_c^q \Big\} + w_7 f_d^q \tag{3.35}$$

Equation (3.35) differs from equation (2.3), (2.2) as it does not include a term for the last step and is independent of k. While the inequality constraints refer to equation (3.1), the equality constraints refer to the state equation (3.23).

The general form of the objective function, which is used in the further analysis, is given by:

$$J = \sum_{k=0}^{K-1} \{ \Phi[\boldsymbol{x}(k), \boldsymbol{u}(k)]\} \tag{3.36}$$

where u is the control vector, comprising longitudinal and lateral accelerations. The general vector-based representation of (3.1) is:

$$\boldsymbol{x}(k+1) = f[\boldsymbol{x}(k), \boldsymbol{u}(k)] \tag{3.37}$$

The Hamiltonian function, including the equality and inequality (3.23) constraints, for this problem is defined as:

$$\widehat{H}[\boldsymbol{x}(k), \boldsymbol{u}(k), \boldsymbol{\lambda}(k+1), \boldsymbol{\mu}(k)] = \boldsymbol{\Phi}[\boldsymbol{x}(k), \boldsymbol{u}(k)] + \boldsymbol{\lambda}(k+1)^T \boldsymbol{f}[\boldsymbol{x}(k), \boldsymbol{u}(k)] + \boldsymbol{\mu}(k)^T \boldsymbol{h}[\boldsymbol{x}(k), \boldsymbol{u}(k)] \tag{3.38}$$

where $\boldsymbol{\lambda}(k)$ are the co-states, associated with the state equations, and $\boldsymbol{\mu}(k)$ are multipliers, associated with the control constraints. Based on these, the necessary conditions of (local) optimality, to be used in the numerical solution algorithm, are given next. We have the state equation.

$$\boldsymbol{x}(k+1) = \frac{\partial H}{\partial \boldsymbol{\lambda}(k+1)} = f[\boldsymbol{x}(k), \boldsymbol{u}(k)] \tag{3.39}$$

With the control condition given by:

$$\frac{\partial H}{\partial \boldsymbol{u}(k)} = 0 \tag{3.40}$$

The co-state equation given by:

$$\boldsymbol{\lambda}(K) = \frac{\partial H}{\partial \boldsymbol{x}(k)} \tag{3.41}$$

The complementarity conditions are:

$$\boldsymbol{\mu}_i \boldsymbol{h}_i[\boldsymbol{x}(k), \boldsymbol{u}(k)] = 0, \ \ \boldsymbol{\mu}_i(k) \geq 0 \tag{3.42}$$

As a result, the requirements for optimality (2.7) are met. Finally, the boundary conditions are:

$$\boldsymbol{x}(0) = \boldsymbol{x}_0 \tag{3.43}$$

$$\boldsymbol{\lambda}(K) = 0 \tag{3.44}$$

3.2.1 Solution

The stated OCP's solution must be attained using a powerful numerical solver that supports real-time feasibility.

The current OCP is solved using a very effective gradient-based feasible direction algorithm (FDA). The underlying technique takes advantage of the state equations' explicit structure and applies the necessary optimality conditions to map the OCP into a Nonlinear Programming (NLP) problem in the reduced space of control variables. As a result, the algorithm tries to reach a control trajectory $u(k)$, $k = 0, .., K-1$, which corresponds to a local minimum of the cost function in the $mK - dimensional$ space, where m is the quantity of control variables. As a result of the state variables being eliminated, the problem dimension gets significantly reduced.

The FDA benefits from the fact that the gradient gets reduced when $g(k) = \left[\frac{\partial f}{\partial u(k)}\right]^T \lambda(k+1) + \frac{\partial \Phi}{\partial u(k)}$ equals the reduced gradient.

The FDA is consists of four gradual steps: Firstly, an initial guess for the control variables -initial trajectory is required. Next, the state variables, the Lagrange multipliers, the Kuhn-Tucker multipliers, and the reduced gradient are calculated in order for the first iteration to begin. The next step is the specification of a search descent direction, in which line optimization may start to find the scalar step a using this search direction, in order to calculate the subsequent state variables, the Lagrange multipliers, the Kuhn-Tucker multipliers, and the reduced gradient.

FDA is an iterative process that starts with a user-specified plausible initial-guess control trajectory and may calculate reduced gradients. Upper and lower (potentially state-dependent) constraints on the control variables can be easily assessed by the method [54], [52].

Each FDA iteration uses the updated gradient $g(k)$ to compute the descent direction (such as a conjugate gradient or quasi-Newton direction) and generate an improved feasible control trajectory based on line-search that minimizes the objective function value compared to the previous iteration, while satisfying the state equations and control

constraints. The improved control trajectory acts as the starting point of the next iteration, and so forth. The method has global convergence, which means it starts from any feasible initial-guess and concludes to a local minimum.

When the gradient's magnitude sufficiently approaches zero, the minimum is practically obtained, and the algorithm's iterations are completed. At algorithm convergence, all necessary conditions of optimality are satisfied. It is noteworthy that an initial-guess trajectory closer to the ideal one may lead to less iterations, it should be emphasized.

Among several conjugate-gradient and Quasi-Newton methods, the Polak-Ribiere method was proven to be the most appropriate for this OCP, so it was used for finding search directions inside FDA. The approach is efficient enough to be considered for real-time applications

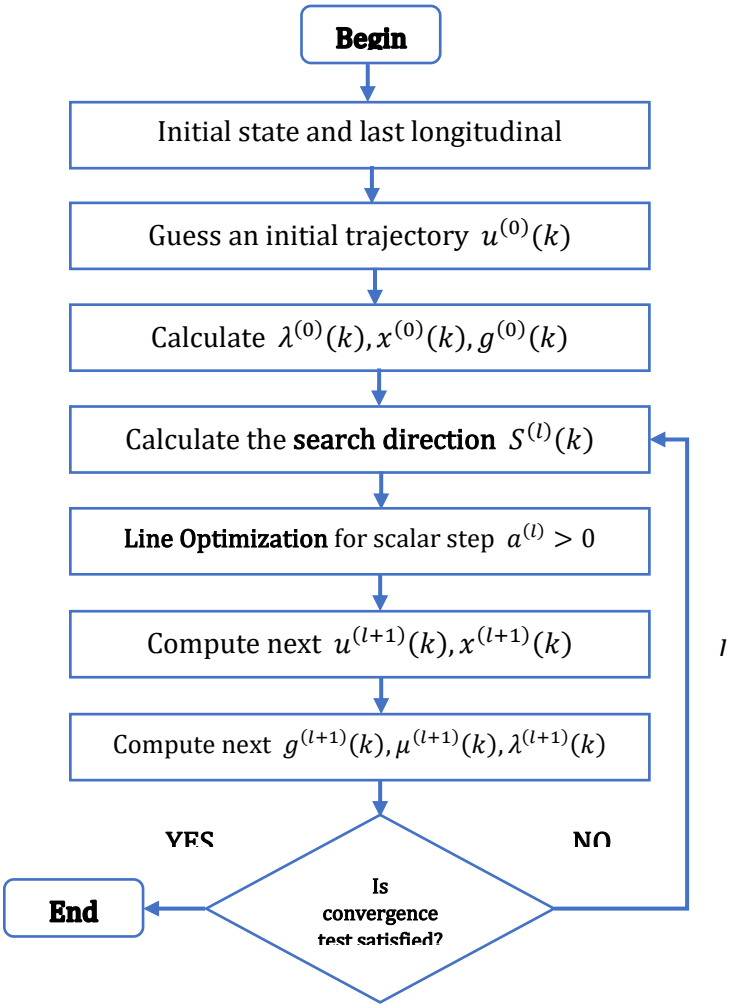

Figure 3. 4: Schematic Representation of Algorithmic Steps

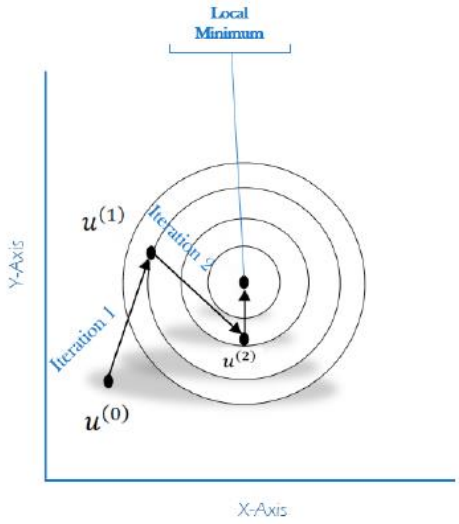

Figure 3. 5: Feasible Direction Algorithm

3.2.2 Model Predictive Control (MPC)

The development of MPC as a quasi-feedback control scheme has enabled for the implementation of optimization and optimal control techniques in real time. As opposed to tracking desirable values for system states, the current application, known as economic MPC, tries to minimize a quasi-physical objective criterion.

An FDA is integrated into an MPC scheme in the current application to offer real-time numerical solutions of the specified OCP that indicate the most convenient vehicle trajectories. The MPC scheme is applied, independently to all vehicles populating a ring-road infrastructure, to examine and evaluate the approach under the novel requirements of lane-free traffic and vehicle nudging, in addition to evaluating its impact on traffic level. The OCP predicts future action requirements, according to its time horizon in order to avoid myopic acts. This is considered advantageous for the pursued vehicle jobs, particularly for higher efficiency (vehicle advancement), safety (collision avoidance), and passenger convenience (smooth paths).

It is assumed that vehicles communicate and share their decisions. Thus, each ego vehicle knows about the decided future trajectories of all its obstacles, though this prediction may not be accurate, as decisions of the obstacles may have to be updated according to MPC. Considering long time horizons for the OCP is not recommended due to the dynamic nature of traffic and the inherent uncertainty of the neighbor vehicles' activity. So, prediction of movement for other vehicles gets progressively inaccurate over time. Through trial and testing, it was determined that time spans of the range of 8 seconds are a very good choice in terms of performance, taking into account the dynamic, but uncertain, nature of traffic.

The MPC framework starts each FDA call in an event-based mode, with modified initial EV states and updated obstacle trajectory predictions. The FDA calls, which force the EV to compute a new trajectory, are brought on by the following circumstances [52]:

- The planning horizon is larger than the application period in order to prevent the vehicle from acting in a myopic manner. The vehicle has already applied the portion of the most recent generated trajectory that corresponds to a pre-specified application period, which in this case is half of the planning horizon.
- Any of the dynamic obstacles' paths has a significant variance (0.2 m longitudinally or 0.1 m laterally).
- This is essential to avoid collisions brought on by improper estimation of the movement of the actual obstacles.
- A new obstacle enters the IZ of the EV.

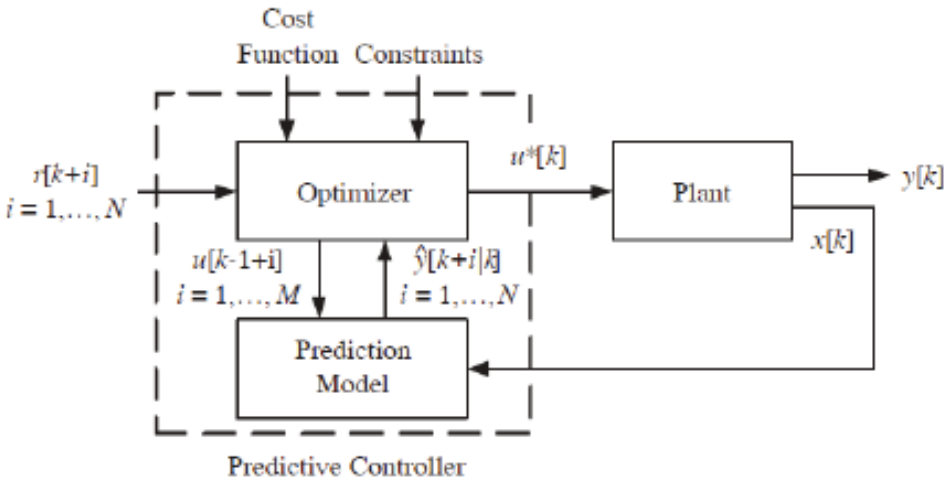

Figure 3.6: MPC Scheme
(Source: [58])

As previously mentioned, minimizing the objective function does not ensure that the EV will always be generated with a collision-free trajectory. So, using the projected trajectories of the obstacles as a guide, the FDA's generated trajectories are examined for any potential collisions. Checks are made for potential longitudinal or lateral collisions, and if one is spotted, the relevant new OCP is stated, along with the necessary preventive measures. Based on study [52], a longitudinal collision with i^{th} obstacle is detected if all the following checks return true:

- $x_1^q(0) < o_{i1}^q(0)$ i.e., the initial position of the EV's center is behind the obstacle's center, otherwise no longitudinal collision is conceivable.
- $\left(o_{i1}^q(k) - \frac{e_l^q}{2} - \frac{o_{il}^q}{2} - \omega_{1em}^q x_3^q(0)\right) < x_1^q(k) < \left(o_{i1}^q(k) + \frac{e_1^q}{2} + \frac{o_{il}^q}{2} + \omega_{1em}^q x_3^q(0)\right)$, for any k within the time horizon $0 < k < K$, to check longitudinal overlap of length and emergency time-gap on rear and front sides of the EV, where $\omega_{1em} = 0.5\omega_1$. Figure 3.7 shows a case of an overlap.

- $\left(o_{i2}^{q}(k) - \frac{e_w^q}{2} - \frac{o_{w2}^q}{2} - \varepsilon\right) < x_2^q(k) < \left(o_{i2}^{q}(k) + \frac{e_w^q}{2} + \frac{o_w^q}{2} + \varepsilon\right)$,
  to check lateral overlap of width on either side of the EV, with a small positive safety margin ε. Figure 3.7(b) depicts a case of lateral overlap.

The OCP is reformulated with a new upper limit in the state-dependent bound and aims to follow the obstacle if a collision is observed. On the other hand, and similarly to the longitudinal direction, a lateral collision can be identified if all three of the following conditions are met:

- lateral alignment check:
  $\left(o_{i1}^{q}(k) - \frac{e_l^q}{2} - \frac{o_{il}^q}{2} - \varepsilon\right) < x_2^q(0) < \left(o_{i1}^{q}(k) + \frac{e_1^q}{2} + \frac{o_{il}^q}{2} + \varepsilon\right)$

- longitudinal overlap checked of the width between the vehicle and the obstacle:
  $$\left(o_{i2}^{q}(k) - \frac{e_w^q}{2} - \frac{o_{w2}^q}{2} - \varepsilon\right) < x_1^q(k) < \left(o_{i2}^{q}(k) + \frac{e_w^q}{2} + \frac{o_w^q}{2} + \varepsilon\right)$$

- overlap lateral check:
  $$\left(o_{i2}^{q}(k) - \frac{e_w^q}{2} - \frac{o_{w2}^q}{2} - \varepsilon\right) < x_2^q(k) < \left(o_{i2}^{q}(k) + \frac{e_w^q}{2} + \frac{o_w^q}{2} + \varepsilon\right),$$
  where ε is a small safety margin.

Thus, if the initial positioning of the vehicles is as shown in Fig. 3(a) and evolves to a position as shown in Figure 3.7(c) during the course of the trajectory, this is categorized as a lateral collision.

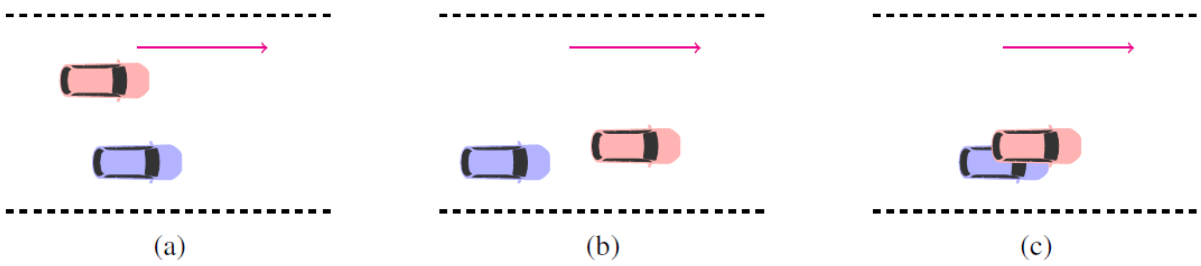

Figure 3.7: Illustration of collision detection: (a) Longitudinal overlap, (b): Lateral overlap, (c): Longitudinal and lateral overlap
(Source: [52])

In case of a collision detection the OCP is reformulated with updated upper and lower bounds in the state-dependent bounds, which limit lateral movement to a distance of 0.15 m or less from the starting point.

Moreover, as proposed on [52] a longitudinal speed adjustment is required due to two issues:

- in cases of high vehicle densities, where there is little space for maneuvers and overtaking of downstream obstacles. In these circumstances, vehicles tend to travel in groups with similar speeds, which mostly are lower than their desired speeds.
- In lane-based traffic, when the longitudinal speed in all lanes is low, due to congestion and even fast vehicles have no space to get out of traffic. In such case, maintaining a high target speed in the OCP may result to aggressive forward-acceleration behavior of the EV. This behavior may lead discomfort of passengers due to acceleration bursts or even to collisions.

To address these issues, an adaptive desired speed $u_{d_1}^q$ is defined in (3.45) as stated in [52], is calculated prior to every new trajectory computation. $u_{d_1}^q$ may be limited to values lower than V_{des}, to address the above two concerns. In more detail, the adaptive desired speed vd1 is always limited to a positive increment V_{incr1} above the current longitudinal ego speed $x_3(0)$, which addresses the first issue above, since the desired speed targeted by the OCP is never higher than V_{incr1} above the current vehicle speed $x_3(0)$, hence the longitudinal acceleration will not take unreasonably high values.
To prevent from the second issue mentioned, a second limit is included in (3.45), which is considered only at dense traffic, i.e., if $D_d > D_{bar}$, where D_d (in veh/km) is the downstream vehicle density, defined as the number of obstacles included in the downstream part of the IZ, divided by the zone's length; and D_{bar} is a density threshold, selected around the critical density value. Specifically, if $D_d > D_{bar}$, the adaptive desired speed v_{d1} is additionally limited to a positive increment Vincr2 above the current average downstream longitudinal speed D_v of the vehicles included in the downstream part of the IZ. This second limit addresses the second issue above, as, at higher densities, the EV has no strong incentive to accelerate beyond the average speed of surrounding vehicles.
Summing up, the longitudinal target speed V_{des}^q as well as the initial longitudinal speed may differ significantly, which could lead to excessive acceleration values and consequent passenger discomfort. Furthermore, cars often move in groups with identical longitudinal speeds less than their target speed, due to high traffic density. To face those two issues, the objective function's required longitudinal speed must be adjusted as depicted below:

$$u_{d_1}^q = \begin{cases} \min\{x_3^q(0) + V_{incr1}^q, V_{des}^q\}, & D_d \le D_{bar} \\ \min\{x_3^q(0) + V_{incr1}^q, D_u + V_{incr2}^q, V_{des}^q\}, & otherwise \end{cases} \quad (3.45)$$

3.2.3 Collisions-Emergency Rule

Regarding the safety features of the model, the EV ought to remain clear of accidents with other vehicles by treating them as moving obstacles. This is a necessary condition that must be stated appropriately in a sub-objective that considers both the potential for vehicle nudging and the distinctive features associated with lane-free vehicle movement. As described briefly in Section 3.1.2 it is essential that the EV sensors or V2V communication have access to the current states (position and speed) of the surrounding

vehicles to avoid accidents while generating the path of the EV. Each vehicle also communicates its generated path planning to surrounding vehicles. Undoubtedly, the accuracy of short-term predictions of the relative movement of nearby vehicles is limited, and this may result in the development of a different path. As a result, the algorithm might need to be rerun as many times as needed to replan the path to be followed by the vehicle.

4

Simulation Set up

In Chapter 4, the EmV enters our lane-free environment and modifications start taking place in order to test the reaction of traffic to the entry of an EmV, with different goals and characteristics. Section 4.1 provides details on the specially created extension proposed in [40], which is used as a tool for the simulations and the observation of the behavior vehicle population, as an EmV, during the present work, enters the environment. Section 4.2 demonstrates the stages of testing taken place for the case of the EmV entrance in the CAV population. by presenting the proposed Active [4.2.1] and Passive [4.2.2] approaches of modifications.

4.1 Simulation Environment - TrafficFluid-Sim

A custom - made extension, called TrafficFluid-Sim proposed in [40] was created within the well-known and widely used Simulation of Urban Mobility (SUMO) simulator [59] to execute traffic-level simulations in a lane-free environment. The extension to the open-source codebase of SUMO was extended and used to communicate control inputs and other information with SUMO. The API utilizes the MPC framework, which, when necessary, calls the FDA algorithm. Due to the lane-free structure of the road, the default car-following and lane-changing models of SUMO are not appropriate for the vehicle movement; therefore, the extension is utilized to incorporate the proposed vehicle movement strategies.

In more detail, TrafficFluid-Sim is a microscopic simulator, which aims to V2V and/or V2I communication. The development of this extension was based on the two principles of the novel paradigm called TrafficFluid. Firstly, the vehicles travel in a lane-free environment, hence the vehicles can be located anywhere on the road. SUMO's open-source software is expanded and utilized to exchange information, including control inputs, with other

systems. The API incorporates the MPC framework, which, when necessary, calls the FDA algorithm. The extension is used to incorporate the suggested vehicle movement techniques, because the default car-following and lane-changing models of SUMO are ineffective for vehicle movement, due to the road's absence of lanes. Due to lane-free traffic, SUMO detectors are used to measure flow, but they are set to span the entire road width at their designated points, which measures the total cross-section flow.

Therefore, the extension provides an application programming interface (API) for establishing the lateral position of the cars and their desired speed in the longitudinal direction, as well as a dynamic library for lane-free vehicle movement control (API). Additionally, the dynamic library enables C/C++ programming development, enabling the creation of coding structures that include initialization and finalization routines. Through programming, the user can create control strategies and test them using the SUMO. Another useful gadget of the API is its wide range of information regarding the vehicle's characteristics, such as its width or length, or its status, its position or speed and their own control through their unique ID. Additionally, the API offers details about the roadway on which the vehicles are travelling, like its length and width.

4.2 An Emergency Vehicle Enters the Network

The proposed vehicle-movement strategy is based on the defined OCP, its numerical solution using an FDA, and its real-time MPC deployment. The method is individually implemented to all cars traveling on a 1 km long and 10.2 m wide extended lane-free ring-road in order to test each vehicle-level characteristics and evaluate the creation of traffic-level characteristics. In this work, simulations took place for gradually increasing traffic densities (50, 100 and 150 vehicles). Randomly, eight different vehicle classes are taken into consideration; except from the EmV which belongs in the 9th class and has greater dimensions (length: 6.2 m and width 2.3 m), according to the dimensions of a Type II ambulance. Table I lists the associated measurements for each class.

Figure 4.1: Type II ambulance

Class	I	II	III	IV	V	VI	VII	VIII	IX
Length (m)	3.2	5.15	4.25	4.55	4.6	3.9	3.4	5.2	6.2
Width (m)	1.6	1.84	1.8	1.82	1.77	1.7	1.7	1.88	3.2

Table 4.1 : Vehicle classes and dimensions

Vehicles begin each simulation moving at a stop. The lateral space is divided into four virtual lanes for homogenous initial placement of the vehicles with sufficient two-dimensional spacing between them, (see Figure 4.2) and the longitudinal space is divided into $n = 4$ sections, where n is the number of vehicles (density) being taken into consideration. As a result, the two-dimensional ring-road surface is divided into exactly n cells, each of which is evenly spaced out, with some two-dimensional random deviations inserted around its center for each car. Based on their initial lateral placement, individual vehicles are given the required longitudinal speeds. One for each virtual lane, the considered longitudinal desired speed range is [25, 35] m/s, and this range is divided into four equal desired speed zones.

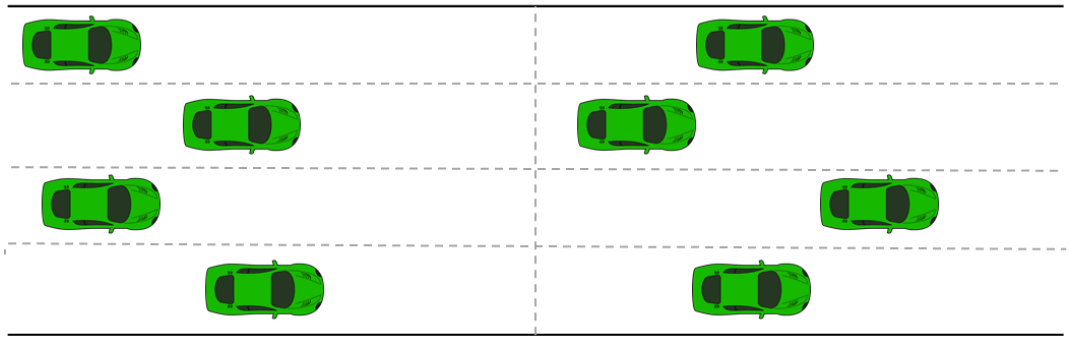

Figure 4.2: Initial placement for requlars passenger vehicles
(Source: [37])

Following the placement of each vehicle and the assignment of their desired longitudinal speeds, the cars begin to move from zero initial speed, in accordance with the defined strategy, attempting to reach their target speed, while avoiding other vehicles in front of and around them.

At first, there are no lanes in the space where a car can drive, thus it can move freely on the road. Meanwhile, when other vehicles are in their interaction zone, the vehicles use the nudging effect to push them. This simulator's aim is to enable the use of various movement methods, including the nudging effect, for lane-free environments.

On the given model which represents daily traffic in varying traffic densities, types of cars and conditions, emergency incidents may arise, such as in real life. For example, an ambulance or a fire truck moving through traffic may need space to move faster than the rest of the vehicle population. With human lives at stake, the Ambulance, Firetruck, or

police car must be handled differently from any other car with fast intentions. With cooperation among the automated vehicles, emergency situations can be handled in an efficient manner. In the current work, it is assumed that there is an EmV that must pass through traffic, intending both passive and active cooperation with other vehicles, to complete its mission. Testing the environment's reaction to the emergency entrance in the vehicle network with simulations was the next step that took place in order to observe our alterations, starting from low to gradually denser traffic. In both passive and active approaches, the desired speed of the EmV was higher than the rest of the vehicle population. Moreover, on the passive approach, the EmV had special characteristics and aims, such a smaller aura that made it travel/move closer to other vehicles. All other vehicles adjusted their behavior to this alteration, without any further intervention. On the contrary, in the active approach, the EmV communicated the emergency case to its neighbor vehicles, so they could cooperate and help it pass through traffic more easily. A variety of cases was tested in order to create a "green corridor" for the safe and independent passage of EmV through dense traffic. The passive and active approach will be described briefly in the following sections.

w1	w2	w3	w4	w5	w6	w7	ω1	ω2
0.01	0.01	0.03	7.0	0.01	0.2	0.35	0.5	0.1

Table 4.2: Parameters of the objective function

Table 4.2 summarizes all the parameters referring to the objective function (3.35) safety parameters, crash avoidance etc. The parameters have been selected after various simulations. The large value of w_5 = 7.0 refers to the weight of the ellipsoid and its role is to enforce the obstacle avoidance. The simulation duration is half an hour, while the flow values are recorded for the last 10 min. Moreover, various densities of vehicles starting from 25 and end up 350 in different numbers of replications have been used.

4.2.1 Non - Cooperative Approach

All scenarios were observed in 1hour simulations. Since all vehicles have zero initial speed, the addition of the EmV in all cases took place on the 10th minute of simulation, when the vehicles had accelerated and reached a stable point.

Scenario 1.1: Higher target speed for the Emergency Vehicle

As previously stated, all vehicles travel at a speed that ranges between 25 and 35 m/s *(=90-126km/h)*. So, the first scenario of simulations taking place was to add an EmV in the network with different target speed. Instead of setting a desired speed in the given range, the target speed for our EmV was fixed to 40m/s (*=144km/h*) in this and in the following simulation scenarios.

Scenario 1.2: Decrease of time-gap parameters

The time-gap design parameters (ω1 and ω2) in both longitudinal and lateral directions of each CAV were decreased to 70% of their nominal values in this scenario. More specifically, the aura was decreased, regarding how other vehicles were discerned by the EmV. All the surrounding vehicles within the interaction zone of the vehicle controlled are treated as obstacles. An aura around each obstacle in the shape of positive valued ellipsoid is considered. It is assumed that vehicles communicate and share their decisions. Thus, each ego vehicle knows about the decided future trajectories of all the obstacles within its interaction zone. Decisions of the obstacles though, may have to be updated according to Model Predictive Control (MPC). As it has been analyzed briefly in Section 3.1.2, the specified ellipsoid is used to construct a sort of potential function that penalizes the vehicle's approach to the obstacle and acts as a collision avoidance term.

By adjusting the time-gap parameters ω1 and ω2, the size of the ellipsoids neighboring to the EmV are decreased and the EmV becomes more flexible on the road sacrificing a part of safety, since it may get closer to other vehicles if needed. This variation was inspired by human driving in which, in case of an emergency, we drive more aggressively. In the simulations that took place, we decreased the safety parameters to values still ensuring safety. The values taken in consideration did not result to any crashes.

Scenario 1.3: Centering the Emergency Vehicle on the Road

Staying on course, to increase the EmV's real time speed, the simulations were observed, and it was noticed that the vehicle had sometimes the tendency to get stuck into the left or right "lanes", near the road boundaries, and as a result had no choices to maneuver and overpass slower vehicles to reach its goals. So, a lateral v_{dy} was set, such as in Faros' work, in order to keep the EmV on the middle of the road. The results of this variation will also be displayed on Chapter 5 proving that centering had a positive effect on the real time speed of the vehicle.

4.2.2 Active Approach - Cooperation

Moving on to the active approach, «the siren of the EmV is activated». By this means, the emergency case is shared to all neighbor, to the emergency, vehicles. They cooperate by i) giving less priority to their target speed, ii) opening the way for the EmV to pass and finally, iii) by creating a "green corridor" for the safe and independent passage of EmV.

The variations adopted in the non-cooperative level (Scenario 1) were the base case for any further alteration on the active scenarios. Target speed = 40m/s and smaller auras for the vehicles seen by the EmV were changes kept at all further levels.

Below is a flow chart with the changes made on the initial model for the creation of the green corridor for the EmV.

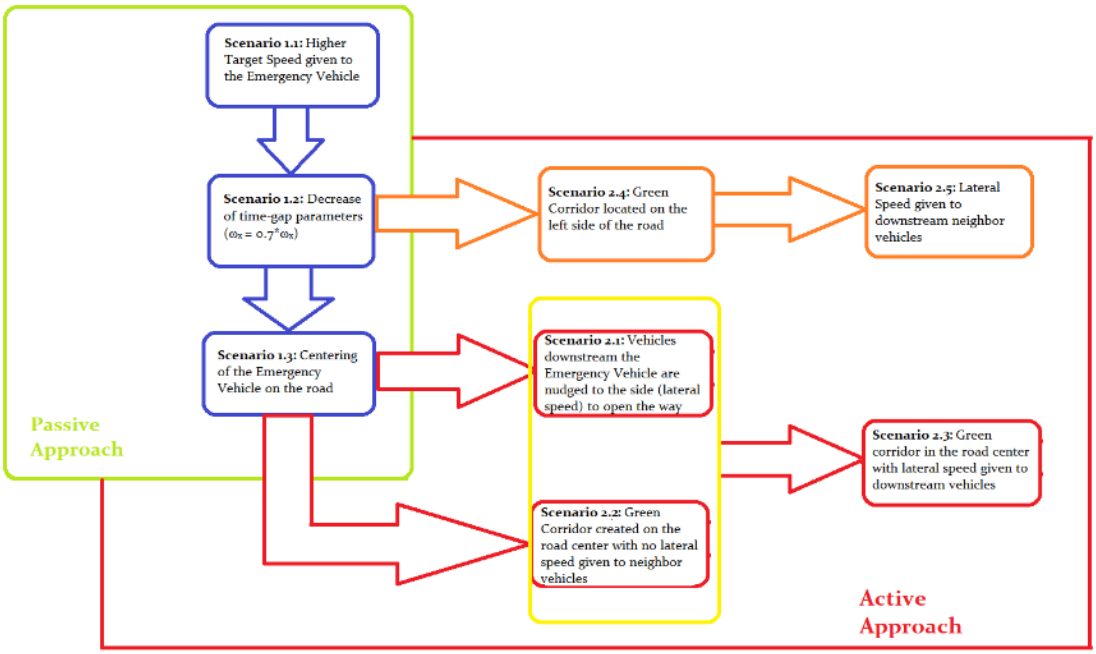

Figure 4.3: Schematic representation of scenarios in Passive and Active Approach

Scenario 2.1: Vehicles downstream the Emergency Vehicle are nudged to the side to open the way with the EmV centered on the road

Cooperation starts with the vehicles in front of the EmV starting to open the way for it to pass through, by giving them a small lateral speed ($V_{dy} = \pm 0.1$) and as a result, moving them to the side. Regarding their lateral position compared to the EmV's, the neighbor vehicles are moved to the right or to the left-hand side in order to open the way. In addition, to the lateral speed given, to other vehicles, the EmV has the tendency to drive in the middle of the road.

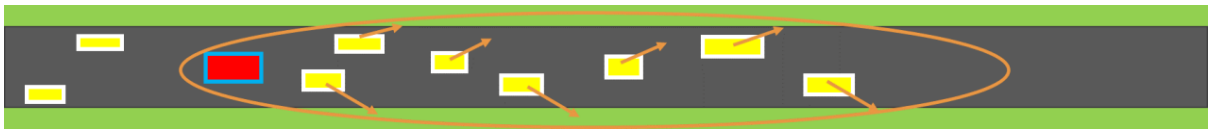

Figure 4.4: Scenario 2.1 - Lateral Speed given to downstream vehicles in a certain radius

Scenario 2.2: Green Corridor created on the road center with no lateral speed given to neighbor vehicles

On this testing phase, different road boundaries are given to the vehicles in front of the EV. The road boundaries, from their design, are a hard bound making it impossible for the CAVs to violate it. In this means, the creation of a green corridor is a more drastic variation than the lateral speed given to the front neighbor vehicles. The width of the corridor varies depending on the width of the EV and the simulation taking place.

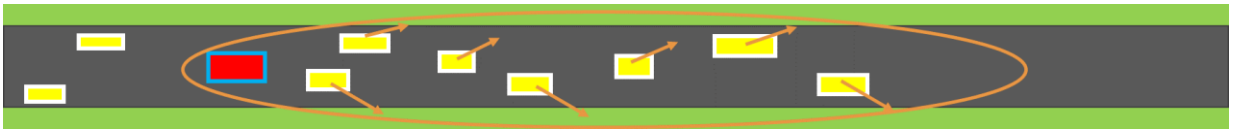

Figure 4.5: Scenario 2.2 - Green corridor in the middle of the road

Scenario 2.3: Green Corridor created on the road center with lateral speed given to neighbor vehicles

After changing the lateral bounds of the downstream to the EmV vehicles, a lateral speed is also given to the vehicles to direct them to the side. The combination of these two variations will theoretically bring even better results in the EmV's performance.

Figure 4.6: Scenario 2.3 – Lateral speed given to downstream vehicles outside the green corridor

Scenario 2.4: Green Corridor reallocated to the left side of the road

On experimental Scenarios 2.4 and 2.5 we change the location of the green corridor in order to test if its position affects its efficiency in any way. At first, the green corridor is created by changing the hard bound of the road width as it is noticed by the downstream to the EmVs, vehicles. So, the hard bound of the vehicles is at about 8.5m instead of 10-ε. That way, our EmV has space to travel independently of any traffic conditions.

Figure 4.7: Scenario 2.4 - Green corridor on the left side of the road

Scenario 2.5: Green Corridor reallocated to the left side of the road with lateral speed given to neighbor vehicles

In Scenario 2.5, adding up to the change of the lateral bound, a lateral speed is also given to the vehicles downstream the Emergency. So, all vehicles travelling near the left side of the road, are given a lateral speed to move to the right.

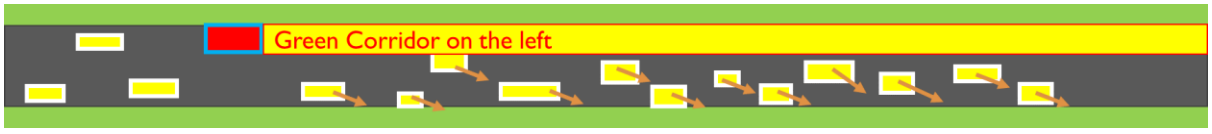

Figure 4.8: Scenario 2.5 - Green corridor on the left side of the road while a lateral speed is given to downstream to the EmV vehicles

Does the lateral speed help the green corridor be formed more easily? Does it help the EmV reach its goals? Does the EmV perform better than with the corridor in the middle of the road? The results will be performed and analyzed in Chapter 5.

5

Results

The statistical analysis and outputs shown in tables and diagrams of the scenarios described in Chapter 4 are presented in the present Chapter. In Section 5.1, the calculated quantities taken into consideration in order to test the efficiency of the changes made in the code, are presented. In Section 5.2 the traffic and vehicle level results for our scenarios are provided categorized in Passive and Active Approach, based on cooperation with other vehicles.

5.1 Experimental Setup

Analyzing several metrics, including the average flow and other statistical quantities, offers the study of various scenarios. A statistical analysis can be used to determine whether the suggested methodology is effective, and efficient.

5.1.1 Evaluation Metrics

Flow (veh/h)

The number of cars passing from a reference location in a unit of time is known as flow (q), and it is estimated over the final 30 minutes of a one-hour simulation to ensure that data are collected after the traffic has reached a steady state.

Heuristic Percentage

The heuristic percentage represents how many times the FDA function was recalled over the total number of times called. In Section 3.2.3 the reasons why the algorithm might need to be recalled are explained briefly.

Average Computational Time (CPU Time)

The Average CPU time was checked throughout all our code alterations to test the efficiency of our changes. There were different ways to implement the scenarios described

below by altering the given model. Therefore, the CPU times determined whether the changes improved efficiency and did not affect the algorithm's performance overall. Although we made a lot of changes regarding the target speed, the time-gap, the hard bounds of the vehicles, as shown on the table below, in terms of execution times and average CPU, they do not affect the algorithm's performance negatively.

Traffic Density		**50**			**100**			**150**	
Scenario	**Flow**	**Heur. %**	**Avg. CPU**	**Flow**	**Heur. %**	**Avg. CPU**	**Flow**	**Heur. %**	**Avg. CPU**
1.1	5391	0.014	0.006	10422	0.019	0.017	15049	0.007	0.024
1.2	5398	0.031	0.006	10533	0.137	0.017	15058	0.124	0.024
1.3	5397	0.031	0.006	10481	0.135	0.018	15122	0.138	0.025
2.1	5394	0.039	0.006	10520	0.150	0.017	15027	0.147	0.025
2.2	5391	0.148	0.007	10442	0.580	0.019	15142	1.002	0.026
2.3	5383	0.166	0.007	10438	0.531	0.018	15109	0.837	0.027
2.4	5392	0.278	0.007	10453	1.276	0.022	15165	1.952	0.035
2.5	5387	0.335	0.007	10508	1.044	0.021	15168	2.046	0.036

Table 5.1: Metrics of simulations

Metrics

- *Average Speed of EmV*
- *Average Speed of the rest traffic (Excluding the EmV)*
- *Flow*
- *Heuristic Percentage*
- *Average CPU*

Crashes

Since safety is the major issue in creating an automated vehicle model, the number of crashes was the most important factor taken into account to keep or discard changes made in the code, accordingly. As a result, simulations with crashes were discarded. The aim of the thesis is to implement a model that may help save more lives by helping decrease the emergency response time to an accident. No meaning in that if other lives are put to risk.

5.2 Traffic and Vehicle Level Results

On the first stage of testing the EmV's response to changes, we set the EmV a higher target speed (=40m/s) than the rest of the vehicle population. The EmV's target speed is 5 m/s higher than the fastest vehicle on the road and 15 m/s than the slowest one. As a result, it aims to travel much faster than the rest of the vehicle population and the vehicle environment is called to adapt to this alteration without further intervention. So, in the Non-Cooperative or Passive Approach of alterations, we aim to test the response of the system to the change in one vehicle's movement. For all scenarios, metrics such as the EmV's longitudinal real time speed, in compliance with the vehicle's adaptive desired

speed in throughout the entire simulation, will be plotted, such as its longitudinal and lateral position, acceleration and speed.

The adaptive desired speed v_{d1} as proposed in [52] is defined in (3.45) and is computed prior to every new trajectory calculation for use in the desired-speed sub-objective. Based on (3.45), v_{d1} may be limited to values lower than V_{des1}, to address the above two concerns. Specifically, the adaptive desired speed v_{d1} is always limited to a positive increment V_{incr1} above the current longitudinal ego speed $x_3(0)$, since the desired speed targeted by the OCP is never higher than V_{incr1} above the current vehicle speed $x_3(0)$, hence the longitudinal acceleration will not take unreasonably high values.

5.2.1 Non-Cooperative Approach

Scenario 1.1

In the first stage of testing, a higher target speed (40m/s) is given to the EmV. Its real time speed increases, as plotted in Figure 5.1. Figures (a), (b) and (c) represent the same scenario, in gradually increasing traffic densities from 50 to 150 vehicles accordingly. As it may be noticed, in low-traffic densities the EmV manages to keep up with its target speed for most of the simulation time, although it has some velocity drops ~5m/s frequently in an hour and a significant drop of about 10m/s once, which results to an average speed of 39m/s for the entire simulation, after the 10th minute, where the new target speed is activated. The rest of the vehicles' average speed is 29.35m/s, much lower than the speed of the EmV. Inferentially, the population's speed doesn't negatively affect the vehicles performance, which is rational, since the EmV has space to maneuver and make overpasses in low traffic densities.

As traffic density starts to increase and reach 100 vehicles on the road, reaching the target speed of 40m/s is still implementable, but maintaining it for more than 2.5 minutes becomes harder, resulting to a major drop on the average speed of the EmV to 32.12m/s, which is much closer to the average speed of the rest of the vehicle population (28.69m/s). It is noticed here that the average speed of the vehicle population is also decreased, as traffic density increases, which seems rational since vehicles travel closer to each other, they have less space to make overpasses, and as a result focus less on reaching their target speeds.

Moreover, for 150 vehicles on the road, reaching the target speed of 40m/s becomes infeasible. The max speed reached by the EmV is 36m/s and is only achieved for less than a minute. As traffic density increases, the average speed (27.76m/s) of the vehicle population effects the EmV's performance more. As a result, more drastic measures must be taken, other than changing the desired speed of the vehicle of interest.

For all the simulations plotted below labels (a), (b) and (c) will be used to determine the traffic density for each test, where: (a): 50 vehicles, (b): 100 vehicles, (c): 150 vehicles.

The figures regarding the longitudinal real time speed of the EmV also show the adaptive desired speed

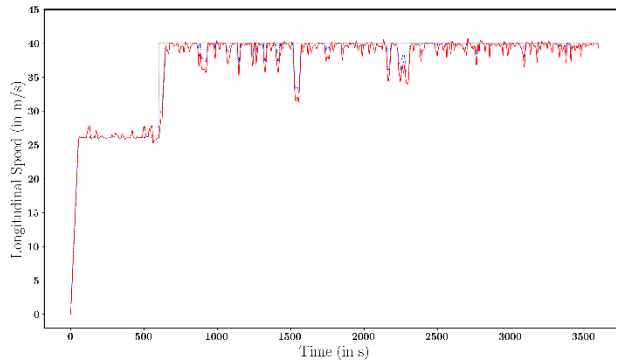

(a): 50 vehicles

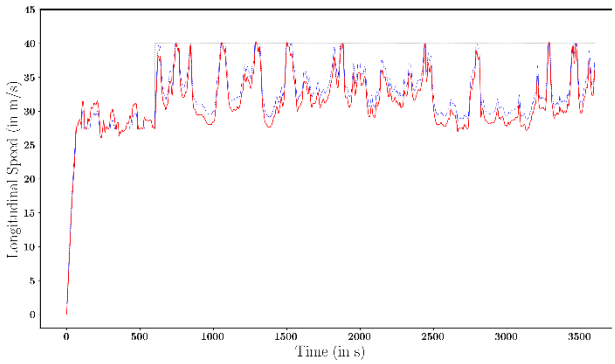

(b): 100 vehicles

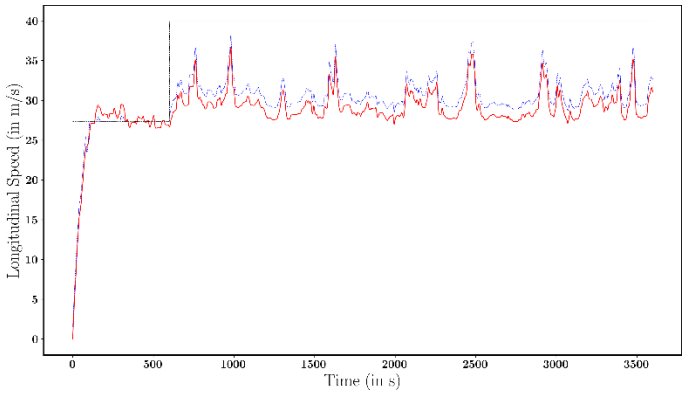

(c) : 150 vehicles

Figure 5.1: Scenario 1.1 - EmV's real time longitudinal speed (m/s)

Regarding the rest of the EmV's behavior, some useful information is plotted in the Figures below such as its lateral speed, longitudinal and lateral acceleration.

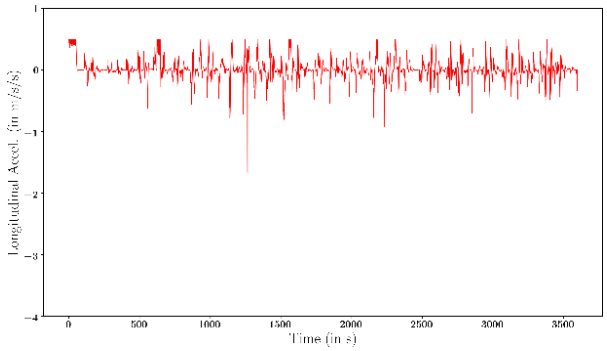

(a): 50 vehicles

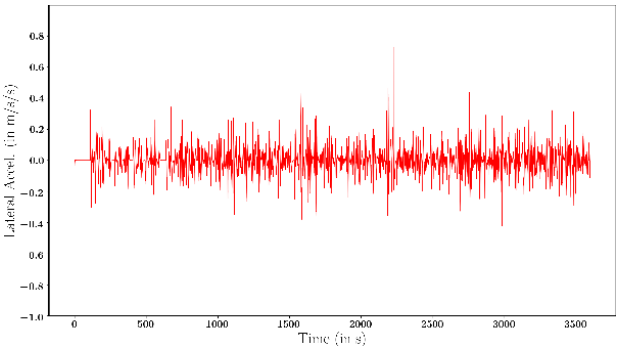

(a): 50 vehicles

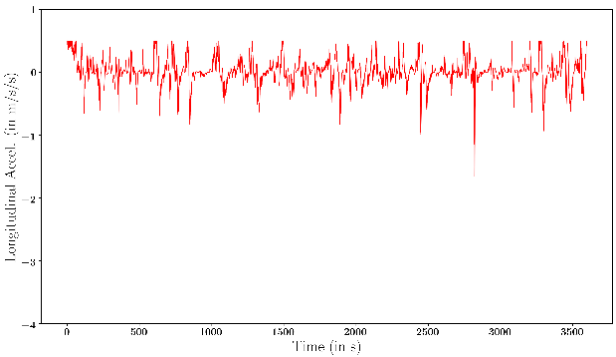

(b): 100 vehicles

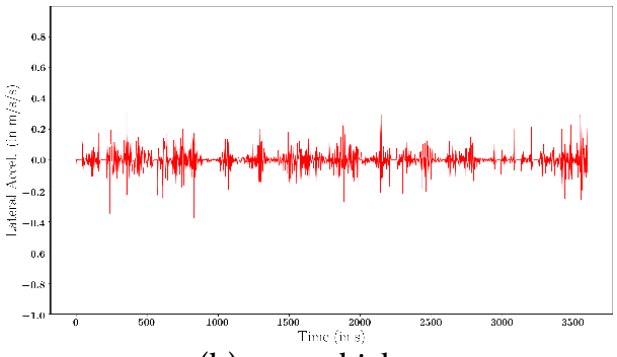

(b): 100 vehicles

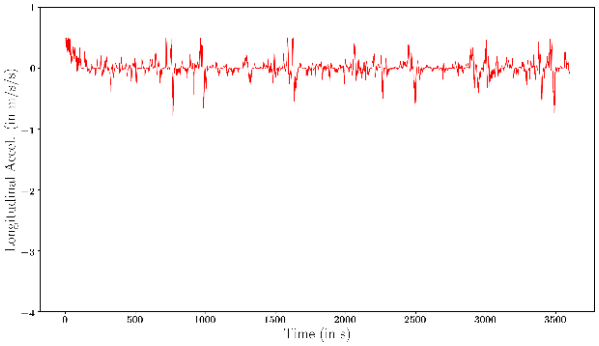

(c) : 150 vehicles

Figure 5.2: Scenario 1.1 - Longitudinal Acceleration (m/s/s)

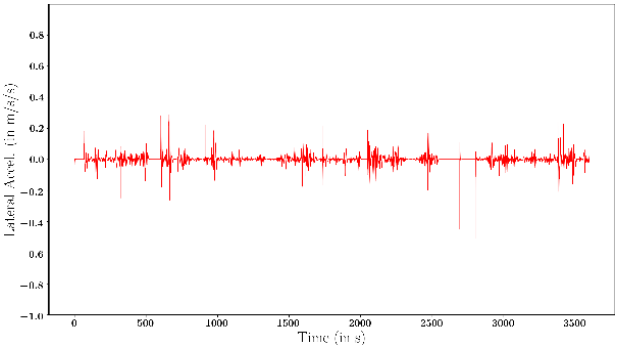

(c) : 150 vehicles

Figure 5.3: Scenario 1.1 - Lateral Acceleration (m/s/s)

Figures 5.4.a-5.4.c plot the lateral speed during the 1-hour simulation for the stated traffic densities. It can easily be noticed that, as the traffic density increases, the EmV starts to become less flexible in terms of utilizing all the lateral space of the road. As a result, the lateral speed magnitude becomes smaller as we add vehicles to the network.

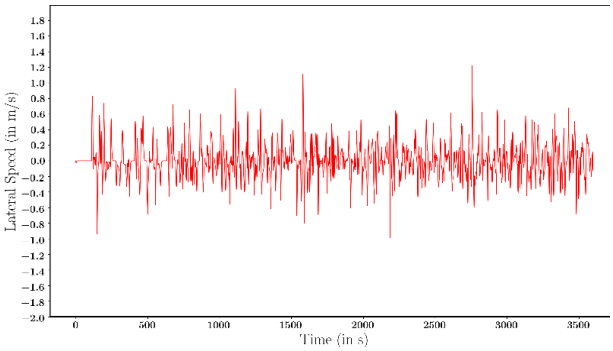

(a): 50 vehicles

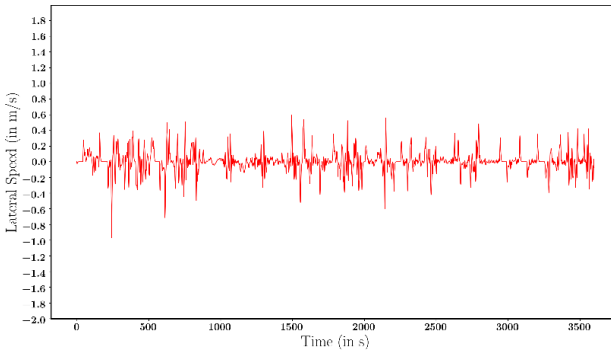

(b): 100 vehicles

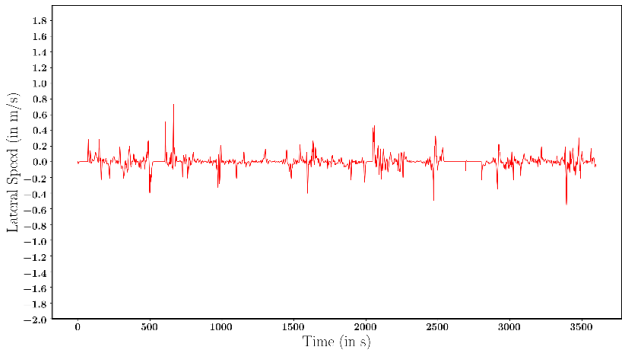

(c) : 150 vehicles

Figure 5.4: Scenario 1.1 - Lateral Speed (m/s)

Scenario 1.2

Moving on to the next simulation scenario, where the time gap of the EmV is decreased, it is crucial to compare the results to the previous stage of variations, in order to measure the effectiveness of this change. As we decrease the time-gap, a noticeable increase in the average speed of the EmV is seen, compared with the corresponding to the previous stage of variation, where only the target speed was changed. A major increase is noticed for 100 vehicles on the road, with an average speed from 32.12m/s to 36.62m/s. The EmV seems to keep a higher longitudinal speed for a longer time. Furthermore, moments where it travelled with a velocity near the average speed levels (29m/s-30m/s) for more than 5 minutes are eliminated. In all traffic densities the EmV seemed to move faster with a smaller time-gap. More extensively, for 50 vehicles the average speed continues to have a small deviation from 40m/s, summing up to an average speed of 34.7 m/s, while for 150 vehicles, the average speed increase was almost 2m/s, from 29.34 to 31.41m/s.

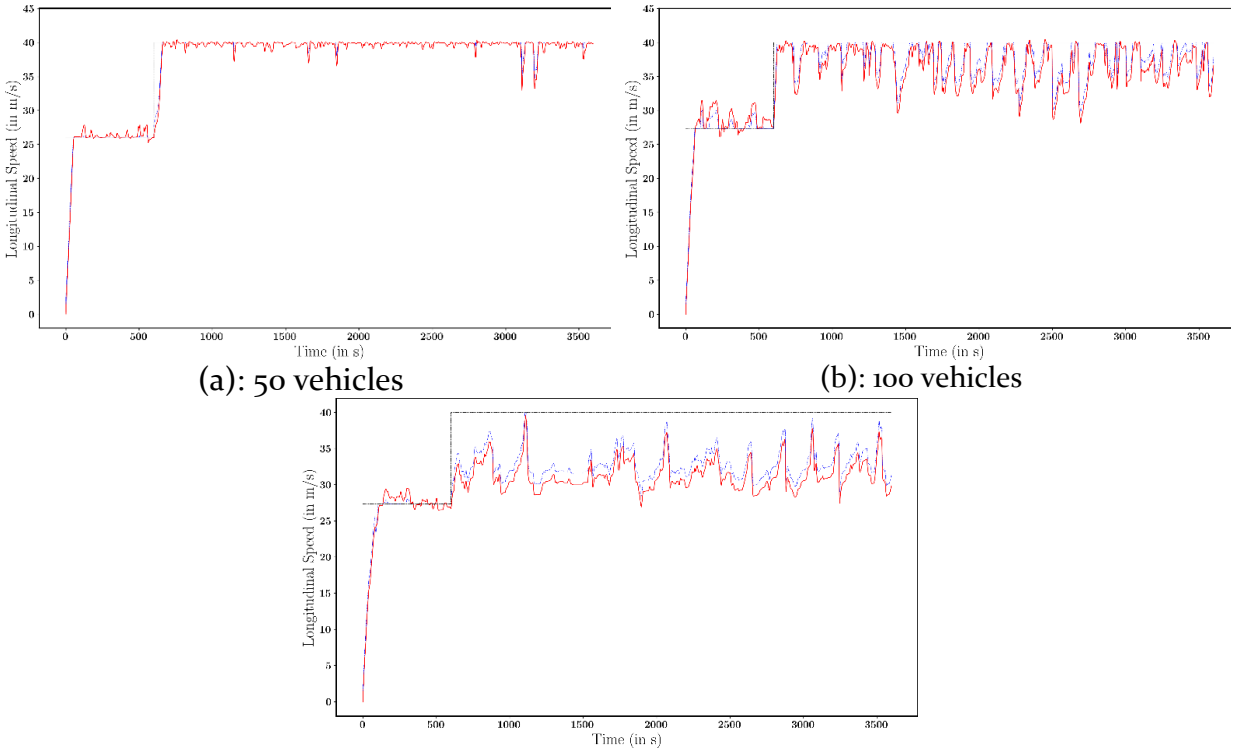

(a): 50 vehicles (b): 100 vehicles

(c) : 150 vehicles

Figure 5.5: Scenario 1.2 - EmV's real time longitudinal speed

Even though it becomes more flexible, no noticeable difference is seen on the lateral speed of the EmV, as its time-gap decreases. Its more flexible behavior though is noticed by observing the simulation videos, where its movement seems riskier by getting closer to neighbor vehicles in order to maneuver and overpass.

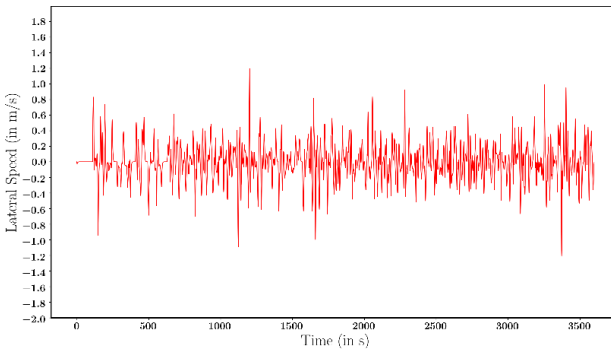

(a): 50 vehicles

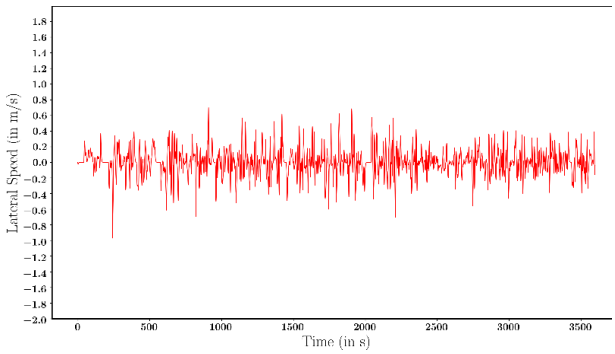

(b): 100 vehicles

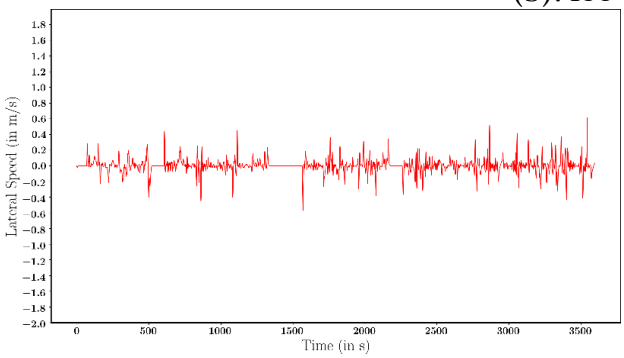

(c) : 150 vehicles

Figure 5.6: Scenario 1.2 - Lateral Speed (m/s)

Regarding the longitudinal acceleration, major drops or ripples infer that the EmV has difficulties passing through some spaces, so it is forced to decelerate. Many major drops are noticed in 100 vehicles traffic density, fact that indicates that the EmV manages to reach high speeds but later on is forced to decelerate.

Moreover, from the lateral acceleration plots shown in EmV's real time longitudinal speed, is similar in each simulation. As traffic density is increased, our vehicle of interest becomes less flexible and makes less maneuvers and overpasses.

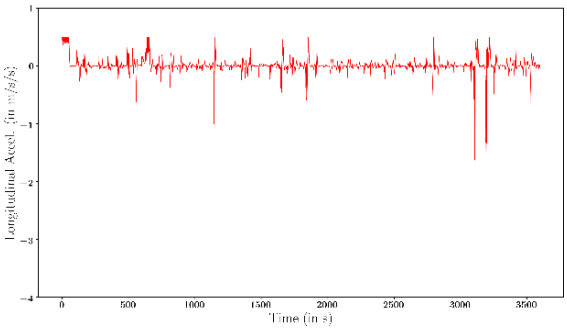

(a): 50 vehicles

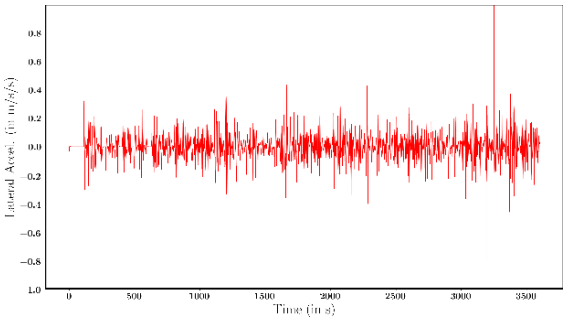

(a) 50 vehicles

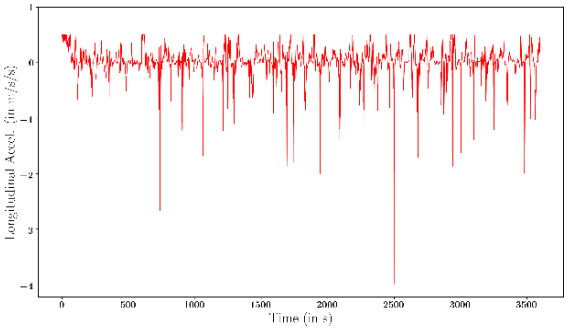

(b): 100 vehicles

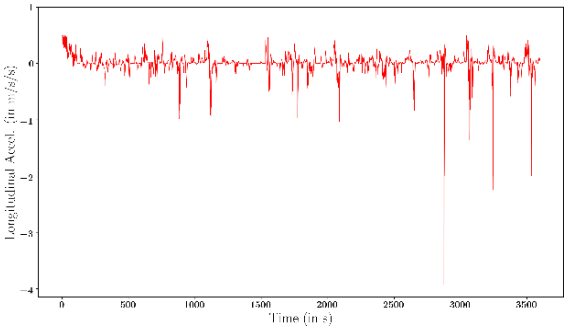

(c) 150 vehicles

Figure 5.7: Scenario 1.2 - Longitudinal Acceleration (m/s/s)

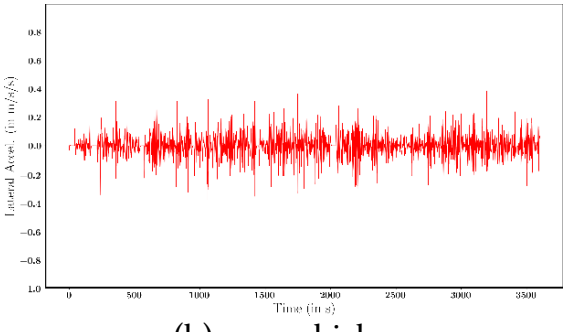

(b): 100 vehicles

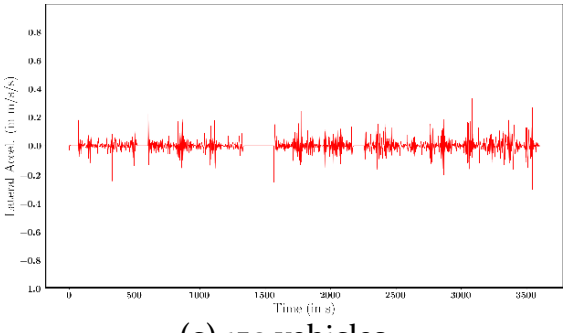

(c) 150 vehicles

Figure 5.8: Scenario 1.2 - Lateral Acceleration (m/s/s)

Scenario 1.3

Finally, in the last scenario of the passive approach, where changes were made only involving the EmV as an individual, without further cooperation with its surrounding vehicles, the EmV was centered in the middle of the road. By giving it a lateral speed, we continuously gravitated it to the center of the road to avoid it from getting stuck in lanes on the road boundary. This change individually, did not result in an improvement of the Emergency Vehicle's longitudinal speed. We assume though, that centering the vehicle, combined with other changes, such as nudging downstream vehicles to the side, will help to its performance improvement.

For 50 vehicles, the average speed remained the same as in the previous simulation, at 39.4m/s, for 100 vehicles the average speed was measured equal to 34.21m/s, so it had a small (0.2m/s) decrease from the previous stage. Last, but not least, the only simulation in which centering was found helpful was for 150 vehicles, where a small improvement was noticed in average speed, resulting at 31.41m/s.

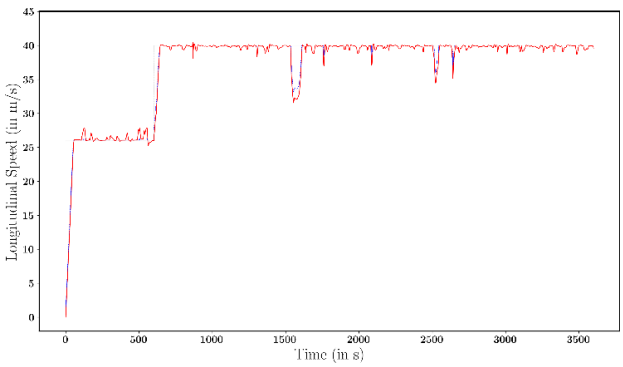

(a): 50 vehicles

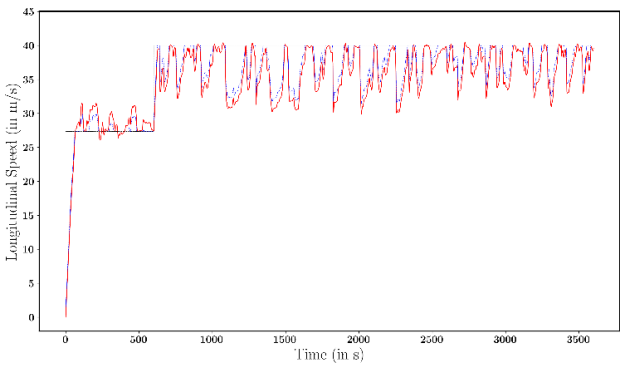

(b): 100 vehicles

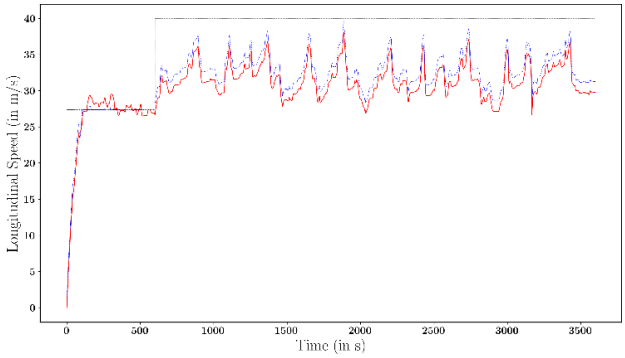

(c) : 150 vehicles

Figure 5.9: Scenario 1.3 - EmV's real time longitudinal speed (m/s)

The lateral speed follows the same pattern, with the EmV being more flexible in low densities, and less in higher ones. Compared to the previous cases, it makes less frequent ripples, since it has the tendency to stay in the middle and not utilize all the lateral space of the road.

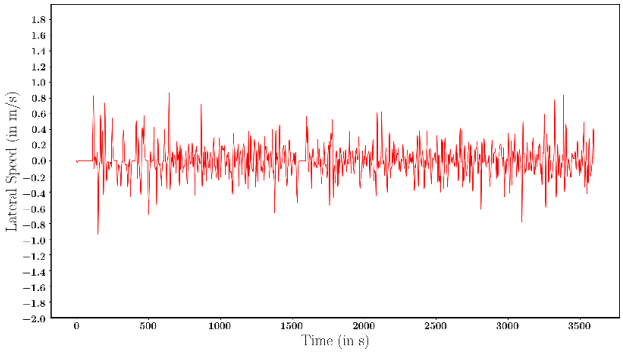

(a): 50 vehicles

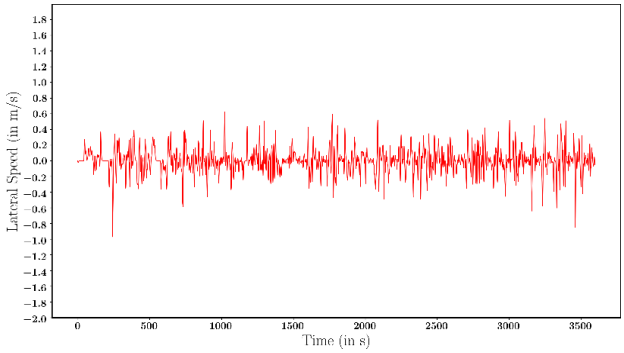

(b): 100 vehicles

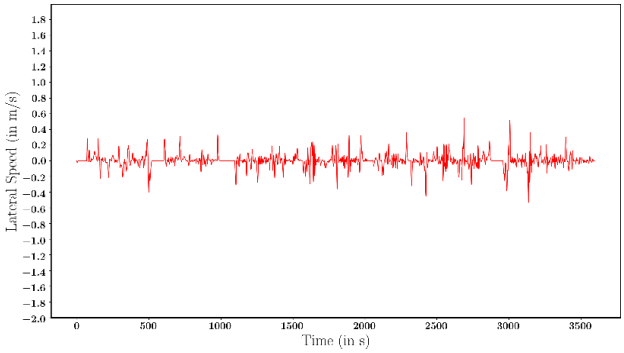

(c) : 150 vehicles

Figure 5.10: Scenario 1.3 - Lateral Speed (m/s)

The lateral acceleration plotted on Figure 5.11 follows the same pattern as the lateral speed.

Finally, the longitudinal acceleration has a similar behavior with the previous scenarios. In 50 vehicles traffic density it keeps its high speed during most of the simulation, in 100 vehicles it makes big decelerations frequently and then gradually recovers and accelerates. Halfway during the simulation, a huge deceleration is captured. And, for 150 vehicles the

EmV finds it seems difficult for the EmV to reach its target speed, but keeps it a slightly higher from the average longitudinal speed, so it has smaller and less frequent ripples.

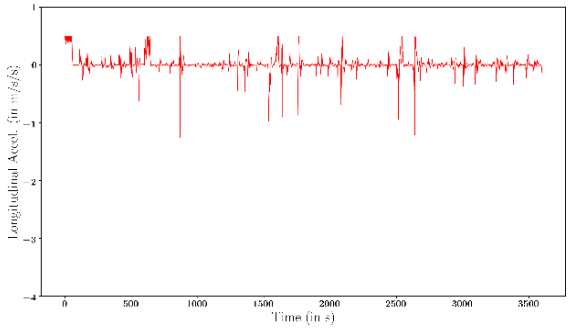

(a): 50 vehicles

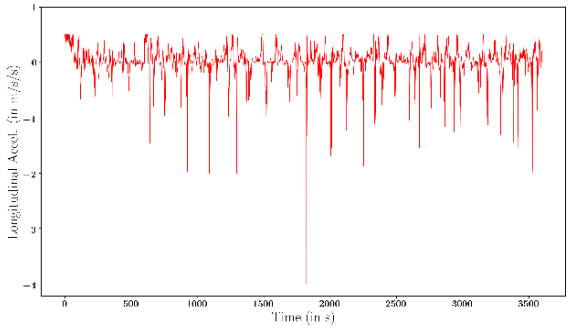

(b): 100 vehicles

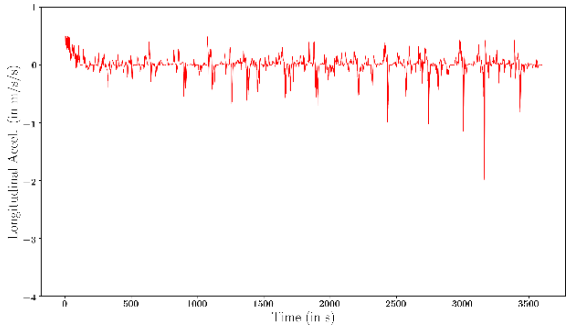

(c) : 150 vehicles

Figure 5.11: Scenario 1.3 - Longitudinal Acceleration (m/s/s)

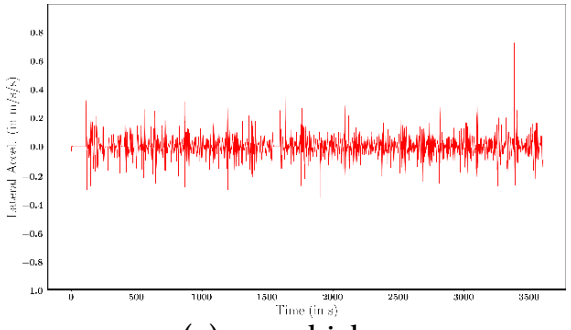

(a): 50 vehicles

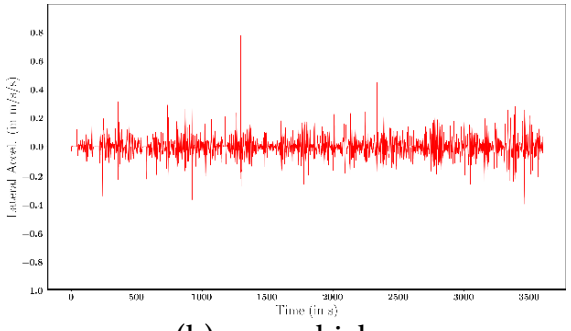

(b): 100 vehicles

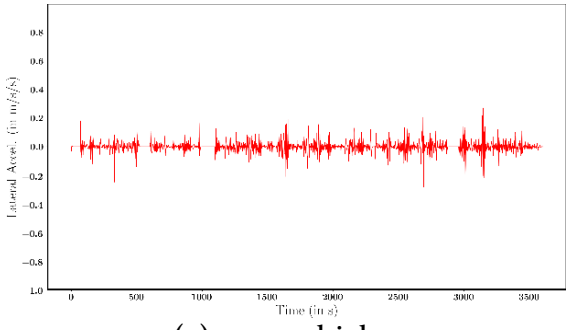

(c) : 150 vehicles

Figure 5.12 Scenario 1.3 - Lateral Acceleration (m/s/s)

5.2.2 Cooperative Approach

Cooperation between the Emergency and its neighbor vehicles starts to take place gradually. As presented in Figure 4.2 the stages of cooperation are firstly tested independently and then, combined. Firstly, (Scenario 2.1) uses Scenario 1.3 as the base case and then gives downstream vehicles to the EmV a lateral speed to move to the side. As a more effective method to create space for the EmV to move freely on Scenario 2.2 a green corridor for the EmV. Trying to improve this method, Scenario 2.3 is invented, where a lateral speed is also given to the vehicles, other than their changed hard bounds. Last, but not least, in Scenarios 2.4 and 2.5 the corridor is moved to the left side of the road.

Scenario 2.1

Starting cooperation, a small lateral speed is given to the neighbor vehicles in front of the EmV to open up the way for it to pass through traffic, while it has been centered in the middle of the road (from previous scenarios). This is the first methodology tested for creating space for the EmV. The results for scenario 2.1, involving the average speed and the flow of the vehicle population are not noted to be influenced by this alteration since their average speed remains the same or in some cases even increases (for 50 or 100 vehicles the population average longitudinal speed is measured equal to 0.02m/s - 0.12m/s higher, accordingly).

Regarding the longitudinal speed of the EmV a significant raise in every traffic density scenario is noted. For 50 vehicles the average speed increases almost 0.2m/s (39.59m/s). For 100 vehicles the improvement is about the same (~0.2m/s) with an avg. speed: 36.76m/s. In the last case, with 150 vehicles, avg. speed: 30.22m/s which is less than the speed measured in Scenario 1.3. In conclusion, this method, individually is not the best solution to giving out EmV space to move.

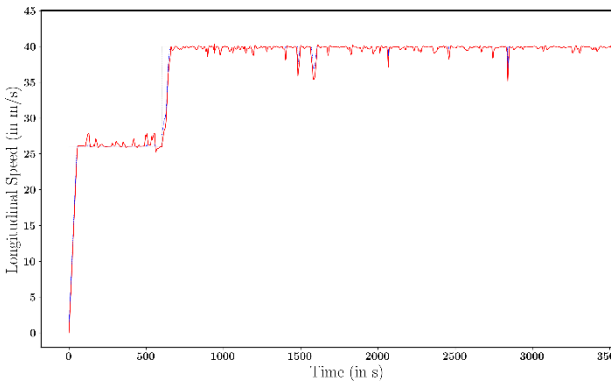

(a): 50 vehicles

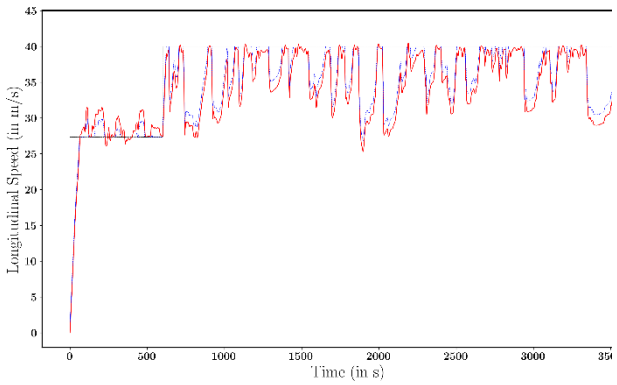

(b): 100 vehicles

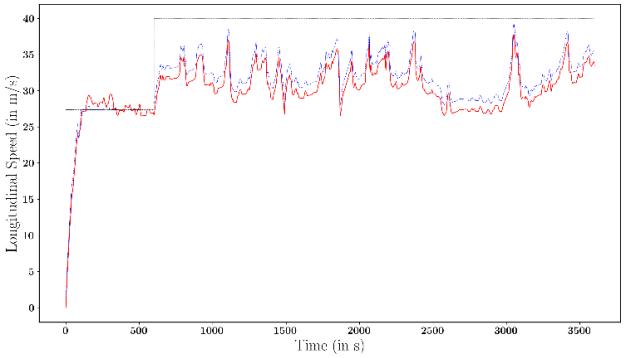

(c) : 150 vehicles

Figure 5.13: Scenario 2.1 - EmV's real time longitudinal speed (m/s)

The EmV is centered, and other vehicles are moved to the side, when possible, so, the plots of lateral speed seem rational, since the EmV moves mainly in the center of the road.

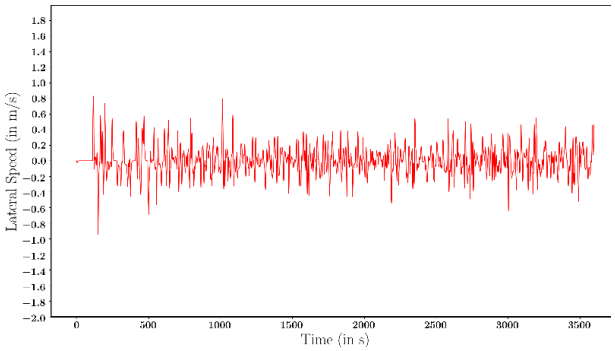

(a): 50 vehicles

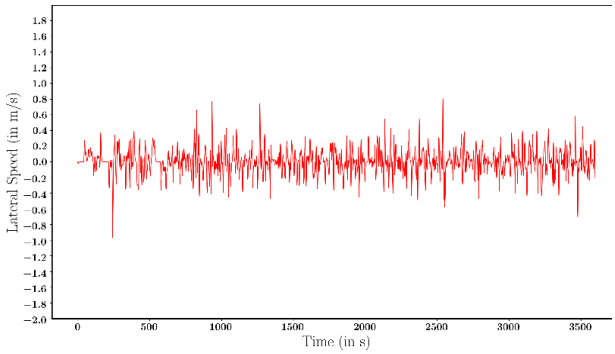

(b): 100 vehicles

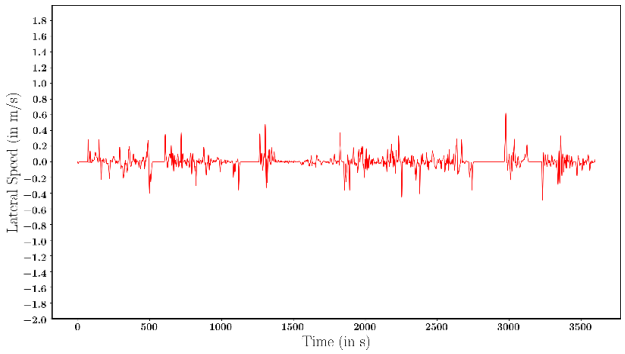

(c) : 150 vehicles

Figure 5.14: Scenario 2.1 - Lateral Speed (m/s)

The speed of the population is a good sign but, regarding the EmV's performance, a noticeable velocity drop (from 31.41m/s in Scenario 1.3 to 30.22m/s) is noticed for 150 vehicles traffic density. Summing up, the lateral speed to the front vehicles is not an effective alteration to help the EmV reach its goals and complete its aim as a faster vehicle. From the simulations, it is noticed that when there is space, the neighbor vehicles obey the "order" and move to the side as shown in the figure below:

Figure 5.15: Timing in scenario 2.1 where downstream vehicles find space to move to the side.

Nevertheless, when there is no space for the vehicles to move to the side, space in not created for the EmV to pass through. In Figure 5.20 a case like that is noticed where making space for the EmV is not feasible.

Figure 5.16: Timing in scenario 2.1 where space is difficulty found for EmV to pass through.

For all traffic densities, the plots for the longitudinal acceleration follow the same pattern so no further conclusion is made. We still notice some major decelerations and figure out that happen due to circumstances like the one captured on Figure 5.16.

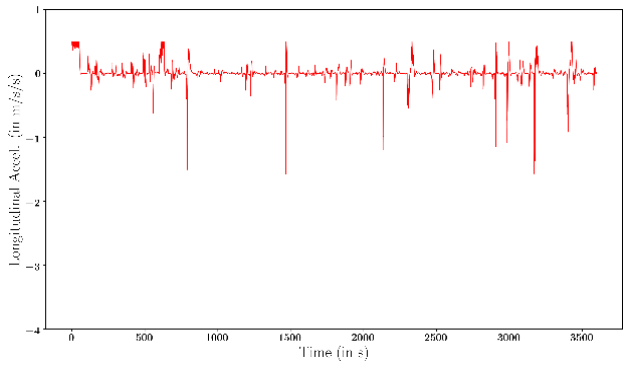

(a): 50 vehicles

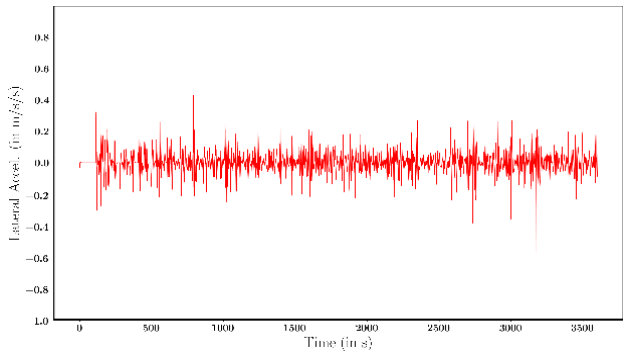

(a) : 50 vehicles

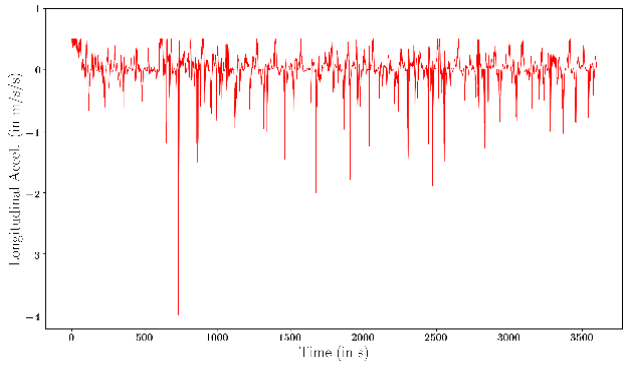

(b): 100 vehicles

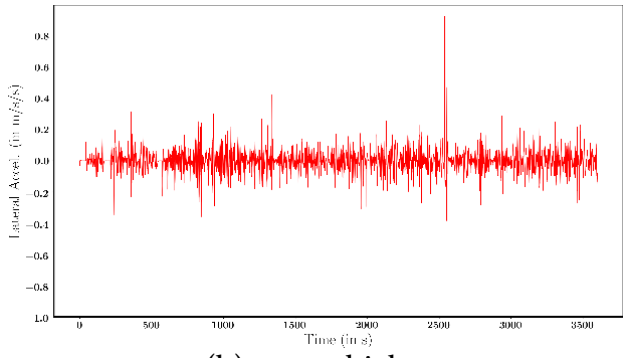

(b): 100 vehicles

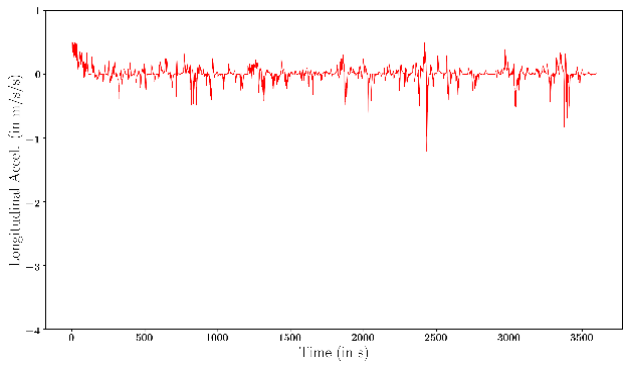

(c) : 150 vehicles

Figure 5.17: Scenario 2.1 - Longitudinal Acceleration (m/s/s)

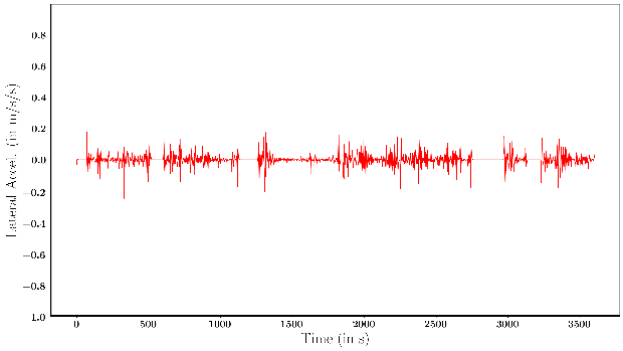

(c) : 150 vehicles

Figure 5.18: Scenario 2.1 - Lateral Acceleration (m/s/s)

Similarly, regarding the lateral acceleration, as in every scenario till now with gradually increasing traffic densities, as the road hosts more vehicles, the lateral acceleration moves in a smaller range, as maneuvers and overpassing become more difficult.

Since the results regarding the average speed of the EmV are not extraordinary improved, we continue with the next step of variations in Scenario 2.2 with a change of the lateral bounds in order to create a green corridor.

Scenario 2.2

On this stage of variations, a green corridor is created for the EmV in the middle of the road, as a more effective solution. By changing the hard bounds of the vehicles in a certain beam in front of the EmV we manage to create an Emergency "lane" in its personalized to EmV dimensions, in order for it to travel faster. More briefly, the neighbor vehicles' hard bounds are adjusted to the EmV's lateral position. By setting the lateral hard bounds of the stated vehicles in front of the EmV accordingly, the road is separated into 3 parts. The vehicles detected on the front left-hand side of the EmV, when the siren is activated, are forced to travel on the top part of the road (bounds [5+ε,10-ε]) and the vehicles on the front right-hand side of the Emergency are forced to travel on the bottom part of the road (bounds [ε,5-ε]). Here, ε is a small safety distance whose value depends on the controlled vehicle's and the EmV's dimensions.

Figure 5.19: Green Corridor in the middle of the road

The EmV's real time longitudinal and lateral speed such as its longitudinal and lateral acceleration are plotted in Figure 5.20 and Figure 5.21.

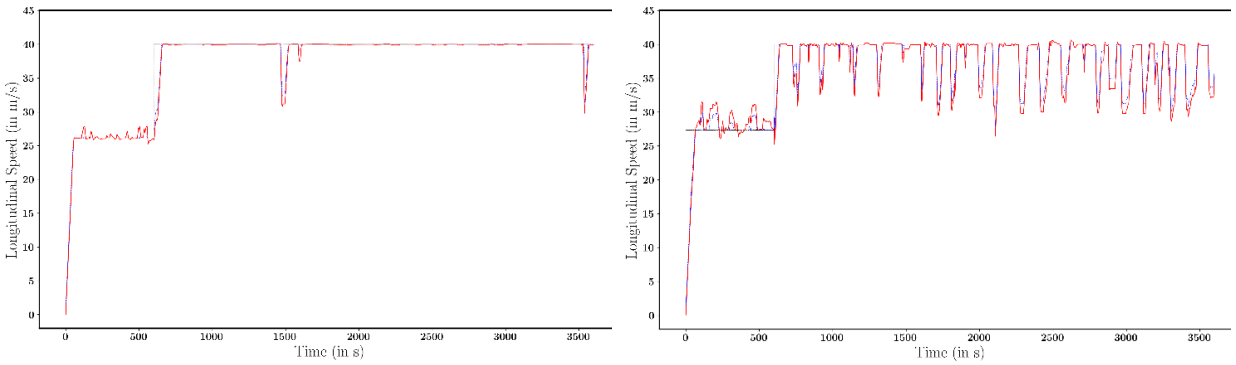

(a): 50 vehicles (b): 100 vehicles

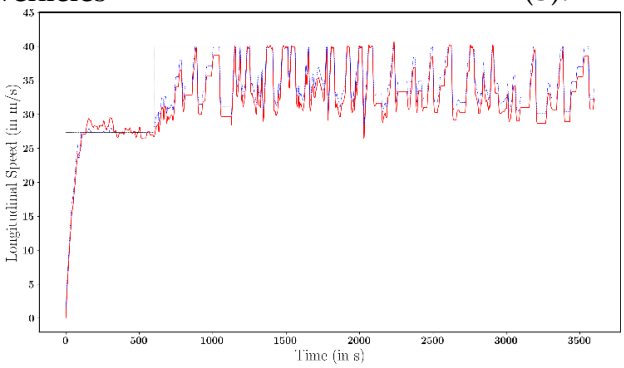

(c) : 150 vehicles

Figure 5.20: Scenario 2.2 - EmV's real time longitudinal speed (m/s)

The results are good, since the average speed of the EmV performs a great improvement for every traffic density (50-150 vehicles) and no crashes are detected, making the green corridor a safe solution to the EmV Problem. In more detail, for 50 vehicles the average speed was 39.83m/s, for 100 vehicles the average speed was 39.08m/s (the greatest till now), and for 150 vehicles 35.76m/s. The results are great. From the simulation videos as well, the vehicles seem to easily adapt and keep up with the change of the hard bounds.

By observing the longitudinal speed of the EmV from the plots on Figure 5.20 in the 50 vehicles traffic density scenario, it is noticed that our vehicle of interest seems to keep its 40m/s speed steady for long periods for the first time. As traffic density increases, the need for the green corridor becomes more critical, since keeping a high real time speed becomes more difficult. The results are noticeably improved, compared to all scenarios taken into consideration till now. For 100 vehicles, the average speed reaches 39.08m/s, which is a record high and for 150 vehicles the average speed of the EmV is 35.76m/s, which is 1.6m/s higher than Scenario 2.1 with the lateral speed given to vehicles downstream the EmV and 7.1m/s higher than Scenario 1.3 without the corridor. The EmV travels with 40m/s during most of the simulation and performs some drops that are quickly corrected. Even for 150 vehicles traffic density, our vehicle reaches its target speed for the first time! In both 100 and 150 vehicle cases, the reason for the velocity drops is dense traffic, that makes even the hard bound difficult to be activated, without intervening furthermore to the network's safety features.

Moreover, this change of the hard bounds does not seem to affect the traffic's behavior in the big picture, regarding the average speed of the population, which is not decreased. To the contrary, it is even increased for the 150 vehicles' case by 0.21m/s.

Travelling in the green corridor, the EmV's lateral speed moves into a much smaller range: from [-0.8m/s,0.8ms] to [-0.3m/s-0.3m/s]. Which means that our vehicle utilizes the corridor and stays in it.

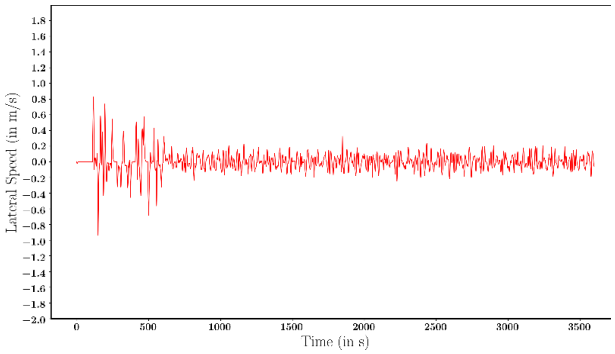

(a): 50 vehicles

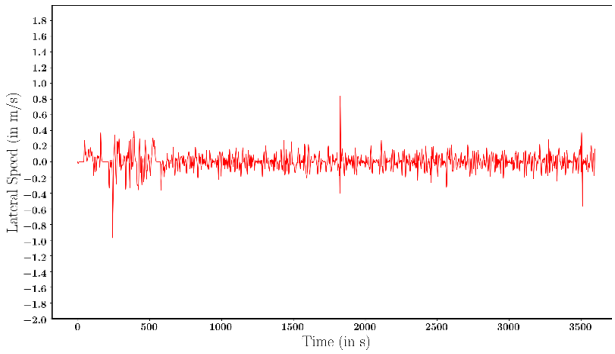

(b): 100 vehicles

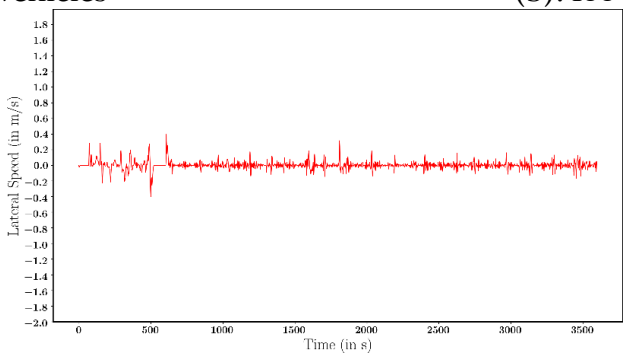

(c) : 150 vehicles

Figure 5.21 Scenario 2.2 - Lateral Speed (m/s)

Regarding the longitudinal acceleration no major drops are captured during 50 vehicles' simulation and most of them are seen during the 150 vehicles' simulation. In Scenario 2.3 we will try to improve that as well.

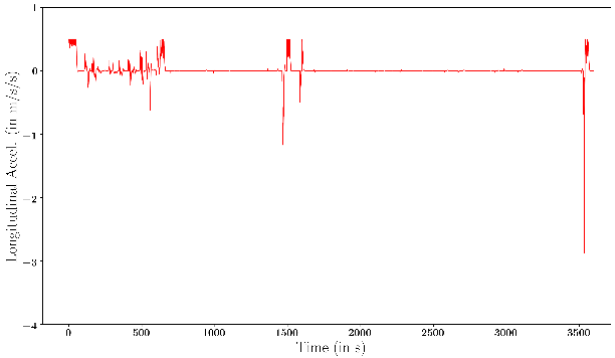

(a): 50 vehicles

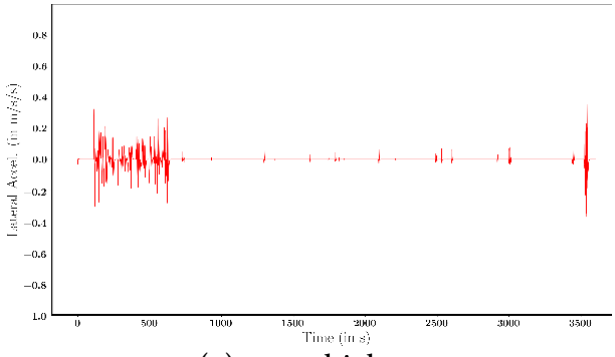

(a): 50 vehicles

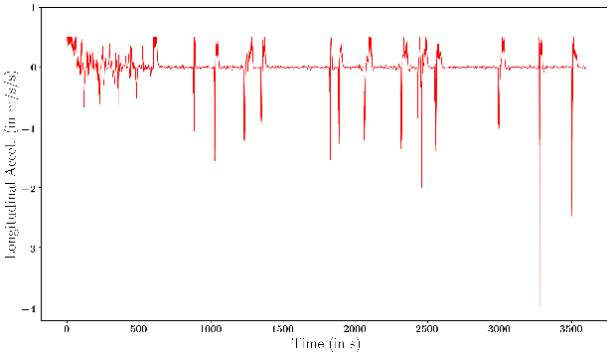

(b): 100 vehicles

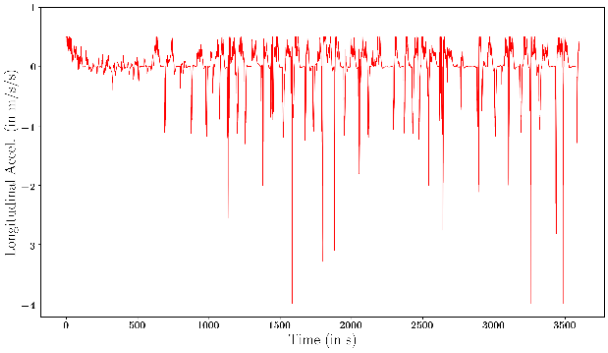

(c) : 150 vehicles

Figure 5.22 Scenario 2.2 - Longitudinal Acceleration (m/s/s)

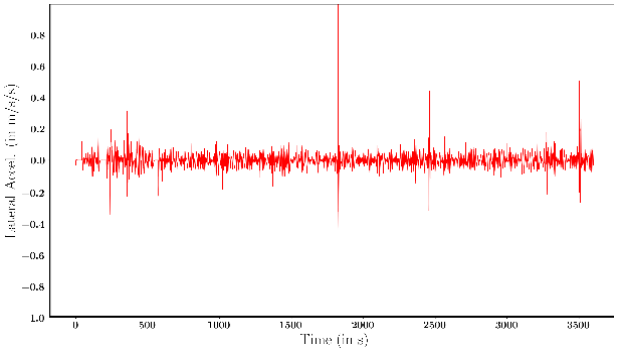

(b): 100 vehicles

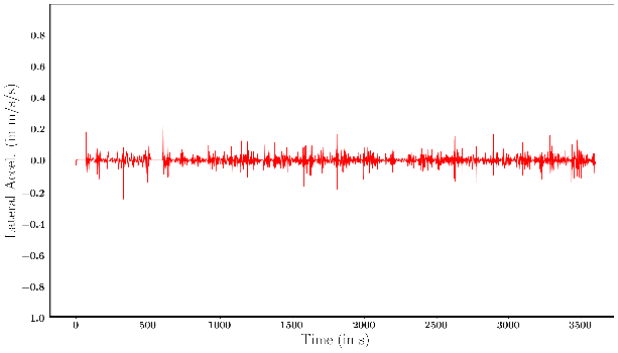

(c) : 150 vehicles

Figure 5.23: Scenario 2.2 - Lateral Acceleration (m/s/s)

Scenario 2.3

On the next stage of variations, we try to improve the green corridor's efficiency further by also giving a lateral speed to the downstream neighboring vehicles. Theoretically, this will "help" them move more quickly to their right or left part of the road and will correct the longitudinal speed drops noticed on the previous scenario (2.2). Our estimation was correct since the drops become much rare. In more detail, for 100 vehicle the noticeably velocity drops are only 5 compared to 20 on scenario 2.2. As a result, the average speed is also increased from 39.08m/s to 39.35m/s which is not huge, but shows that the modifications move in the right direction. On the other hand, for 150 vehicles, the average speed of the EmV is slightly decreased by 0.08m/s (from 27.92m/s to 27.84m/s).

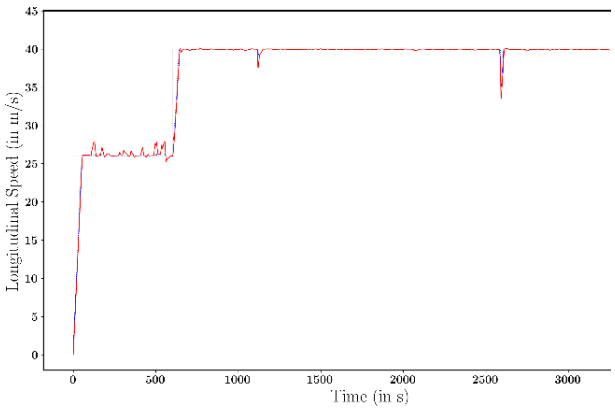

(a): 50 vehicles

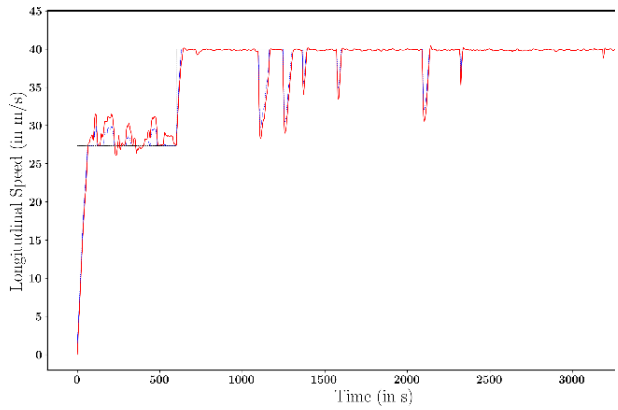

(b): 100 vehicles

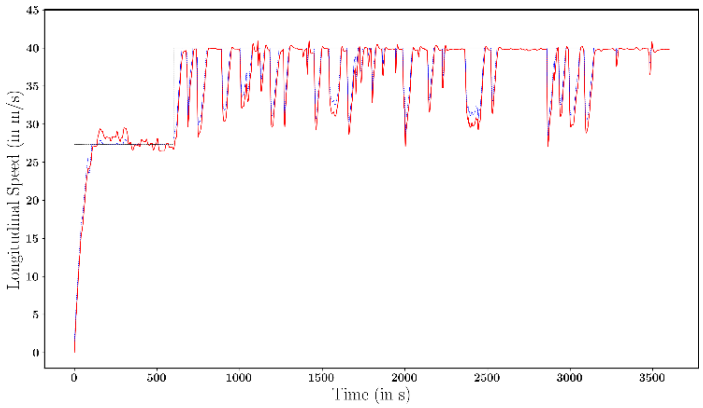

(c) : 150 vehicles

Figure 5.24 Scenario 2.3 - EmV's real time longitudinal speed (m/s)

The lateral speed shown below keeps following the same pattern and no further conclusion is made by it.

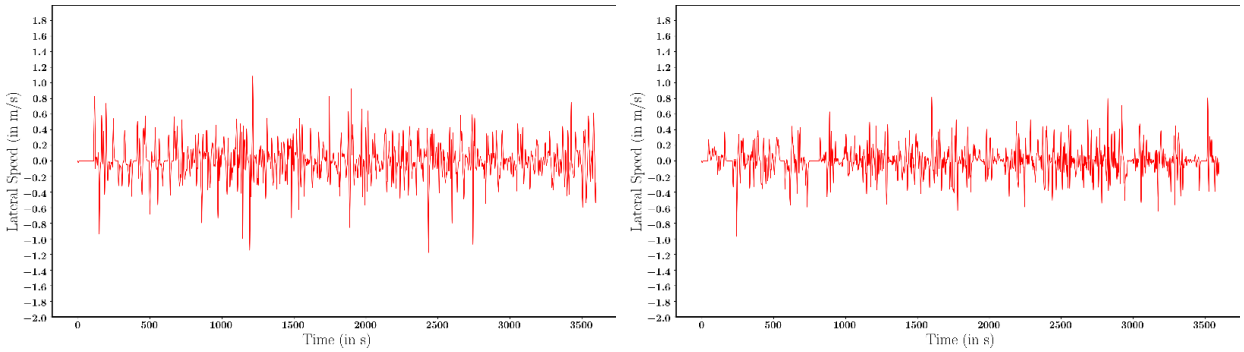

(a): 50 vehicles (b): 100 vehicles

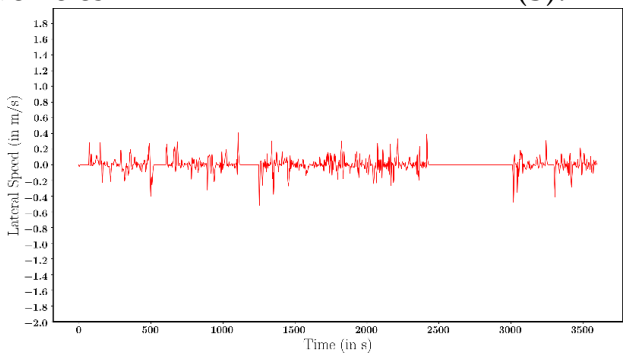

(c) : 150 vehicles

Figure 5.25: Scenario 2.3 - Lateral Speed (m/s)

By giving the neighbor vehicles lateral speed, we help the EmV efficiently reach its goals, since a noticeable improvement is detected in its longitudinal accelerations. In both 100 and 150 vehicles' simulations the EmV decelerates more than half times less compared to Scenario 2.3. In conclusion, giving a lateral speed is a change to be kept in our method.

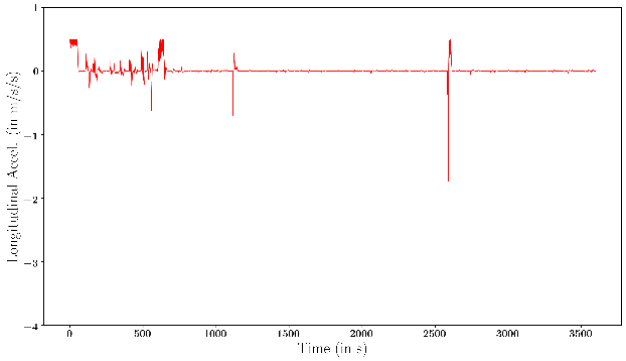

(a): 50 vehicles

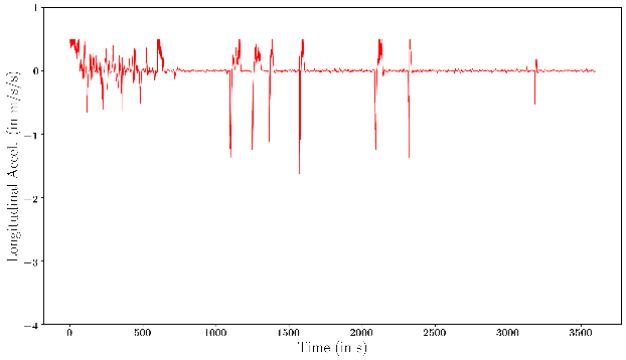

(b): 100 vehicles

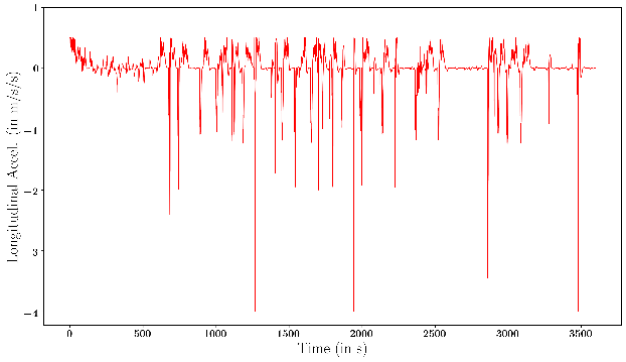

(c) : 150 vehicles

Figure 5.26: Scenario 2.3 - Longitudinal Acceleration (m/s/s)

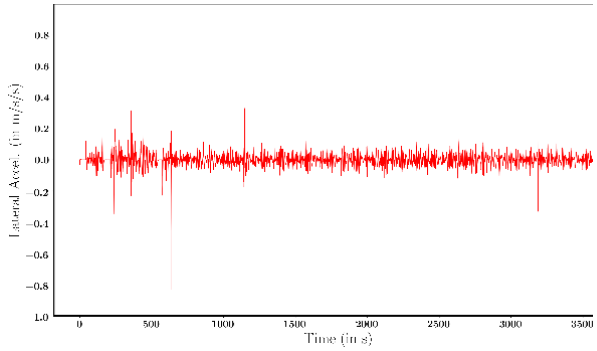

(a) : 50 vehicles

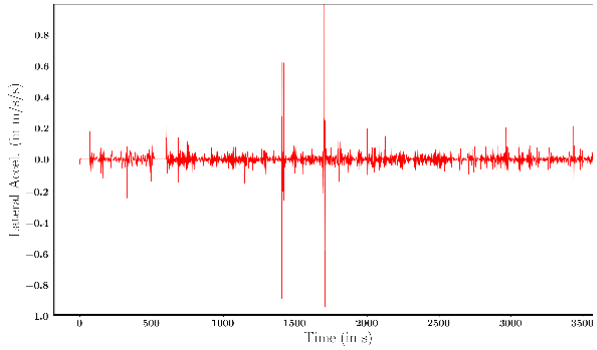

(b): 100 vehicles

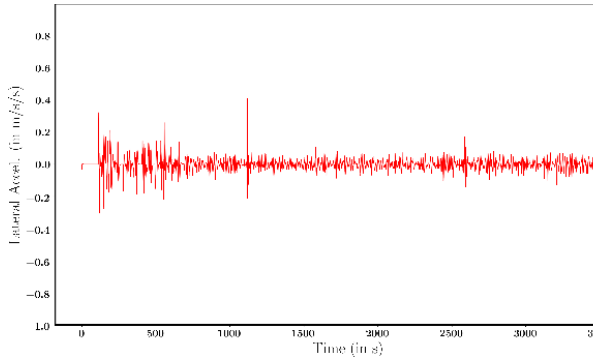

(c) : 150 vehicles

Figure 5.27: Scenario 2.3 - Lateral Acceleration (m/s/s)

Scenario 2.4

Intuitively, it is believed that moving to the center of the road gives more choices to any independent vehicle traveling on the road, since it can easily make overpasses and maneuvers to any direction needed. In Faros' diploma thesis [38], it was tested and proven that this intuition was correct. So, in this stage of alterations the same issue was tested for the green corridor. In human driven vehicles, the EmV corridor is set to be the right lane. On the contrary, in Scenario 2.2 and 2.3 the green corridor was emplaced in the center of the road, since the EmV independently was measured to move faster, when travelling close to the road center. In Scenario 2.4 the green corridor is created with the same methodology as described in the previous two cases, but is located on the left side of the road, without giving any lateral speed to downstream vehicles yet.

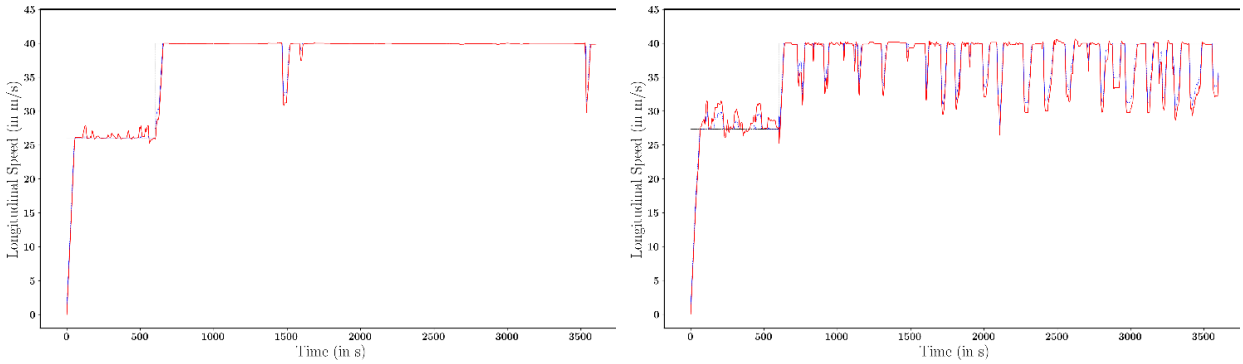

(a): 50 vehicles (b): 100 vehicles

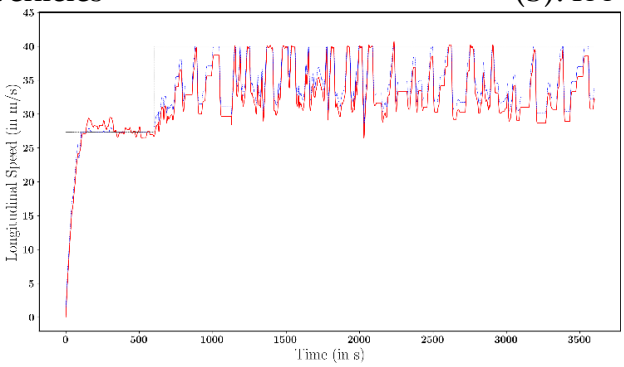

(c) : 150 vehicles

Figure 5.28: Scenario 2.4 - EmV's real time longitudinal speed (m/s)

By evaluating the results regarding the average speed of the EmV, the relocation of the corridor is not a good practice since the average speed drops in all traffic density scenarios. From 0.3m/s in low traffic density (50 vehicles) to 2.34m/s (in 150 vehicles). In detail, for 50 vehicles, avg. speed: 39.61m/s, for 100 vehicles, Avg. Speed: 37.56m/s, and for 150 vehicles, Avg. Speed:33.42m/s. The average speeds are compared to Scenario 2.2, where no lateral speed is given to the downstream vehicles, only the hard bounds are altered. And the results are better for the corridor in the middle. Before we come to a conclusion, Scenario 2.3 will be compared to the next Scenario taking place (2.5), where lateral speed is given additionally.

More briefly, in 150 vehicles, when vehicles travel having the same longitudinal position (in parallel), even if the hard bound is changed, it is not evitable to move to the side and risk crashing with those vehicles. In Figure 5.29 a case like that is spotted, where two vehicles are in the green corridor of the EmV.

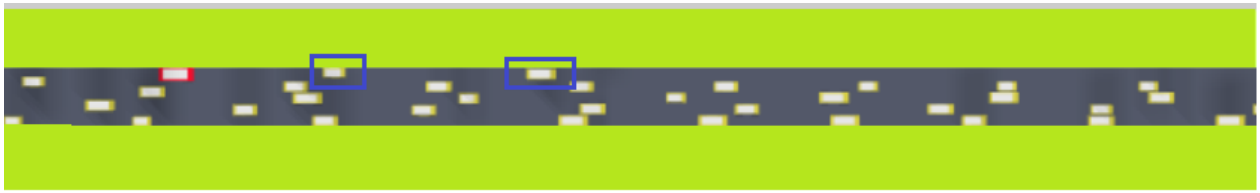

Figure 5.29: Timing in scenario 2.4 where the green corridor on the left side of the road phases difficulties: there is not always space for vehicles to move to the right in dense traffic.

When the Emergency corridor is placed in the left side of the road the lateral speed of our vehicle of interest is kept steady for the first time. In these means, it is easier for the EmV to stay in its lane, since it doesn't get "nudged" by other vehicles.

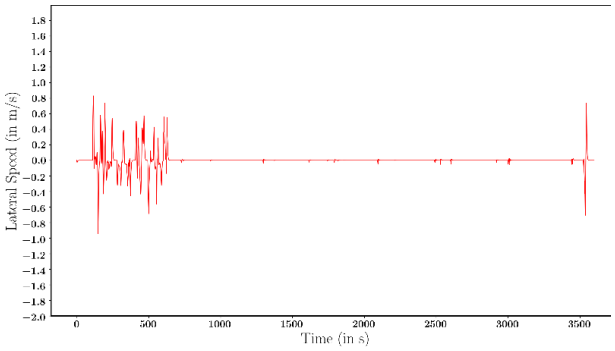

(a): 50 vehicles

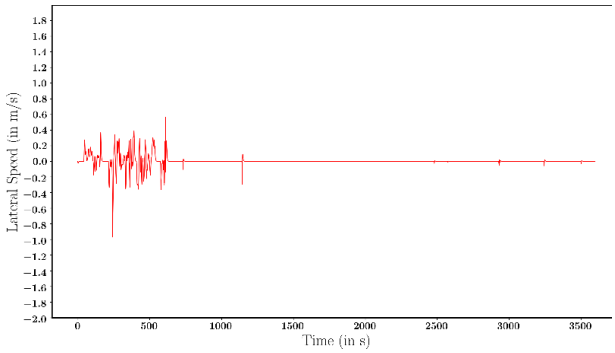

(b): 100 vehicles

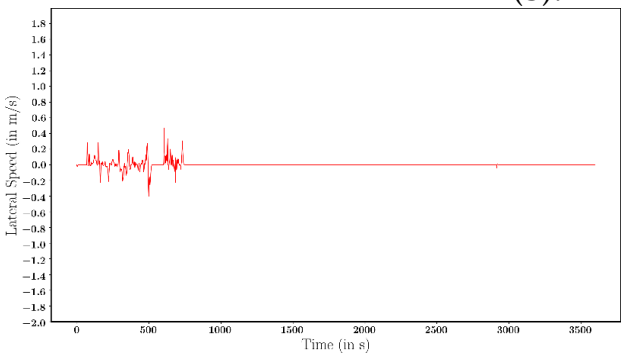

(c) : 150 vehicles

Figure 5.30: Scenario 2.4 - Lateral Speed (m/s)

The lateral acceleration is kept close to 0 after the activation of the corridor which shows that the EmV stays and utilizes the green corridor created. Though the longitudinal acceleration performs many ripples and moves in a wide range, especially regarding the negative longitudinal acceleration. In this means, even a corridor is created for the Vehicle to move freely and independent from the rest of the vehicle population, it is forced to decelerate noticeably a couple of times during the simulation.

From the video it is seen that the decelerations take place due to the vehicles that travel for some seconds on the green corridor.

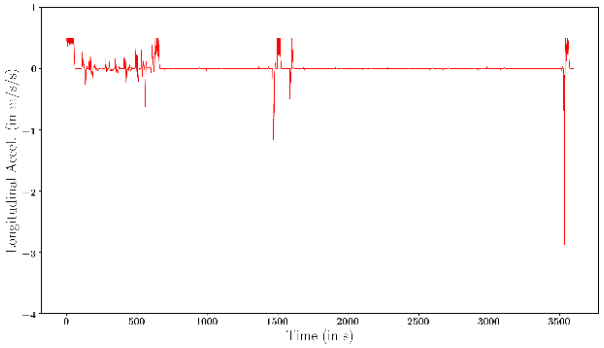

(a): 50 vehicles

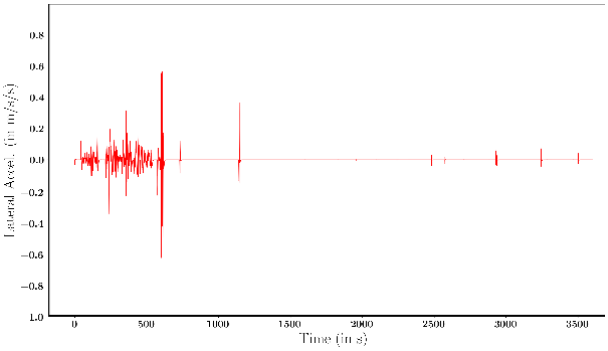

(a): 50 vehicles

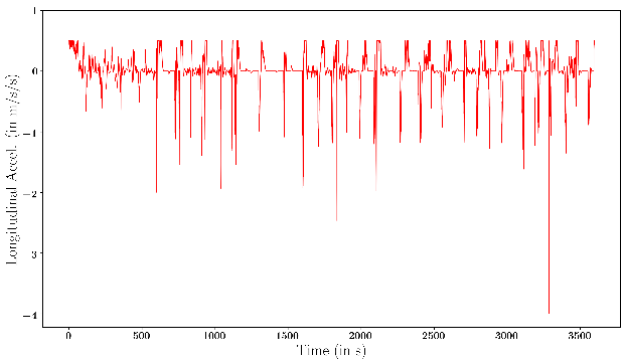

(b): 100 vehicles

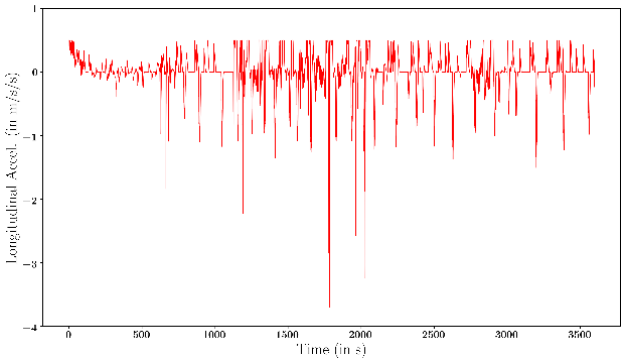

(c) : 150 vehicles

Figure 5.31: Scenario 2.4 - Longitudinal Acceleration (m/s/s)

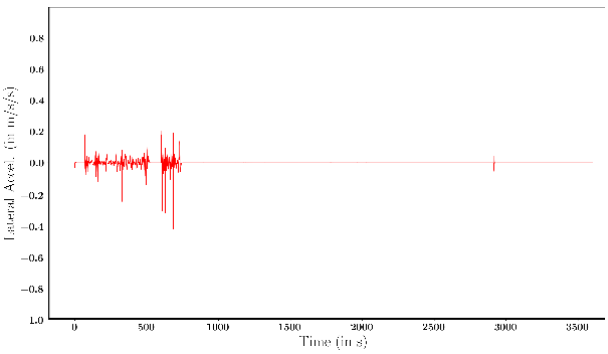

(b): 100 vehicles

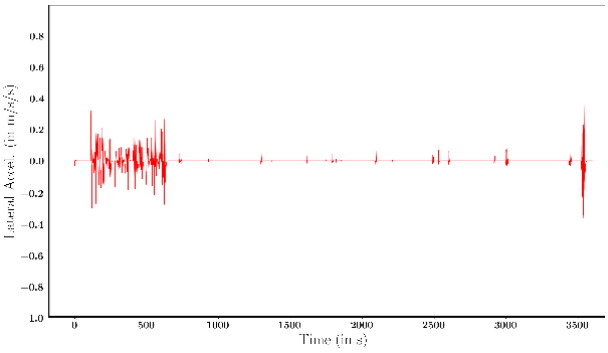

(c) : 150 vehicles

Figure 5.32: Scenario 2.4 - Lateral Acceleration (m/s/s)

Scenario 2.5

In the last stage of variations, a lateral (negative) speed is given to all traffic population in order to move to the right part of the road. Compared to Scenario 2.4 with no lateral speed and the green corridor on the left part of the road, an improvement is noticed regarding the average speed of the EmV. Nevertheless, the longitudinal average speed results are still appreciably lower than Scenario 2.3 with the green corridor in the center of the road.

In more detail, for 50 vehicles the average speed was measured equal to 39.63m/s, which is 0.2 m/s lower than in Scenario 2.3. For 100 vehicles the average speed was equal to 38.34m/s, 1m/s less than the Scenario we compare it to. And finally, for 150 vehicles the average speed was measured much less, almost 4m/s less than in scenario 2.4, equal to 33.97m/s. Specially the final measure, can help us reject the left side of the road corridor and conclude to the one in the middle as best practice.

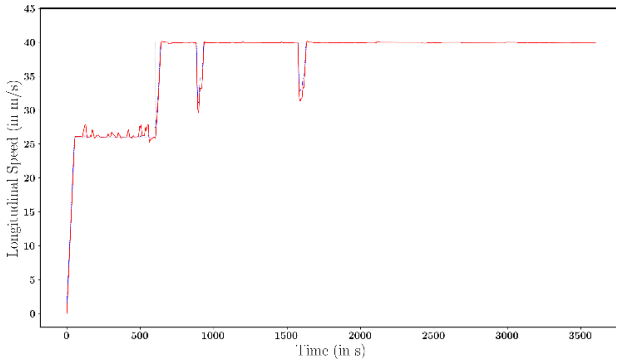

(a): 50 vehicles

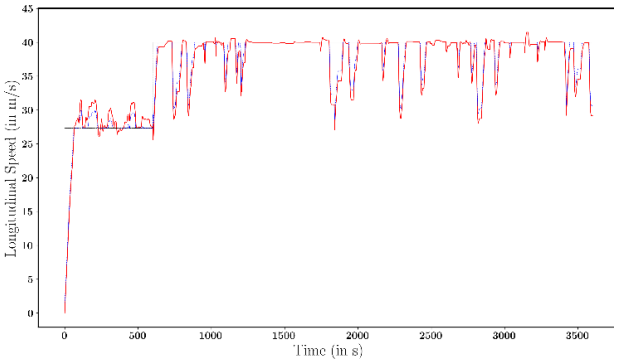

(b): 100 vehicles

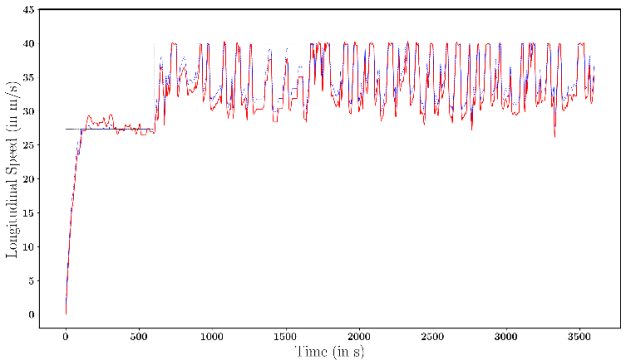

(c) : 150 vehicles

Figure 5.33: Scenario 2.5 - EmV's real time longitudinal speed (m/s)

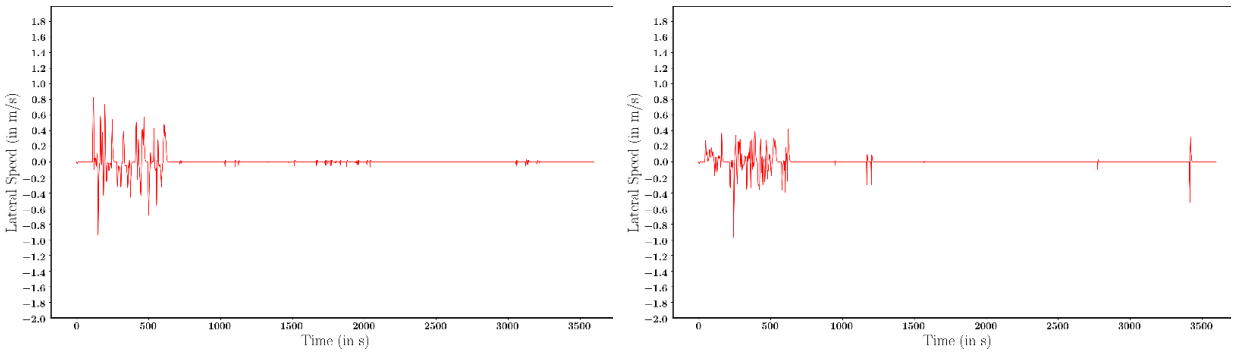

(a): 50 vehicles (b): 100 vehicles

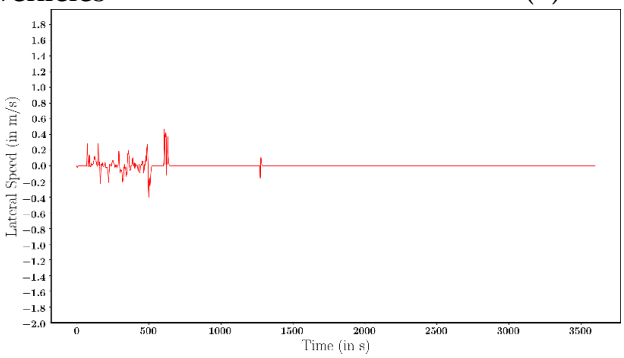

(c) : 150 vehicles

Figure 5.34: Scenario 2.5 - Lateral Speed (m/s)

Longitudinal acceleration has no point to be reviewed at this point. The lateral acceleration follows the same pattern as the lateral speed in both Scenarios 2.4 and 2.5, with a smaller range, almost steady value which infer a very steady, longitudinal movement of the EmV.

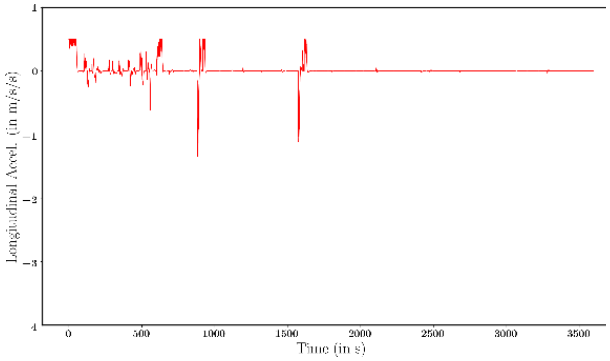

(a): 50 vehicles

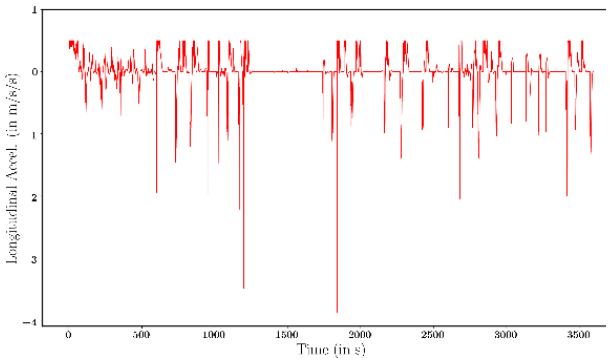

(b): 100 vehicles

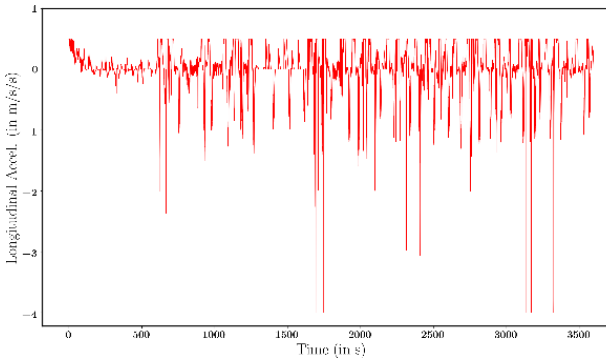

(c) : 150 vehicles

Figure 5.35: Scenario 2.5 - Longitudinal Acceleration (m/s/s)

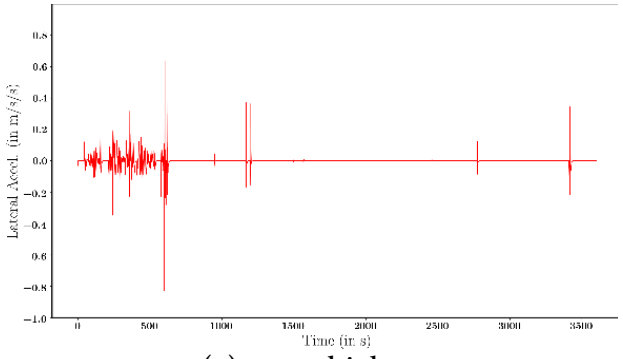

(a): 50 vehicles

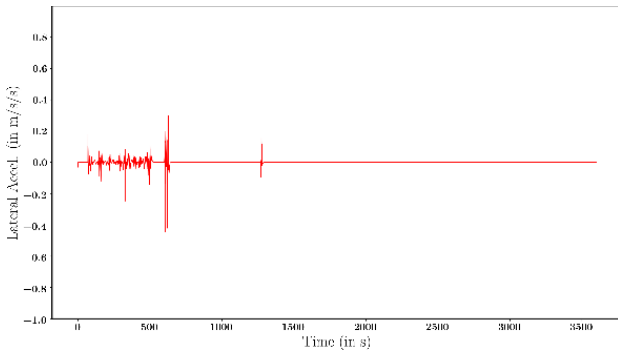

(b): 100 vehicles

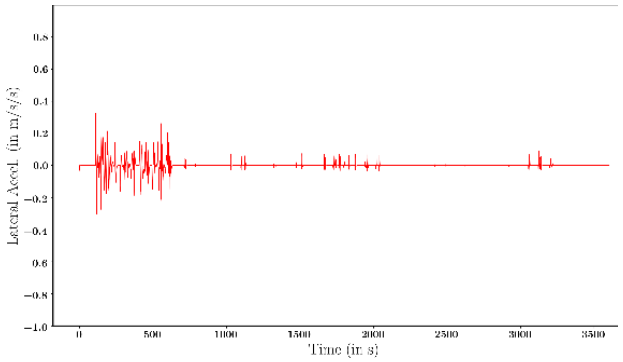

(c) : 150 vehicles

Figure 5.36: Scenario 2.5 - Longitudinal Acceleration (m/s/s)

5.2.3 Comparison of Passive and Active Approaches

As shown on Figure 5.37, the changes made in each stage of the passive approach bring an increase on the real time speed of the EmV and as result to a better average speed in low traffic densities. Specifically, in Scenario 1.2, decreasing the time-gap results to a major increase on longitudinal speed for the EmV (32.12m/s->36.62m/s), as it becomes more flexible on the road. It easily maneuvers and overpasses other vehicle and that is also shown on the plots of the lateral speed and acceleration. Compared to 1.1, Scenario 1.2 has a greater range of lateral accelerations: in a range of (-0.3m/s/s to 0.3m/s/s), with a max lateral acceleration of 0.3m/s/s that is reached only three times during the simulation. The EmV starts to max perform its max accelerations of $(-0.38m/s/s \; - \; 0.38m/s/s)$ ten times during the simulation and its plot is denser. Which proves that it is for sure more flexible. Continuously, when centering is activated on Scenario 1.3 a small decrease in speed (0.21m/s) is noticed for 100 vehicles. Regarding the fact though, that we still have a relevant increase in the average speed for 150 vehicles, the centering alteration is not considered as productive but is kept in the base case for the Active Approach. The improvement in the EmV's performance is present but is not so noticeable.

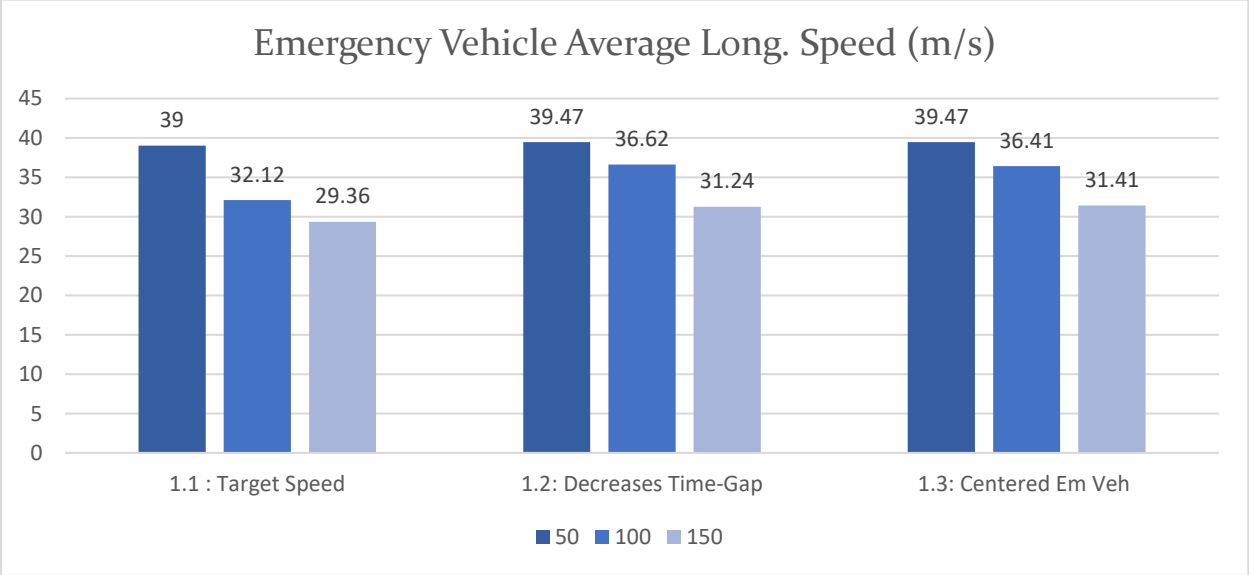

Figure 5.37: Comparison of Non-Cooperative Approach Methods

Other than average speeds as a number, there is a point in comparing the longitudinal speeds during the whole simulation from Scenarios 1.1-1.3. Taking 100 vehicles as a medium case, the diagrams below plot the EmV's longitudinal speed in scenarios 1.1, 1.2 and 1.3.

As we add to our modifications, the EmV seems to reach its higher speed of (40m/s) more frequently and seems to keep it for a longer time.

Taking 100 vehicles as a medium case, Figure 5.38 plots the EmV's average speed for 100 vehicles' traffic density for scenarios 1.1, 1.2 and 1.3.

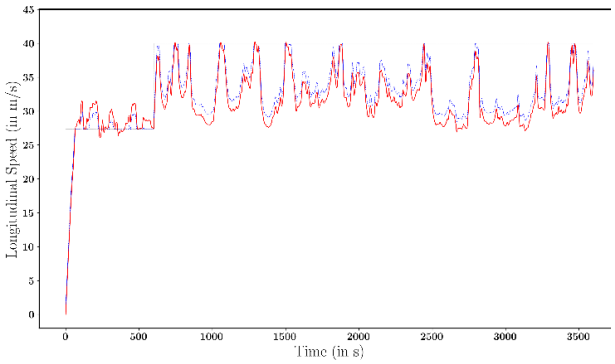

(a) : Scenario 1.1, Avg. Speed: 32.12 m/s,

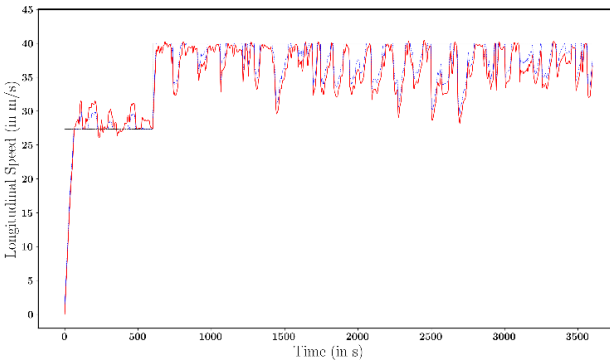

(b) : Scenario 1.2, Avg. Speed: 36.62m/s

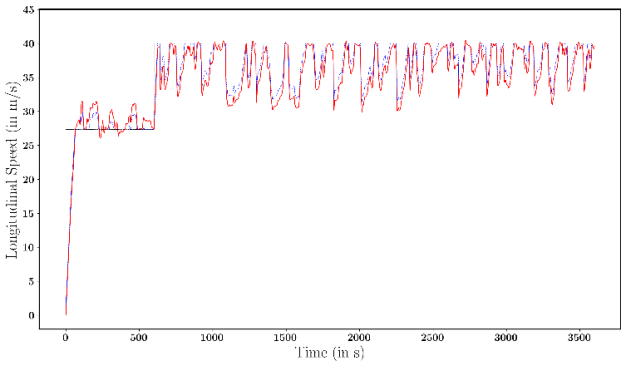

Figure 5.38: EmV's real time longitudinal speed

(c) : Scenario 1.3, Avg. Speed: 36.41m/s

It is noticed that huge instant ripples in velocity drops take place on the longitudinal acceleration which implies that the EmV gets slowed importantly in some cases during the simulation. From the simulation videos, it is found that these major decreases in speed are caused by the vehicles difficulty to get out of slow rows on the road boundaries. As a result, centering is implemented.

Moving on to Scenario 1.3, these ripples in longitudinal acceleration seem to be decreased, but are not eliminated. So, these issues will be resolved by the variations in the Active Approach, where the neighbor vehicles will be called to "help" the EmV reach its goals.

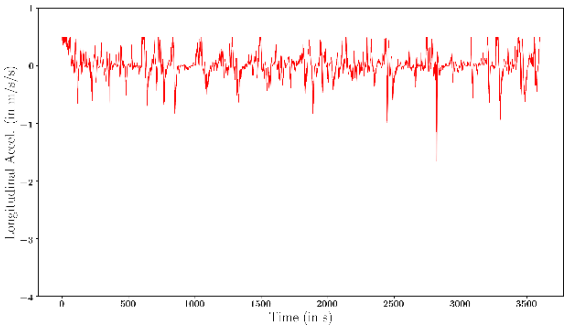

(a) : Scenario 1.1

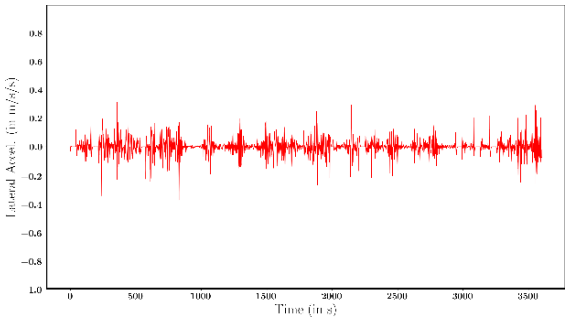

(a) : Scenario 1.1

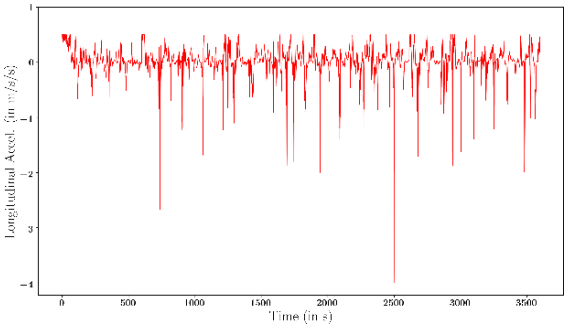

(b) : Scenario 1.2

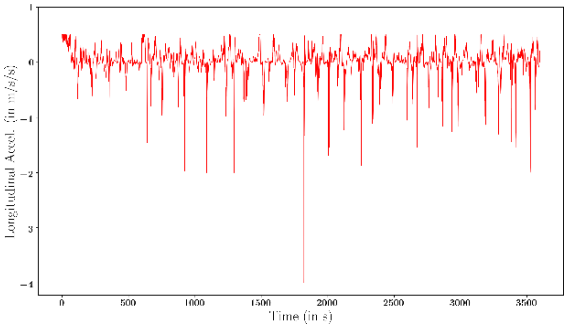

(c) : Scenario 1.3

Figure 5.39: Longitudinal Acceleration (m/s/s)

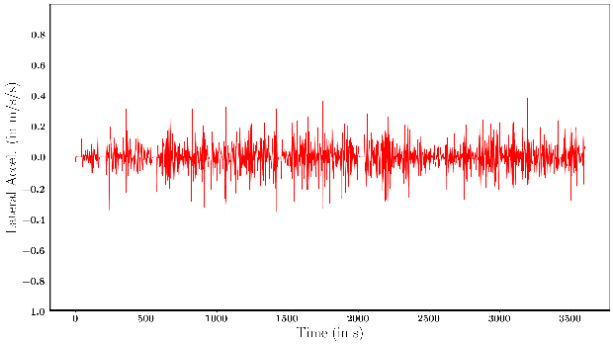

(b) : Scenario 1.2

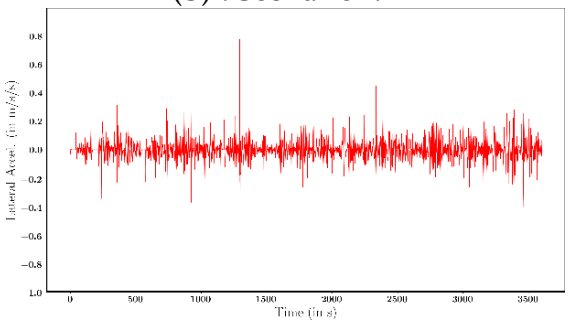

(c) : Scenario 1.3

Figure 5.40: Lateral Acceleration (m/s/s)

Regarding the lateral speed and acceleration, the help us confirm our conclusion that decreasing the time-gap makes it more active and flexible and centering controls this lateral movement in some extent. From 0.7m/s max lateral speed it is dropped to 0.6, which is reached less frequently, and most importantly, during most of the simulation the lateral speeds have an average of 0.3m/s.

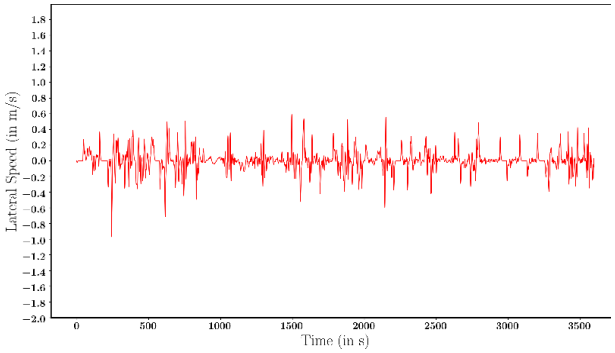

(a) : Scenario 1.1

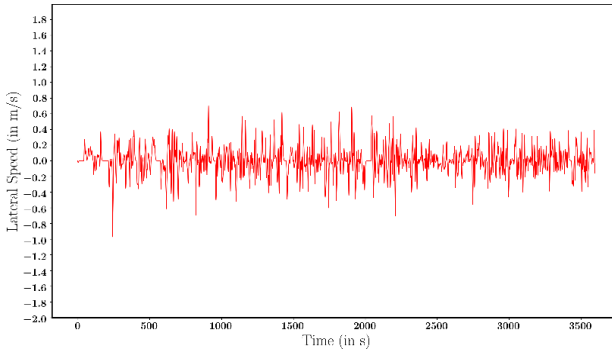

(b): Scenario 1.2

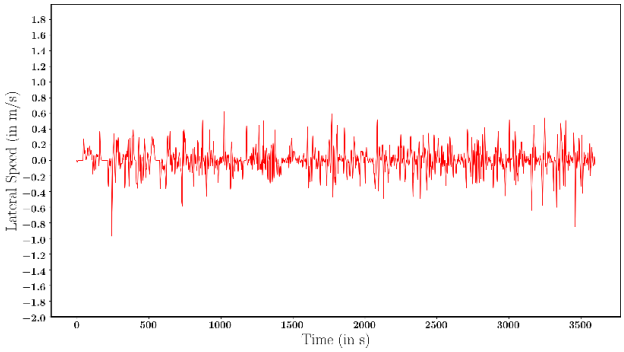

(c) : Scenario 1.3

Figure 5.41: Lateral Speed (m/s)

Moving on the Active approaches, to choose the most efficient strategy for the cooperative approach, it is crucial to compare scenarios for the same traffic densities and the same conditions of simulation in general.

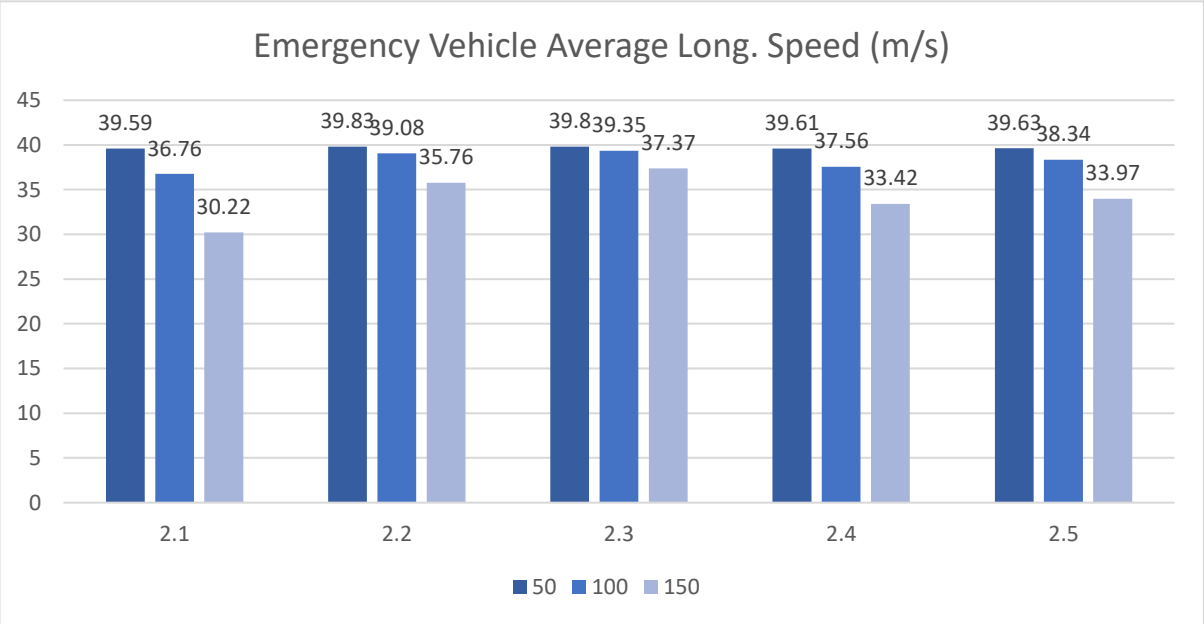

Figure 5.42: Comparison of Active Approach Methods

As shown in Figure 5.42, for 50 vehicles the maximum average speed is noticed during Scenario 2.2 with 39.83m/s, but in low traffic densities the results were good in general. The values that indicate more targeted the efficiency of the different methods are the values of the average speed for 100 and 150 vehicles' traffic density, where opening up the way becomes crucial. For high densities the record highs take place in Scenario 2.3 where the green corridor is created and emplaced in the middle of the road and a lateral speed is given to the downstream neighbor vehicles. 37.37m/s for 150 vehicles in traffic is a great improvement in performance (27.3%) compared to just giving a higher speed to the EmV, without any further alterations and cooperation with other vehicles.

In Figure 5.40, the average speed of the EmV is plotted for 100 vehicles' simulations.

Longitudinal Speed of the EmV for Cooperative Approach all scenarios

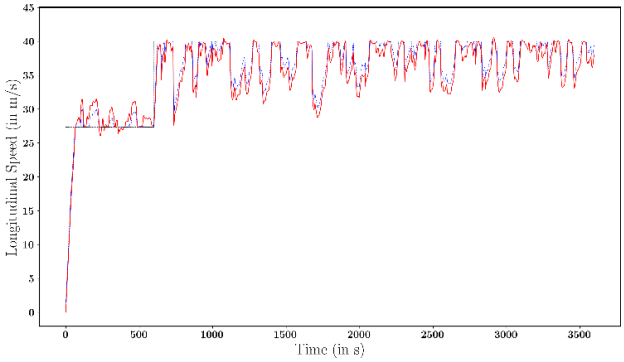

(a) : Scenario 2.1, Avg Speed: 36.37m/s

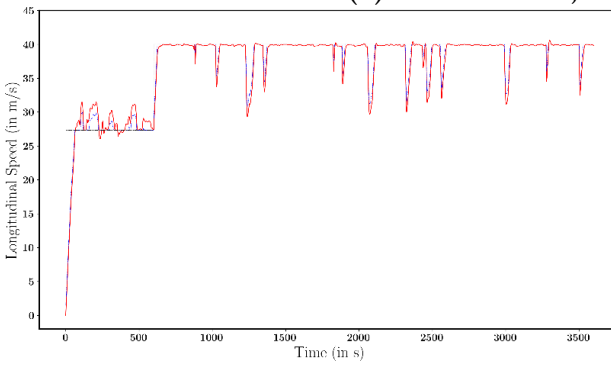

(b) : Scenario 2.2, Avg Speed: 39.08m/s

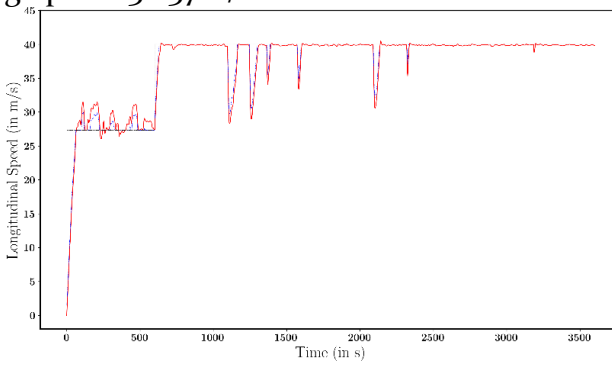

(c) : Scenario 2.3, Avg Speed: 39.35m/s

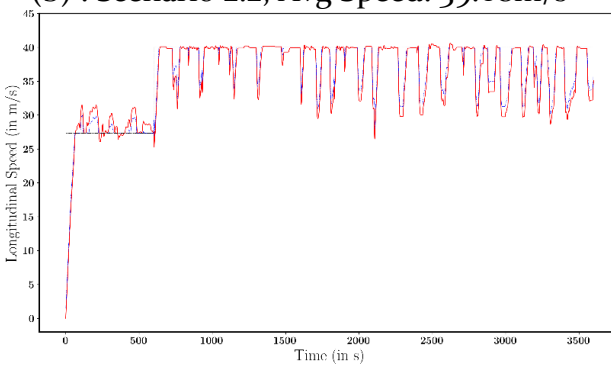

(d) : Scenario 2.4, Avg Speed: 37.56m/s

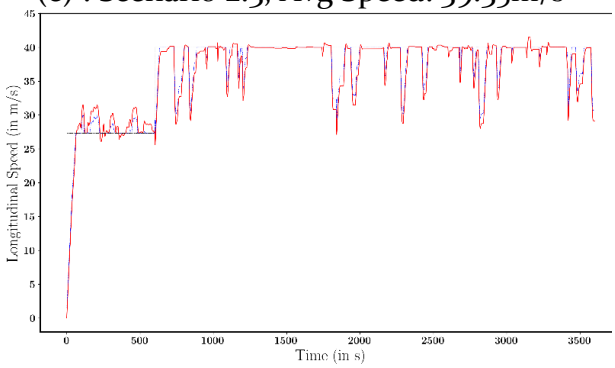

(e) : Scenario 2.5, Avg Speed: 38.34m/s

Figure 5.40: Longitudinal Speed of EmV for all Active Approach Scenarios in 100 vehicle density

As it can be noticed, Scenario 2.2, where the green corridor is first included to our simulations, performs a great increase in average speed compared to Scenario 2.1, where only a lateral speed is given to the downstream neighbor vehicles of the EmV. When these two methods are combined, in Scenario 2.3, the efficiency increases, and we accomplish the greater average speed noted till now.

On the other hand, in Scenarios 2.4 and 2.5,where the corridor is relocated on the left side of the road, performance is not as that good as with the green corridor in the middle of the

road, since it is more difficult for vehicles to move to the side, in cases where four CAVs are travelling in parallel (with the same longitudinal position).

As previously stated, centering of the EmV helps it stay within the green corridor. At first Figure 5.49(a) we center the EmV and give a lateral speed to its downstream vehicles. The greatest magnitude of all Cooperative Approach methods is noted. In this means, the EmV finds it hard to stay on the space made for it because it faces obstacles in its path. So, we can conclude the lateral speed is not enough for the creation of space. On simulation 2.2 (Figure 5.49(b)), when the hard bounds are changed for downstream vehicles, the magnitude of lateral speed is decreased. Which proves our EmV has an easier time focusing on keeping its target speed without needing to search for space to pass through. As we also give a lateral speed to downstream vehicles, combined with the hard bounds, this range becomes even smaller which is rational. Finally, when we set the green corridor on the left side of the road the range minimizes to an almost constant value since the EmV does not have so many options of sides to move towards and it receives less forces from downstream or upstream neighbor vehicles.

Average Speed of Emergency Vehicle

Summing up, as shown in Figure 5.37 every change in of the non-cooperative approaches had a positive impact on the average speed of the EmV as shown in Figure, without resulting to any collisions, all changes were kept and used as a base case for the Active Approach.

Moreover, the changes made in the cooperative approach had a positive impact (Figure 5.42) regarding the creation of the green corridor in the middle of the road and the lateral speed given to downstream vehicle. Practices, such as locating the green corridor on the left side of the road resulted to decreased performance of the EmV, so it will not be considered best practice.

Tables 5.2 – 5.4 below, show the deviation from the desired speed for the EmV or the difference of the real time speed and the target speed. Deviation from the target speed may not be compared only as a number, since, in low traffic densities, it is easier for the EmV to reach and keep its target speed since it has space to move, overpass and make maneuvers. On the other side, as traffic densities increase, this aim becomes harder, so low deviation from the desired speed is more important. In our case, the smaller deviation for 50 vehicles is noticed in Scenario 2.2. But, this value has a much bigger impact in 100 and 150 vehicle traffic density in which the smaller deviation is seen in Scenario 2.3. Concluding, Scenario 2.3 is the most effective till this point.

50 Vehicles Traffic Density

Scenario	1.1	1.2	1.3	2.1	2.2	2.3	2.4	2.5
Deviation from desired speed (m/s)	1	0.53	0.53	0.41	**0.17**	0.2	0.39	0.37

Table 5.2: Deviation from desired speed – 50 vehicles

100 Vehicles Traffic Density

Scenario	1.1	1.2	1.3	2.1	2.2	2.3	2.4	2.5
Deviation from desired speed (m/s)	7.88	3.38	3.59	3.24	**0.92**	**0.65**	2.44	1.66

Table 5.3: Deviation from desired speed – 100 vehicles

150 Vehicles Traffic Density

Scenario	1.1	1.2	1.3	2.1	2.2	2.3	2.4	2.5
Deviation from desired speed (m/s)	10.64	8.76	8.59	9.78	7.24	**2.64**	6.58	6.03

Table 5.4: Deviation from desired speed – 150 vehicles

In Table 5.4 the average speeds of the EmV are shown in comparison with the average speed of traffic. In order to choose a solution to our problem, we have to take into account the average speed as well. If our changes had a noticeable negative impact on the rest of the vehicle population, we might have to reconsider out methods. In our case, no such thing was noticed, so we did not have to filter our methods. As density increases, the population moves slower due to lack of space. So, reaching the target speed is even more impressive.

Traffic Density	50 vehicles		100 vehicles		150 vehicles	
Scenario	**Avg. Speed EmV**	**Avg. Speed Traffic**	**Avg. Speed EmV**	**Avg. Speed Traffic**	**Avg. Speed EmV**	**Avg. Speed Traffic**
1.1	39.00	29.35	32.12	28.69	29.36	27.76
1.2	39.47	29.38	36.62	29.02	31.24	27.77
1.3	39.47	29.37	36.41	28.85	31.41	27.91
2.1	39.59	29.35	36.76	28.97	30.22	27.71
2.2	39.83	29.33	39.08	28.69	35.76	27.92
2.3	**39.80**	29.27	**39.35**	28.68	**37.37**	27.84
2.4	39.61	29.34	37.56	28.74	33.42	28.00
2.5	39.63	29.31	38.34	28.92	33.97	28.00

Table 5.5: Average speed and Average speed of traffic in every scenario taken place

Safety – Collisions

The table below indicates the collisions that took place in each simulation. *Corner Crashes** are not taken into consideration, since they are not realistically possible and dangerous.

In the Non-Cooperative Approach, no collisions are noted. As a result, all changes may be kept and implemented. On the other hand, as cooperation starts taking place, collisions are an indicator of the efficiency of our method. For example, in Scenario 2.2, for 100 vehicles in traffic, 2 crashes took place and in 150 vehicle traffic, 5 took place. The collisions detected will be observed in the team's future work, in order to be reduced.

Some of the collisions detected, happen while deactivating the altered hard bounds. More specifically, when the EmV passes through the corridor and the vehicles behind it can again, take their original borders, some collisions take place. But, when the green corridor is activated combined with the lateral speed given to the neighbor downstream vehicles, these numbers decrease. So, Scenario 2.2 on its own may be excluded, but may be used when in cooperation with 2.1, resulting to Scenario 2.3 as a good choice.

Regarding the green corridor on the left side of the road, it brought low performance overall and has more crashes (3 in each case) than the corridor in the middle. The reason the crashes occur will be taken into consideration to direct further work. Even if on the specific method, we don't choose to place the corridor in the middle of the road, the conclusion drawn from the crashes may help us reduce them completely.

Traffic Density	50 vehicles	100 vehicles	150 vehicles
Scenario	Crashes		
1.1	0	0	0
1.2	0	0	0
1.3	0	0	0
2.1	0	1(cc*)	0
2.2	0	2	5
2.3	0	1	1
2.4	0	3	1(cc*)
2.5	0	0	3

Table 5.6: Vehicle Collisions

* (cc): Collisions labeled as corner crashes took place between vehicles for *m*seconds at the edges of them which are not realistically possible or dangerous since they refer to vehicles colliding in terms of millimeters.

6

Conclusion

The objective of this diploma thesis was a study regarding the development of a strategy for an EmV to travel through traffic in a lane-free environment with automated vehicles. In the research done so far, the automated vehicles drove in a lane-free environment having a specific range of characteristics and goals. The EmV that entered our given model for the specific study, on the contrary, had greater dimensions and a higher target speed than the rest of the traffic population. This work aims to infer a good strategy for the EmV to travel independently through dense traffic. The main goal of the green corridor was to improve the longitudinal speed of the EmV in various traffic densities, while avoiding collisions.

Firstly, the reaction of the population's response to the entrance of the EmV was observed without taking any further action. Only by giving the EmV the intention to drive faster than other vehicles, was not sufficient. So, on the next stage, the safety time-gap was decreased for the EmV, so it could travel more aggressively and closer to other vehicles and was also centered in the middle of the road to be given more choices for overpasses and maneuvers. These changes were made regarding the Passive Approach of alterations. On the next stage of cooperation with other vehicles, a lateral speed was given to vehicles downstream the EmV in order to open up the way for it to pass through. Regarding the Active Approach, the space for the EmV to pass through independently was made with a different method by changing the hard bounds of the downstream to the EmV vehicles. As it was observed, changing the hard bounds was a more drastic solution and brought the best results in the performance of the vehicle of interest. Finally, the place of the corridor on the road was compared on being in the middle and on the side of the road, and the choice of the middle was found to be more efficient.

All proposed strategies and scenarios were simulated for various densities, in a lane-free environment using a custom-made extension, named TrafficFluid-Sim, which is built for

the Simulation of Urban Mobility (SUMO) simulator, considering a 1km ring-road, with the extension TrafficFluid Sim as proposed in [40]. Moreover, several quantities, like the average longitudinal speed, traffic flow, collisions and statistical measures were taken into consideration for the evaluation of each method.

The conclusion drawn from our test was that a good strategy to help an EmV pass through dense traffic and keep a higher real time speed, was the proposed green corridor in the middle of the road with a lateral speed given to its downstream vehicles. The combination of altering the downstream vehicles' lateral bounds and the lateral speed given to them gives space to the EmV to move and as a result the average speed of the EmV is maintained higher than the rest of the vehicle population. In higher densities (100+ veh/km), where the improvement was critical, we managed to reach 23.2% of longitudinal speed increment, compared to just setting a higher target speed for the EmV. In low densities the vehicles have the essential space to move and to reach the longitudinal desired speeds, while for densities over the critical density, the traffic speed improvement is higher, due to the need for the actual solution of the corridor.

Discussion and Future Work

Firstly, the cases where crashes took place will be investigated briefly, in order to specify the reason why they happen. Methods to avoid collision completely, improving the presented method, will be formed. Also, the proposed strategy will be tested in higher traffic densities, over critical as described in [52], since 150 vehicles which was our extreme case, is still under the critical limit of 200 CAVs on a 1km ring-road. Some thoughts included in our team's future work, on improving the strategy proposed in the present thesis, is to test this strategy in cases at and over critical traffic density. If needed the decrement of the desired speed of front vehicles (e.g., -30%), will be activated, to achieve smaller time gaps between non-EmV vehicles. They will then, be able to travel closer to each other, creating more space for the EmV.

Another thought, inspired by the way emergency vehicles operate in some countries as the U.S, is to add more EmV's in the circuit and test the reaction of our model. In the majority of cases, a police car and a firefighter vehicle attend an ambulance, so, it is crucial to observe the reaction of our model with more than one EmV. Instead of testing the model's reaction to the entrance of one EmV, we may try it for three vehicles, aiming for these three vehicles to travel as a group.

Moreover, the study proposed in [60] regarding dynamic incremental road widening or narrowing may be used as a method to create space for the EmV. In more detail, the direction of the road that includes the EmV will be widened and as a result, the vehicle capacity of the specific direction will be increased, so, the EmV will have more space to overpass, maneuver and reach its goals more easily.

Last, but not least, an improvement or variation to the EmV case will be used to test the CAV movement in a typical freeway instead of a ring-road. In the present experiment, CAVs were travelling in a ring-road, which means that each vehicle that travelled the 1km-road and exited, re-entered the network instantly, with the same features and target speed. On the contrary, in the freeway, new vehicles, with other dimensions and target speeds will be entering the road. In that means, more variability cases will be tested, and observations made will contribute to further improvements of the present method.

References

[1]. Papageorgiou, M., 1998. Some remarks on macroscopic traffic flow modelling. Transportation Research Part A: Policy and Practice, 32(5), pp.323-329.

[2]. Zhang, H.M., 2003. Anisotropic property revisited––does it hold in multi-lane traffic?. Transportation Research Part B: Methodological, 37(6), pp.561-577.

[3]. Lighthill, M.J. and Whitham, G.B., 1955. On kinematic waves II. A theory of traffic flow on long crowded roads. Proceedings of the royal society of London. series a. mathematical and physical sciences, 229(1178), pp.317-345.

[4]. Papageorgiou, M., Mountakis, K.S., Karafyllis, I., Papamichail, I. and Wang, Y., 2021. Lane-free artificial-fluid concept for vehicular traffic. Proceedings of the IEEE, 109(2), pp.114-121.

[5]. Ruan, Hai-lin, et al. "Prehospital Index provides prognosis for hospitalized patients with acute trauma." Patient preference and adherence (2018): 561-565.

[6]. Yu, W., Bai, W., Qi, L. and Luan, W., 2022. State-of-the-art review on traffic control strategies for emergency vehicles. IEEE Access.

[7]. Bishop, R., 2005. Intelligent vehicle technology and trends.

[8]. Popescu-Zeletin, R., Radusch, I. and Rigani, M.A., 2010. Vehicular-2-X communication: state-of-the-art and research in mobile vehicular ad hoc networks. Springer Science & Business Media.

[9]. Diakaki, C., Papageorgiou, M., Papamichail, I. and Nikolos, I., 2015. Overview and analysis of vehicle automation and communication systems from a motorway traffic management perspective. Transportation Research Part A: Policy and Practice, 75, pp.147-165.

[10]. Lo, H.K., Chang, E. and Chan, Y.C., 2001. Dynamic network traffic control. Transportation Research Part A: Policy and Practice, 35(8), pp.721-744.

[11]. Ferrara, A., Sacone, S. and Siri, S., 2018. Freeway traffic modelling and control (Vol. 585). Berlin: Springer.Dudek G, Jenkin M (2010) Computational principles of mobile robotics. Cambridge University Press, Cambridge

[12]. Heinen, F.J. and Osório, F.S., 2002, December. HyCAR-A Robust Hybrid Control Architecture for Autonomous Robots. In HIS (pp. 830-842).

[13]. Meneguette, R.I., De Grande, R. and Loureiro, A.A., 2018. Intelligent transport system in smart cities. Cham: Springer International Publishing.

[14]. dos Santos, C.T. and Osório, F.S., 2004, May. An intelligent and adaptive virtual environment and its application in distance learning. In Proceedings of the working conference on Advanced visual interfaces (pp. 362-365).

[15]. Heinen, F.J. and Osório, F.S., 2002, December. HyCAR-A Robust Hybrid Control Architecture for Autonomous Robots. In HIS (pp. 830-842).

[16]. Dudek, G. and Jenkin, M., 2010. Computational principles of mobile robotics. Cambridge university press.

[17]. Li, X., Xiao, Y., Zhao, X., Ma, X. and Wang, X., 2023. Modeling mixed traffic flows of human-driving vehicles and connected and autonomous vehicles considering

human drivers' cognitive characteristics and driving behavior interaction. Physica A: Statistical Mechanics and its Applications, 609, p.128368.
[18]. Montanaro, U., Dixit, S., Fallah, S., Dianati, M., Stevens, A., Oxtoby, D. and Mouzakitis, A., 2019. Towards connected autonomous driving: review of use-cases. Vehicle system dynamics, 57(6), pp.779-814.
[19]. Jiang, Y., Zhao, B., Liu, M., Yao, Z., 2021. A Two-Level Model for Traffic Signal Timing and Trajectories Planning of Multiple CAVs in a Random Environment. Journal of Advanced Transportation 2021, 9945398. https://doi.org/10.1155/2021/9945398
[20]. Yao, Z., Hu, R., Jiang, Y. and Xu, T., 2020. Stability and safety evaluation of mixed traffic flow with connected automated vehicles on expressways. Journal of safety research, 75, pp.262-274.
[21]. Carrone, A.P., Rich, J., Vandet, C.A. and An, K., 2021. Autonomous vehicles in mixed motorway traffic: capacity utilisation, impact and policy implications. Transportation, pp.1-32.
[22]. Barabas, I., Todoruţ, A., Cordoş, N. and Molea, A., 2017, October. Current challenges in autonomous driving. In IOP conference series: materials science and engineering (Vol. 252, No. 1, p. 012096). IOP Publishing.
[23]. Yu, H., Jiang, R., He, Z., Zheng, Z., Li, L., Liu, R. and Chen, X., 2021. Automated vehicle-involved traffic flow studies: A survey of assumptions, models, speculations, and perspectives. Transportation research part C: emerging technologies, 127, p.103101.
[24]. Olovsson, T., Svensson, T. and Wu, J., 2022. Future connected vehicles: Communications demands, privacy and cyber-security. Communications in Transportation Research, 2(1), p.100056.
[25]. Guo, J., Cheng, S. and Liu, Y., 2020. Merging and diverging impact on mixed traffic of regular and autonomous vehicles. IEEE Transactions on Intelligent Transportation Systems, 22(3), pp.1639-1649.
[26]. Guo, J., Liu, Y. and Fang, S., 2019. Simulated CAVs driving and characteristics of the mixed traffic using reinforcement learning method. In Smart Transportation Systems 2019 (pp. 193-204). Springer Singapore.
[27]. Mahbub, A.I. and Malikopoulos, A.A., 2021. A platoon formation framework in a mixed traffic environment. IEEE Control Systems Letters, 6, pp.1370-1375.
[28]. T Campisi, T., Severino, A., Al-Rashid, M.A. and Pau, G., 2021. The development of the smart cities in the connected and autonomous vehicles (CAVs) era: From mobility patterns to scaling in cities. Infrastructures, 6(7), p.100.
[29]. Chuanjin, L., Xiaohu, Q., Xiyue, H., Yi, C. and Xin, Z., 2003, October. A monocular-vision-based driver assistance system for collision avoidance. In Proceedings of the 2003 IEEE International Conference on Intelligent Transportation Systems (Vol. 1, pp. 463-468). IEEE.
[30]. Ozguner, U., Stiller, C. and Redmill, K., 2007. Systems for safety and autonomous behavior in cars: The DARPA Grand Challenge experience. Proceedings of the IEEE, 95(2), pp.397-412.

[31]. Vis, I.F., 2006. Survey of research in the design and control of automated guided vehicle systems. European journal of operational research, 170(3), pp.677-709.
[32]. Medeiros, A.A., 1998. A survey of control architectures for autonomous mobile robots. Journal of the Brazilian Computer Society, 4, pp.35-43.
[33]. Santa, J., Gómez-Skarmeta, A.F. and Sánchez-Artigas, M., 2008. Architecture and evaluation of a unified V2V and V2I communication system based on cellular networks. Computer Communications, 31(12), pp.2850-2861.
[34]. Poczter, S.L. and Jankovic, L.M., 2014. The google car: driving toward a better future?. Journal of Business Case Studies (JBCS), 10(1), pp.7-14.
[35]. Fagnant, D.J. and Kockelman, K., 2015. Preparing a nation for autonomous vehicles: opportunities, barriers and policy recommendations. Transportation Research Part A: Policy and Practice, 77, pp.167-181.
[36]. Papadoulis, A., Quddus, M. and Imprialou, M., 2019. Evaluating the safety impact of connected and autonomous vehicles on motorways. Accident Analysis & Prevention, 124, pp.12-22.
[37]. Faros, I. 2022. Automated Vehicles in Lane-free Traffic using Optimal Control
[38]. Pocketbook, E.E.E.S., 2020. Country datasheets. European Commission: Brussels, Belgium.
[39]. Union—Current Trends and Issues. [Online]. Available: https://ec.europa.eu/transport/sites/transport/files/2018-transport-in-the-eucurrent-trends-and-issues.pdf
[40]. Troullinos, D., Chalkiadakis, G., Manolis, D., Papamichail, I. and Papageorgiou, M., 2021, September. Lane-free microscopic simulation for connected and automated vehicles. In 2021 IEEE International Intelligent Transportation Systems Conference (ITSC) (pp. 3292-3299). IEEE.
[41]. Cozzi, L. and Petropoulos, A., 2019. Growing preference for SUVs challenges emissions reductions in passenger car market.
[42]. Average, C.O., 2019. emissions from new cars and new vans increased in 2018. European Environment Agency, EEA.
[43]. Krajinska, A., Krajinska, A., Engineer, E. and de Meeûs, S., 2020. Transport & environment. European Federation for Transport and Environment AISBL, pp.15-21.
[44]. Fernandes, P., Tomás, R., Ferreira, E., Bahmankhah, B. and Coelho, M.C., 2021. Driving aggressiveness in hybrid electric vehicles: Assessing the impact of driving volatility on emission rates. Applied Energy, 284, p.116250.
[45]. Anenberg, S.C., Miller, J., Minjares, R., Du, L., Henze, D.K., Lacey, F., Malley, C.S., Emberson, L., Franco, V., Klimont, Z. and Heyes, C., 2017. Impacts and mitigation of excess diesel-related NO x emissions in 11 major vehicle markets. Nature, 545(7655), pp.467-471.
[46]. Correia, G.H.D.A. and van Arem, B., 2017. Estimating urban mobility patterns under a scenario of automated driving: Results from a model application to Delft, The Netherlands (No. 17-04613).

[47]. Lu, Q., Tettamanti, T., Hörcher, D. and Varga, I., 2020. The impact of autonomous vehicles on urban traffic network capacity: an experimental analysis by microscopic traffic simulation. Transportation Letters, 12(8), pp.540-549.
[48]. Hancock, P.A., Nourbakhsh, I. and Stewart, J., 2019. On the future of transportation in an era of automated and autonomous vehicles. Proceedings of the National Academy of Sciences, 116(16), pp.7684-7691.
[49]. Bandeira, J.M., Macedo, E., Fernandes, P., Rodrigues, M., Andrade, M. and Coelho, M.C., 2021. Potential pollutant emission effects of connected and automated vehicles in a mixed traffic flow context for different road types. IEEE Open Journal of Intelligent Transportation Systems, 2, pp.364-383.
[50]. Clements, L.M. and Kockelman, K.M., 2017. Economic effects of automated vehicles. Transportation Research Record, 2606(1), pp.106-114.
[51]. Daganzo, C.F., 1995. Requiem for second-order fluid approximations of traffic flow. Transportation Research Part B: Methodological, 29(4), pp.277-286.
[52]. Yanumula, V.K., Typaldos, P., Troullinos, D., Malekzadeh, M., Papamichail, I. and Papageorgiou, M., 2023. Optimal trajectory planning for connected and automated vehicles in lane-free traffic with vehicle nudging. IEEE Transactions on Intelligent Vehicles, 8(3), pp.2385-2399.
[53]. D. Q. Mayne, "Model predictive control: Recent developments and future promise," Automatica, vol. 50, no. 12, pp. 2967–2986, 2014.
[54]. Mayne, D.Q., 2014. Model predictive control: Recent developments and future promise. Automatica, 50(12), pp.2967-2986.
[55]. Connected Autonomous Vehicles - ferrovial (2020). Available at: https://www.ferrovial.com/en/innovation/technologies/connected-autonomous-vehicles/.
[56]. Yanumula, V.K., Typaldos, P., Troullinos, D., Malekzadeh, M., Papamichail, I. and Papageorgiou, M., 2021, September. Optimal path planning for connected and automated vehicles in lane-free traffic. In 2021 IEEE International Intelligent Transportation Systems Conference (ITSC) (pp. 3545-3552). IEEE.
[57]. Faros, I., Yanumula, V.K., Typaldos, P., Papamichail, I. and Papageorgiou, M., A Lateral Positioning Strategy for Connected and Automated Vehicles in Lane-free Traffic.
[58]. Piccirillo, V., Goes, L.C.S., Ramos, R.L.D.C.B. and Balthazar, J.M., Application of Predictive Control Techniques to a Helicopter Blade Sailing System.
[59]. Lopez, P.A., Behrisch, M., Bieker-Walz, L., Erdmann, J., Flötteröd, Y.P., Hilbrich, R., Lücken, L., Rummel, J., Wagner, P. and Wießner, E., 2018, November. Microscopic traffic simulation using sumo. In 2018 21st international conference on intelligent transportation systems (ITSC) (pp. 2575-2582). IEEE.
[60]. Malekzadeh, Milad, Ioannis Papamichail, Markos Papageorgiou, and Klaus Bogenberger. "Optimal internal boundary control of lane-free automated vehicle traffic." Transportation Research Part C: Emerging Technologies 126 (2021): 103060.

[61]. Karafyllis, I., Theodosis, D. and Papageorgiou, M., 2022. Analysis and control of a non-local PDE traffic flow model. International Journal of Control, 95(3), pp.660-678.